

UCSF

UC San Francisco Electronic Theses and Dissertations

Title

Calcium mediated differentiation of ameloblasts via the calcium sensing receptor

Permalink

<https://escholarship.org/uc/item/2nw9j29s>

Author

Chen, James Jian

Publication Date

2011

Peer reviewed|Thesis/dissertation

Calcium mediated differentiation of ameloblasts via the calcium sensing receptor

By

James Chen

DISSERTATION

Submitted in partial satisfaction of the requirements for the degree of

DOCTOR OF PHILOSOPHY

in

Oral Craniofacial Sciences

in the

GRADUATE DIVISION

of the

UNIVERSITY OF CALIFORNIA, SAN FRANCISCO

Dedication and Acknowledgements

I would like to give a special thank you to my mentor Dr. Pamela DenBesten for all of her tireless work on my thesis and for unyielding support as a mentor.

I would like to thank Dr. Dan Bikle and Dr. Chia-ling Tu for their collaboration regarding the K14-Cre-CaSR^{-/-} mice.

I would like to thank Dr. Ralf Heber and Dr. Arndt Klocke for their help with my micro-CT analysis.

I would like to thank the members of my thesis committee, Dr. Tamara Alliston, Dr. Ophir Klein, and Dr. Stefan Habelitz.

I would like to thank my family and especially my wife for their support

Abstract:

Ameloblasts continuously differentiate from epithelial stem cells to maturation stage ameloblasts, modulating and directing the formation of a mineralized enamel matrix. Calcium is required for enamel mineralization, however, as in other epithelial tissues; calcium may also be a modulator for ameloblast differentiation. Several studies have suggested a role for the calcium sensing receptor (CaSR) in ameloblast differentiation.

Hypothesis: Calcium regulates ameloblast differentiation through the activity of the calcium sensing receptor. **Methods:** A primary ameloblast cell culture model was used to determine whether calcium could direct ameloblast differentiation, cellular morphology, and gene expression. Gene expression in response to calcium was assessed via microarray analysis. *In vivo* studies using K14-Cre-CaSR^{-/-} mice treated with a normal diet, low calcium diet or high fluoride diet were completed to determine the role of the CaSR on ameloblast differentiation. Enamel formation, mineralization, and ameloblast differentiation were imaged by microCT, histochemistry, and immunohistochemistry. Gene expression was compared by qPCR. **Results:** *In vitro* primary cell culture data showed that elevated levels of calcium could induce mineralization, changes in cell morphology and gene expression related to dose and time of exposure. Primary ameloblast lineage cells is very heterogeneous, with a proportion of stellate reticulum cells, which accounts for the high levels of collagen Type I levels found in the microarray study. *In vivo* K14-Cre-CaSR^{-/-} mouse model data showed earlier enamel formation compared to wild type mice, with no effects on ameloblast morphology and gene expression. The early enamel formation phenotype in K14-Cre-CaSR^{-/-} mice was

enhanced in the presence of fluoride and in the absence of calcium in the diet.

Conclusion: Calcium can modulate expression of extracellular matrix proteins in a mixed primary cell culture. CaSR activity can influence the timing of enamel formation, but has a limited role in regulating ameloblast differentiation. Calcium mediated changes in gene expression and ameloblast cellular function appears to be controlled through mechanisms other than CaSR.

TABLE OF CONTENTS-

Chapter number and Title-	Page #
1) Introduction, hypothesis, and specific aims	1-35
2) Calcium mediated differentiation of ameloblast lineage cells <i>in vitro</i>	36-141
Publication- Calcium mediated differentiation of ameloblast lineage cells <i>in vitro</i>	38-60
Appendix 1-Calcium mediated activation of the human amelogenin promoter	61-71
Appendix 2-Calcium induced gene expression	72-119
Appendix 3-Characterization of growth enhanced human ameloblasts	120-133
Appendix 4-Detection and localization of CaSR in primary human ameloblasts	134-140
3) Evaluation and characterization of K14-Cre-CaSR ^{-/-} mice	142-174
4) Conclusion	175-181
5) UCSF Library Release	182

LIST OF TABLES AND FIGURES-

Chapter title	Page #
Chapter 2-	
<i>Publication-</i>	
Ameloblast differentiation	43
Ameloblast lineage cell morphology	45
In the presence of calcium	
BrdU immunoassay	46
Von Kossa mineralization assay	47
Markers of ameloblast differentiation	48
Amelogenin expression in response to calcium	49
<i>Appendix 1-</i>	
GFP reporter vector construction	63
Calcium dose dependent amelogenin expression	66
Amelogenin promoter activity in response to	67
calcium	
<i>Appendix 2-</i>	
Derivation of significantly up or down regulated	74
genes	
Significantly upregulated genes relative to	76
Amelogenesis	
Total up and down regulated genes	86
<i>Appendix 3-</i>	
Gene specific primers	123
Cellular morphology of SV40-HA cells	124
Large-T antigen localization	125

SV40-HA expression profile	127
Collagen Type I expression	128
SV40-HA mineralization assay	129
<i>Appendix 4-</i>	
CaSR localization in human fetal tooth buds	137
CaSR levels in primary human ameloblast lineage cells	138
<i>Chapter 3-</i>	
Knockout efficiency in K14-CaSR ^{-/-} mice	151
Incisor phenotype comparison between wild-type K14-CaSR ^{-/-} mice	153
Histological analysis of K14-CaSR ^{-/-} mice	154
Enamel matrix expression in K14-CaSR ^{-/-} mice	155
Amelogenin expression and localization in K14-CaSR ^{-/-} mice	156
Enamel thickness comparison between wild type and K14-CaSR ^{-/-} mice	157-158
MicroCt analysis of wild-type and K14-CaSR ^{-/-} mice	159
Quantified early enamel formation in K14-CaSR ^{-/-} mice	160
<i>Conclusion-</i>	
Proposed model of CaSR and calcium function During amelogenesis	178
Proposed model for reduced CaSR activity	179

CHAPTER 1-INTRODUCTION

Calcium regulation-

Intracellular calcium is an essential ion for many biological processes including muscle contraction, hormone secretion, and neuronal excitation. Extracellular calcium is required for incorporation into hydroxyapatite, the basic building block for mineralized tissues. These critical extracellular and intracellular functions of calcium require tightly controlled plasma calcium levels, regulated primarily through the GI tract (absorption), kidneys (re-uptake), and bone (release). Calcium regulation in these tissues is mediated by hormone signaling molecules including parathyroid hormone (PTH), 1,25-dihydroxyvitamin D (Vit D), and calcitonin.

Of the total calcium found in the human body, most is stored in bone and in the blood. In the blood, 45% of total calcium is present as the free ionized form, and 45% is bound to serum proteins, with only a small fraction associated with other anions such as citrate, sulfate, and phosphates. The aforementioned hormones tightly control these percentages.

Calcium homeostasis is highly regulated in the intestine. Intestinal calcium absorption is regulated by the actions of Vit D on the intestinal epithelia. Vit D regulates calcium absorption by a passive paracellular pathway and an active transcellular pathway [1]. In the paracellular pathway, calcium moves down a concentration gradient between the intestinal epithelial cells at their tight junction interfaces. The active transcellular pathway is dependent on transcriptional regulation by Vit D of calcium channel proteins (TRPV5,6), calcium pumps (PMCA1b), and calcium binding proteins (Calbindin) [1, 2].

The concerted actions of Vit D, calcium channels, calcium pumps, and calcium binding proteins move calcium from the lumen of the intestine into the plasma as depending on the needs of the body.

While the intestinal epithelial cells control the uptake of calcium from the diet, the kidneys contribute to calcium homeostasis by regulating calcium re-uptake from urine. Similar to the activities in the intestine, calcium reuptake by the nephrons occurs both passively and actively. Active calcium re-uptake occurs in the thick ascending limb of the loop of Henle and in the distal convoluted tubule and the connecting tubule [3-5]. Whereas in the passive re-uptake pathway, calcium is reabsorbed in the proximal tubule where it follows sodium reabsorption [6]. Similar to intestinal epithelia, calcium channels, pumps, and transport proteins are responsible for the active movement of calcium from the lumen of the nephrons into the blood stream.

The body's ability to regulate the amount of calcium intake and excretion is indeed a vital component of the overall calcium homeostasis mechanism. As mentioned earlier, bone is a huge reservoir of calcium in the human body, where it is stored in the form of hydroxyapatite ($\text{Ca}_{10}(\text{PO}_4)_6(\text{OH})_2$) in bone. Bone is a dynamic tissue and is always in a state of constant remodeling, with a balancing act occurring between deposition and resorption. The actions of both osteoblasts and osteoclasts determine which process will prevail. Both osteoblast and osteoclast activity is driven by the calcium regulating hormones PTH, Vit D, and calcitonin [7]. PTH's stimulatory effects on osteoblast activity can either be anabolic or catabolic [7].

Calcium homeostasis is a dynamic process with multiple integrated feedback loops, for example: PTH, calcitonin, and Vit D are responsible for controlling the level of

calcium in the plasma, and the synthesis of all three hormones is determined by the level of calcium in the serum. PTH and Vit D are release into the blood stream occurs when there is a decrease in the level of free calcium in the plasma, and conversely calcitonin is upregulated when there is an over abundance of calcium in the plasma [3].

PTH regulation is a good example of how the calcium feedback-loops function. The G-protein coupled receptor, calcium sensing receptor (CaSR), is located on the surface of parathyroid cells and responds to changes in the concentration of ionized calcium by regulating PTH expression and secretion. Under low ionized calcium levels, inactive CaSR allows the release of stored PTH, but under high levels of ionized calcium active CaSR will decrease the expression and secretion of PTH [8, 9]. The importance of CaSR activity to calcium regulation is illustrated by genetic mutations in the CaSR gene that lead to varying degrees of hypercalciuria and hypocalcemia [9]. We will discuss the molecular details of CaSR function and its role in cellular regulation in greater detail later.

Ionized calcium is important for the function of almost all the cells in the body. Calcium is required for muscle function, neuronal communication and activity, and is a co-activator for thousands of proteins, development of mineralized tissues, and countless cellular functions. With regards to cellular functions, calcium regulates cell differentiation, cell proliferation, and gene expression. All of these functions are very cell type specific. For example, keratinocytes differentiate at levels of calcium above 0.1mM, but osteoblasts proliferate at similar calcium levels [10, 11]. For mineralized tissues (bone, dentin and enamel), calcium has an additional role in forming a mineralized matrix, which requires cellular transport into the extracellular space.

Dis-regulated calcium homeostasis and its effect on tooth formation-

The importance of calcium homeostasis on cellular function becomes apparent when naturally occurring mutations disrupt various aspects of calcium regulation. Either an increase or a decrease in calcium serum levels can lead to a broad spectrum of effects on the human body. Since calcium is needed very early on during development and is critical for cellular function, early loss of calcium regulation leads more severe and permanent the damage. In adults the normal level of calcium in the blood ranges from 2.2-2.6mM. Symptoms generally appear in hypercalcaemia patients when the calcium levels increase to around 3.0mM, and severe hypercalcaemia occurs at 3.75-4.0mM calcium. In symptomatic hypocalcaemia the blood levels of calcium are usually less than 2.1mM.

Hyper- and hypocalcaemia can be caused by multiple genetic and environmental factors, some which are due to a singular factor, and some due to factors working in concert with each other. The most common cause of hypercalcaemia is primary hyperparathyroidism. The hallmark signs of hypercalcaemia are known as “stones, moans, bones, groans, and overtones.” Stones are associated with high levels of free calcium in the kidneys leading to mineralized calcium stones. Moans are associated with fatigue, lethargy, and depression, where altered neuronal signaling is the major cause. In order to achieve such high levels of serum calcium, bone turnover is increased. The rapid bone turnover leads to pain in the bones. Groans are associated with the loss of regulation in the gastrointestinal tract, which lead to constipation. Lastly, overtones are associated with neuronal signaling, which leads to depression and confusion. In addition

hypercalcaemia can lead to abnormal heart rhythms, which in severe cases can lead to cardiac arrest.

Hypercalcaemia dramatically affects organs dependent on calcium signaling, but in other systems such as dental hard tissues there appears to be minor effects. The most commonly reported tooth related effect of hypercalcaemia is increased tooth movement during orthodontic traction [12].

Hypocalcaemia, on the other hand, presents with very different signs and symptoms compared to hypercalcaemia. In a hypocalcemic state, mineralized tissues, cardiovascular, and neuronal tissues are primarily affected. Often patients report a feeling of “pins and needles” around the mouth and lips due to altered neuronal signaling. The effect on mineralized tissues, especially bone is dramatic. Children with Rickets related to reduced calcium uptake, present with severe bony abnormalities such as disturbed growth and structure. Unlike hypercalcaemia, hypocalcaemia that occurs early in fetal development and infancy can lead to pronounced enamel defects. Children with Rickets, due to a deficiency or impaired metabolism of Vit D, phosphorus, and/or calcium, often have varying degrees of hypoplastic and hypomineralized enamel [13]. Hypocalcaemia can cause enamel malformation in both the primary and permanent dentition, and such malformations become highly susceptible to dental decay [14, 15].

Hypocalcaemia is a biochemical sign of an underlying disease or syndrome. Enamel hypoplasia seen in hypocalcaemic patients could be due to a lack of calcium in the serum and/or disruptions in ameloblast cell function that stems from the underlying cause of hypocalcaemia. Patients with childhood Rickets, as mentioned earlier, present with varying degrees of hypoplastic enamel. The reduction in serum calcium levels in

childhood Rickets is predominately due to insufficient Vit D, though there is a rare x-linked dominant form called Vit D resistant rickets [16]. Vitamin D deficiency is directly correlated with blood calcium levels, and more recent evidence has shown enamel forming ameloblasts express the nuclear vitamin-D receptor (VDR) [17]. Some studies using VDR null mice have reported a direct role of vitamin-D on ameloblast differentiation and function [18, 19]. The enamel phenotype seen in VDR null mice could not be rescued by calcium supplementation, and thus, indicating a specific role for VDR during ameloblast differentiation.

Hypoparathyroidism is another underlying cause of hypocalcaemia that presents with severe enamel hypoplasia [20, 21]. Enamel hypoplasia is related in part to the decrease in calcium levels of the blood, but many of the signaling molecules and receptors responsible for hypoparathyroidism also play an integral part in enamel formation. PTH is a vital signaling molecule for calcium homeostasis, with evidence now showing PTH also works in conjunction with PTHrP to direct tooth formation in an autocrine fashion [22]. PTH does not directly control ameloblast cellular function or differentiation, but rather indirectly regulates ameloblast cytodifferentiation via regulation of odontoblast cellular function [22]. The exact mechanism by which PTH controls tooth formation remains to be understood, but the prevailing hypothesis is that PTH controls tooth formation through a combination of a direct signaling component and an indirect calcium regulatory mechanism.

Another vital calcium regulatory protein is the calcium sensing receptor (CaSR). The role of the CaSR in calcium homeostasis is demonstrated by the disruptions of calcium homeostasis following both loss and gain of function CaSR mutations [9].

Genetic mutations that inhibit CaSR signaling can vary depending on the mutation and whether one or two copies of the CaSR allele are affected. The results of milder losses of function in the CaSR gene can be seen in familial benign hypercalcaemia (FBH). These patients present with mild to moderate hypercalcaemia, normal PTH levels, and low rates of urinary calcium excretion [23]. Inactivating mutations that occur in both alleles lead to severe state of hypercalcaemia known as neonatal severe hyperparathyroidism (NSHPT), resulting in life-threatening severe hypercalcaemia, failure to thrive, and under-mineralization of bone [24].

As one would expect, gain-of-function mutations in CaSR have the opposite effect, resulting in a varying degree of hypocalcaemia, and on occasion, seizures during childhood [23]. Gain-of-function CaSR mutations are classified under autosomal dominant hypocalcaemia. These mutations can occur sporadically or in conjunction with specific syndromes. Bartter syndrome type V, with symptoms of hypocalcaemia, metabolic alkalosis, hypercalciuria, and hyperaldosteronism are due to a gain-of-function mutations in the CaSR [25]. Both loss and gain of function mutations can affect the level of serum calcium, however, only gain-of-function mutations (resulting in hypocalcaemia) have been associated with enamel/dental defects, namely hypoplastic enamel in humans [26]

Similar to Vit D and PTH, the effects of the CaSR on tooth enamel formation could be due to both direct and indirect control of ameloblast differentiation. CaSR mouse germ-line knockout studies showed dramatic changes in tooth formation, and CaSR has been shown to be expressed in pre- and secretory ameloblasts in multiple species [30]. Little is known if and how CaSR has a direct role in ameloblast

differentiation [27-29]. Further studies involving all three calcium regulatory proteins will be needed to determine what their roles are in enamel formation and tooth development.

Enamel formation-

Specialized cells direct the formation of bone, dentin and enamel. Both osteoblasts and the neural crest derived odontoblasts are of mesenchymal cell origin, where as enamel is synthesized by the epithelially derived ameloblasts. After enamel is formed, the ameloblasts terminally differentiate and are lost from the enamel surface as the tooth erupts. Therefore, fully formed enamel cannot regenerate if it is lost or damaged. These factors are what make replacing enamel difficult in the field of dentistry. Currently, there is no substance that comes close to the same physical and mechanical properties as that of enamel,

The formation of the mammalian tooth is heavily dependent on epithelial-mesenchymal signaling. Tooth formation shares common signaling molecules with other organs derived from the ectoderm, such as hair, mammary glands, salivary glands, and kidneys. [31].

Tooth development and formation occurs through several distinct morphological stages: the placode, bud, cap, and bell stages. The bell stage is when cytodifferentiation of ameloblasts and odontoblasts occurs [31]. The first stage of tooth formation is the placode stage, and it is defined by thickening of the oral ectoderm. During this stage, signals from the oral ectoderm induce condensation of the underlying neuromesenchyme. Signaling pathways including members of the fibroblast growth factor (FGF), bone morphogenic protein (BMP), sonic hedgehog (Shh), and wingless (Wnt) families drive

the expression of various transcription factors of the neuromesenchyme (Msx1, Barx1, Gli1-2-3 and others) while under the transcriptional control of *Pitx2* [31, 32]. A review article by Jernvall and Thesleff elegantly illustrated many of the signaling interactions between epithelial and mesenchymal cells [31]. Once triggered by signals from the oral ectoderm, the neuromesenchyme then signals back to the oral ectoderm to perpetuate the signaling cascade into the bud stage of tooth development.

Early in ameloblast differentiation Shh is expressed at high levels by the stratum intermedium and preameloblasts. In *Smo*^{-/-} (receptor for Shh) enamel organs neither preameloblasts or stratum intermedium cells undergo the characteristic morphological changes characteristic of this stage of cytodifferentiation [47]. Secondly, members of the FGF family of signaling molecules have been identified in the inner enamel epithelium of developing molars [49], suggesting a possible regulatory mechanism for ameloblast cytodifferentiation [38]. Finally, members of the BMP family have also been suggested to be involved in ameloblast cytodifferentiation. *In vitro* culture of E13.5 mouse molars in the absence of BMP-4 expression lacked the proper cuspal development in addition to a complete absence of the enamel layer [50]. All the above mentioned growth factors/signaling molecules appear to be important for ameloblast cytodifferentiation, concurrently a new body of evidence is available showing in addition to organic signaling molecules, inorganic molecules may also be important in ameloblast differentiation.

As the tooth bud progresses from the bud stage to the cap stage, a signaling center begins to form in the dental epithelium called the enamel knot [33]. Under the regulation of specific transcription factors (p21, Msx2, Lef1), signaling molecules from the enamel knot promote the development and organization of the underlying dental mesenchyme

[31, 34-37]. As further tooth development occurs in the bell stage, secondary enamel knots form in areas of future cusp tips. These secondary enamel knots continue to express BMP's, FGF's, and Shh signaling molecules to guide species specific cusp patterns [31]. During the bell stage, cytodifferentiation of both ameloblasts and odontoblasts begin at or near the secondary enamel knots.

The formation of enamel and dentin during the bell stage begins in a similar fashion to the initial placode stage. Here, epithelial to mesenchymal signaling again plays a major role in cytodifferentiation. A final set of signals from preameloblasts signal preodontoblasts to polarize and begin the transition into a secretory cell [38]. Once differentiated, odontoblasts lay down the first layer of collagen matrix, which will become the first layer of dentin (mantle dentin). Upon the initial mineralization of the mantle dentin by odontoblasts, preameloblasts undergo their final mitotic division and begin to reorganize their cellular components in preparation for protein secretion [38]. Unlike odontoblasts, upon exit out of the cell cycle ameloblasts will progressively differentiate through several other distinct stages (presecretory, secretory, transitional, maturation).

As preameloblasts begin to terminally differentiate, they undergo polarization by shifting their nuclei from the center of the cells to a basal-lateral position, and develop a prominent endoplasmic reticulum near the Golgi apparatus. Another major change that occurs during this critical stage of ameloblast differentiation is a change in matrix composition. Preameloblasts are separated from the preodontoblasts by a basement membrane containing collagen Type IV, laminin's, nidogen, and other basement membrane components [39, 48]. Upon initiation of differentiation, ameloblasts alter their

expression profile as they shift expression to enamel matrix proteins, which occurs in conjunction with the loss of the basement membrane [39-41].

Of the enamel matrix proteins, amelogenins and ameloblastin comprise the largest portion of proteins secreted by the ameloblasts. Amelogenins make up most of the secretory enamel matrix proteins, and they provide the scaffolding onto which hydroxyapatite crystals combine to form enamel rods [42]. Some splice variants have been shown to signal the ameloblasts resulting in increased amelogenin expression, while others have been shown to alter ameloblast morphology *in vitro* [43, 44].

Ameloblastin is an enamel specific glycoprotein found at the cell surface, and is expressed during the pre-secretory/secretory stages but diminishes in maturation stage [45]. The function of ameloblastin is to promote adhesion between ameloblasts and the enamel matrix. Mutations in the ameloblastin gene are associated with poor enamel matrix formation and inhibition of mineralization, leading to hypoplastic (thin) enamel [40, 41]. More recent evidence has shown that amelogenin and ameloblastin function synergistically to maintain ameloblast differentiation [46].

The first layer of predentin although rich in proteinaceous growth factors and signaling molecules also contains a high level of inorganic ions needed for dentin mineralization, among those ions is calcium. Calcium serves to form hydroxyapatite minerals, but appears to also play a role cell signaling. Calcium is known to control differentiation and proliferation in multiple cell types, and preliminary studies on tooth development suggest it may be an important signaling molecule for ameloblast differentiation. The first line of evidence for the role of calcium as a signaling molecule in tooth development is an *in vivo* mouse model in which there was a complete absence

of PTH expression due to parathyroid gland removal [51]. In this mouse model, ameloblast morphology was greatly disorganized and little to no enamel matrix was present [51]. Additionally, two *in vitro* studies found that in the presence of higher than normal calcium levels in the culture media caused primary ameloblasts to organize into hierarchical structures with two distinct cell populations [29, 52]. These changes in cell morphology were associated with increased amelogenin expression, and decreased cell proliferation [29, 53]. The concentrations of calcium used in all of the *in vitro* studies were within the same range as what is detected in the developing tooth bud (0.1 to 0.5 mM) [54, 55].

The mechanism behind extracellular calcium mediated ameloblast differentiation is not clear, but a prime candidate for initiating the signaling cascade is CaSR. Again, we will discuss the many signaling networks that CaSR is associated with later, but for now we will focus on the role of CaSR in tooth development. CaSR expression begins in the preameloblast stage and continues up to the secretory stage in both mice and humans [56]. Moreover, germ-line CaSR^{-/-} mice are vastly smaller than their wild type counterparts in overall stature as well as tooth morphology [30]. Histological analyses of these mice show a dramatic decrease in the thickness of both dentin and enamel matrix [30].

However, the mouse model used for these studies of CaSR function were germ-line knockout mice, and therefore it is possible that the severely hypomineralized tooth phenotype is due to an indirect effect of poor calcium regulation. It is also interesting to note that though the neomycin cassette inserted into exon 5 would disrupt the full length CaSR transcript, and alternatively spliced form, which lacks exon 5, would not have been affected [10].

The Calcium Sensing Receptor-

Discovery and expression:

A substantial amount of work has focused on proteins that require calcium for their activity, proteins that bind calcium, and proteins that regulate calcium levels. It wasn't until the early 90's that a receptor specific for extracellular calcium was discovered. This calcium sensing receptor (CaSR) was cloned from bovine parathyroid cells and responded to changes in extracellular calcium [57]. Brown and colleagues determined that CaSR is a G-protein coupled receptor (GPCR) with an extracellular domain that can bind calcium and an intracellular signaling domain. [58].

Human CaSR gene is located on chromosome 3q13.3-21 and spans over 50KB of genomic DNA [59]. Human CaSR cDNA consists of seven exons, with the first exon being a 5'-untranslated region and the remaining six exons encoding a 1078 amino acid protein [60]. CaSR has been found in multiple different mammalian species, cow [8], dog [61], rat [62], mouse [10], and rabbit [63]. The CaSR promoter is unique in that it contains TATA and CAAT boxes, along with a second GC-rich promoter without a TATA box [64]. This particular two-promoter structure of CaSR is believed to be involved in its tissue specific gene regulation [64].

Several splice variants of the CaSR gene have been identified and described. The effect of the different splice variants on CaSR function vary considerably from no apparent effect to an inhibitory effect depending on the tissue type [65]. One splice variant contains a 30-nucleotide insertion within exon 7, though the subsequent effect of the 10 amino acid insertion had no apparent effect on CaSR function in *Xenopus* extracts [60]. Another alternatively spliced CaSR variant lacking exon 3 is found in the human

cytotrophoblasts and parathyroid cells [66]. This splice variant encodes a truncated and presumably inactive receptor; however, the effect of this particular splice variant has yet to be determined.

A splice variant with a known effect on CaSR function occurs in exon 5. This splice variant results in an in-frame deletion of 77 amino acids that results in a truncated version of CaSR as well as an markedly altered glycosylation pattern [10]. This truncated CaSR interferes with the function of full-length CaSR through dimerization which then dampens the responsiveness to elevated calcium levels in keratinocytes, but still retains some signaling capacity [10]. This means that in the CaSR knockout mouse analyzed by Sun and co-workers, which disrupted exon 5 expression in the full length transcript, some residual CaSR activity could have remained.

Protein Structure of CaSR:

CaSR is 120 kDa membrane protein with 7 transmembrane domains [57, 67, 68]. The N-terminal 613 AA makes up the extracellular domain. The extracellular domain is highly post-translationally modified, with nine potential glycosylation sites. Detection of CaSR by Western blotting results in three different protein bands that range from 100 to 200 kDa [69]. The lowest band at 120kDa represents the non-glycosylated form [69]. The two other bands represent an intermediate form of CaSR and the mature form of CaSR. The mature form of CaSR has an equivalent mass of 150-160 kDa, and is fully glycosylated with carbohydrates containing a high mannose content [69]. Glycosylation occurs at eight-conserved N-linked glycosylation sites- Asn90, Asn130, Asn261, Asn287, Asn468, Asn488, Asn261, Asn287, Asn446, Asn468, Asn488, and Asn541- and these sites are critical for cell surface expression [70]. Often a 200 kDa band is seen on

Western blot analysis, and represents the dimerized form of mature CaSR [71]. Only the dimerized and mature form of CaSR is found at the cell surface [71] In contrast, the alternatively spliced exon 5 variant produces a product that is around 130kDa with a significantly different glycosylation patten (only mannose glycosylation) [68].

The importance of the extracellular domain of CaSR is highlighted by the numerous naturally occurring mutations found in patients with disorders of calcium homeostasis [9]. The exact structure of CaSR has not been determined, but based on its homology to other members of the GPCR superfamily the predicted extracellular domain structure would produce a bilobed Venus-fly-trap arrangement [72]. Based on the predicted structure and the Hill coefficient, mature dimerized CaSR is hypothesized to bind anywhere from three to five Ca^{2+} ions [73]. The specific sites of calcium binding to CaSR are located at Ser147, Ser170, Asp 190, Tyr218, Glu297, Glu378, Glu379, Thr396, Asp398, Glu399, Glu224, Glu228, Glu229, Glu231, and Glu232 [74-76].

Not only does glycosylation determine cellular localization and CaSR function, but a series of conserved cysteines also play a role in localization and function. The extracellular domain consists of 14 highly conserved cysteines spread throughout- Cys60, Cys101, Cys236, Cys358, Cys395, Cys542, Cys546, Cys561, Cys562, Cys565, Cys568, Cys582, Cys585 [72]. Mutation analysis of each conserved cysteine resulted in decreased cell surface expression and biological activity [72]. Two of the above 14 cysteines are directly involved in dimerization, Cys101 and Cys236 [77].

The transmembrane domain of CaSR consists of 7 hydrophobic regions that form helices linked to one another via alternating intra- and extracellular loops. This orientation of the transmembrane domain is characteristic of all GPCR's, but at same

time, there is very low homology in the transmembrane domain among the GPCR family members. It is hypothesized that the conformational changes in the transmembrane domain occur in response to calcium binding in the extracellular domain and a change in conformation will then induce activation of different G-proteins [65]. This hypothesis was supported by evidence from Zhao *et al*, who found an mutation in the seventh transmembrane region led to a constitutively active form of CaSR [78]. Another putative function of the transmembrane domain is protein dimerization, this was supported by a study by Zhang *et al*, who found transmembrane domains 5,6 and 7 were important for dimerization [79]. Lastly, in regards to the transmembrane domain, the extracellular loops are not directly involved in calcium binding but they are targets of calcimimetics and calcilytics that potentiate the response to calcium [80].

The intracellular domain contains 222 amino acids, of which most are the hydrophilic amino acid variety [57]. Unlike the other two major domains, very few naturally occurring mutations occur in the intracellular domain and in general it is the least conserved among species. In the intracellular domain, two regions are highly homologous between species- AA863-925 and 960-984. Several studies have identified, and confirmed with alanine scanning those 20 amino acids in the proximal region of the intracellular domain are responsible for initiating signaling cascades and for cell surface localization [81, 82]. Alanine scanning is a method whereby each residue is individually changed to alanine by site directed mutagenesis, to identify residues important for function.

The activity of the intracellular domain of CaSR can be regulated through three protein kinase C (PKC) phosphorylation sites, located at Thr888, Ser895, and Ser915

[65]. These PKC phosphorylation sites act as a means of feedback inhibition on CaSR. In addition to PKC phosphorylation sites there are two predicted Protein Kinase A (PKA) phosphorylation sites, but these sites appear to have a very minor effect on CaSR activity [83].

Cellular localization of CaSR:

The site of function of CaSR is at the cell surface; however, multiple steps in protein organization and modification are needed to assure correct cellular distribution. In general for GPCR's, the arrangement of helices within the transmembrane domain are under strict quality control, but are still prone to failure [84]. Often times correct folding of GPCR's is quite difficult and is often delayed [84]. This low efficiency in biosynthesis is compounded by the fact that misfolded proteins in the ER are subject to endoplasmic-reticulum-associated degradation (ERAD). More specifically, CaSR is subject to proteosomal degradation via the E3 ligase, Dorfin, which acts as a quality control step during CaSR biosynthesis [85]. Dorfin specifically interacts and directs polyubiquitination within regions of the carboxy-terminus of CaSR [85]. Targeting of CaSR to ERAD occurs during protein translation and folding; however, CaSR can be diverted from degradation by both cellular and pharmacochaperones [86]. These chaperones provide the necessary time required for proper protein folding [87]. Cavanaugh and colleagues have shown this ER checkpoint for CaSR maturation is critical for providing a readily available supply of CaSR localized in the ER [87].

Once CaSR has been correctly folded and dimerized in the ER, it is then shipped to the Golgi for final processing into the full mature form. CaSR translocation to the Golgi and finally to cell surface is dependent on a class of receptor activity-modifying

protein (RAMP's). The RAMP family of proteins regulate a host of various molecular functions ranging from-receptor trafficking, glycosylation, ligand specificity, to second messenger production [88]. In the case of CaSR, RAMP's 1-3 are responsible for CaSR transport to the golgi followed by cell surface expression [65]. In cells such as COS-7 cells, that do not express any member of the RAMP family, CaSR is retained in the ER with no cell surface expression [89]. The dependence of CaSR on RAMP activity for cellular translocation provides yet another means of tissue specific regulation.

Intracellular signaling of CaSR:

The cellular functions that CaSR promote all begin with signaling through the intracellular domain of activated CaSR. The intracellular domain of GPCR's interacts with various heterotrimeric G-Proteins. Heterotrimeric G-proteins are a class of proteins that consist of three subunits α , β and γ [90]. Upon activation by calcium binding, CaSR associates with the heterotrimer G_{α} , G_{β} , and G_{γ} [90]. There are many different classes of the α -subunit, each binding to different membrane receptors and different downstream effectors (i.e. I, Q, S, etc.) [90]. The use of bacterial toxins such as cholera toxin and pertussis toxin are used to illustrate the different substrate specificities of various α -subunits (Cholera toxin binds to $G_{s\alpha}$ and pertussis toxin binds to $G_{i\alpha}$). These toxins greatly aid in identifying which heterotrimeric G-protein signaling pathway is associated with CaSR [90]. Cholera toxin does not affect CaSR mediated cellular response, whereas pertussis toxin has an effect [57]. This shows that $G_{s\alpha}$ does not play an important role in CaSR mediated signaling and that $G_{q\alpha}$ and $G_{i\alpha}$ may be the predominate G-proteins

activated by CaSR. Binding of GPCR's to a heterotrimeric G-protein complex induces the exchange of GDP for GTP on G_{α} subunits, which cause the dissociation of the trimer to G_{α} -GTP and $G_{\beta\gamma}$ [90]. G_{α} and $G_{\beta\gamma}$ are upstream of multiple pathways, among which are MAPK, PKC, and Phospholipase C- γ (PLC).

CaSR interacts with various G_{α} subunits all of which can trigger different downstream effects. Upon activation by CaSR, $G_{q\alpha}$ activates PLC γ which then catalyzes the hydrolysis of inositol triphosphate (IP₃) from phosphatidyl inositol diphosphate (PIP₂) from the inner cell membrane [57]. IP₃ then localizes to the smooth ER, where it opens calcium channels [57]. The spike in intracellular calcium activates calcium-binding enzymes (CaM kinase), which then propagates the initial signal from calcium to the nucleus, where gene expression occurs [57]. As calcium levels increase in the cytosol, store-operated calcium channels open in the cell membrane, to further increase the cytosolic calcium levels [91]. Diacylglycerol (DAG) is a byproduct from the enzymatic cleavage of PIP₃, and is an activator of the PKC pathway [57]. Activated PKC can phosphorylate other regulatory proteins (Src), upstream targets of transcription factors (MAPK pathway), and possibly feedback to inhibit CaSR activity [57, 92-94]. Active CaSR mediates the release of $G_{\beta\gamma}$ from G_{α} , where $G_{\beta\gamma}$ can activate PI3K pathway, which is important for localization of small GTPases (Rac1 and cdc42) to the plasma membrane [9]. There are many different downstream targets of CaSR, and there is a substantial amount of cross talk among them.

Although CaSR activity has been linked to PLC, PI3K, and PKC pathways, activation of these pathways is cell type specific [57]. This cell specific activation could explain why the same level of CaSR activation (same concentration of extracellular calcium) induces opposite effects in different cell types [57]. It is also possible that CaSR uses several downstream pathways to amplify the initial signal at the plasma membrane. In keratinocytes, activated CaSR induces changes in gene expression through activation of the transcription factor AP-1 [67]. AP-1 is the downstream target of the MAPK pathway, specifically Rac/cdc42-PAK1-MKK4/7-JNK pathway [95]. Although activation of AP-1 occurs in a linear fashion beginning from Rac/cdc42, the connection between Rac/cdc42 and the initial signal at the plasma membrane can be very complicated. Rac/cdc42 activation has been implicated as the downstream target of all of the previously mentioned pathways either directly or indirectly [96]. Therefore the path from activated CaSR to cellular response is complex and has been proven to be fairly redundant.

CaSR signaling in ameloblasts:

CaSR is expressed in a wide range of tissues: teeth, bone, brain, kidney, intestine, breast, parathyroid, and liver [67, 92, 97]. Many of the cell types in which CaSR is expressed do not have an active role in the maintenance serum calcium level; therefore, this would suggest that CaSR activity maybe important for other basic cellular functions. Ameloblast are no different from any of the cells used to determine the CaSR signaling pathway. Ameloblasts express all of the major proteins involved intracellular signaling [56, 98]. With all the players present in ameloblasts, one would suspect calcium to regulate CaSR activity, which in turn, will activate a host of downstream pathways. A

complete study on role of calcium and CaSR on ameloblast differentiation and proliferation is in part the focus of the work reported in this dissertation.

Hypothesis:

Extracellular calcium induces differentiation of ameloblasts, mediated through the calcium sensing receptor.

Specific Aims:

1. *To determine the effect of extracellular calcium on human ameloblast lineage cell function in vitro.*

The role of calcium mediated changes in cell directed tooth tissue differentiation and biomineralization was investigated using both primary ameloblast lineage cells and immortalized ameloblast lineage cell. The response of these cells to extracellular calcium, including changes in cell morphology, proliferation, differentiation, mineralization and gene expression was characterized.

2. *To determine the role of the CaSR in enamel formation using an epithelial specific CaSR knockout mouse model.*

Ameloblasts and forming enamel in epithelial cell specific K14-Cre-CaSR^{-/-} mice were characterized by histomorphology and immunohistochemistry. Enamel matrix gene expression was quantified and compared by real-time PCR. The relative mineral density between K14-Cre-CaSR^{-/-} and wild type mice molars and incisors was quantified and compared following imaging by microCT analysis. Further microCt analysis was done

on mice treated with either the addition of fluoride in drinking water, or decrease of calcium in the diet,

Rationale and significance:

Enamel is the only mineralized tissue in our body that does not have a regenerative capacity. Defects in ameloblast directed enamel formation lead to dramatic enamel malformations, most of which greatly affect the ability of an individual to eat in comfort without pain. Early loss of enamel greatly affects the ability to of individuals to properly thrive without the help of invasive and costly dental procedures. However, the mechanisms by which ameloblasts form and differentiate are still largely unknown, primarily due to limited cell based strategies for tooth regeneration.

The goal of the studies reported in this thesis was to determine the potential role of calcium in initiation of ameloblast differentiation, and the role of the CaSR in mediating this effect. We utilized two unique models to address these questions. First, we used a human ameloblast cell culture system, developed in our laboratory to determine whether calcium can specifically direct ameloblast differentiation. Secondly, in collaboration with the Bikle Lab (UCSF and SF VA Hospital) we analyzed the developing incisors from a knockout mouse model in which exon 7 of CaSR was conditionally deleted in cells, including ameloblasts, which express cytokeratin 14.

Previous *in vivo* CaSR studies using germ-line CaSR^{-/-} mice have shown a significant phenotype with the formation of hypoplastic enamel, however the question remained as to whether the phenotype was in large part due to an indirect loss of calcium regulation, making analysis of the conditional CaSR knockout an ideal next step.

In this dissertation, I describe the results of my studies to determine the roles of calcium in directing ameloblast differentiation, and whether the CaSR contributes to calcium mediated enamel organ epithelial cell differentiation.

References:

1. Perez, A.V., et al., *Minireview on regulation of intestinal calcium absorption. Emphasis on molecular mechanisms of transcellular pathway*. *Digestion*, 2008. **77**(1): p. 22-34.
2. Song, Y., et al., *Calcium transporter 1 and epithelial calcium channel messenger ribonucleic acid are differentially regulated by 1,25 dihydroxyvitamin D3 in the intestine and kidney of mice*. *Endocrinology*, 2003. **144**(9): p. 3885-94.
3. Renkema, K.Y., et al., *Calcium and phosphate homeostasis: concerted interplay of new regulators*. *Ann Med*, 2008. **40**(2): p. 82-91.
4. Hoenderop, J.G., B. Nilius, and R.J. Bindels, *Epithelial calcium channels: from identification to function and regulation*. *Pflugers Arch*, 2003. **446**(3): p. 304-8.
5. Hoenderop, J.G., B. Nilius, and R.J. Bindels, *Calcium absorption across epithelia*. *Physiol Rev*, 2005. **85**(1): p. 373-422.
6. de Groot, T., R.J. Bindels, and J.G. Hoenderop, *TRPV5: an ingeniously controlled calcium channel*. *Kidney Int*, 2008. **74**(10): p. 1241-6.
7. Taylor, J.G. and D.A. Bushinsky, *Calcium and phosphorus homeostasis*. *Blood Purif*, 2009. **27**(4): p. 387-94.
8. Brown, E.M., et al., *Cloning and characterization of an extracellular Ca(2+)-sensing receptor from bovine parathyroid*. *Nature*, 1993. **366**(6455): p. 575-80.
9. Brown, E.M. and R.J. MacLeod, *Extracellular calcium sensing and extracellular calcium signaling*. *Physiol Rev*, 2001. **81**(1): p. 239-297.

10. Oda, Y., et al., *The calcium sensing receptor and its alternatively spliced form in keratinocyte differentiation*. J Biol Chem, 1998. **273**(36): p. 23344-52.
11. Yamauchi, M., et al., *Involvement of calcium-sensing receptor in osteoblastic differentiation of mouse MC3T3-E1 cells*. Am J Physiol Endocrinol Metab, 2005. **288**(3): p. E608-16.
12. Midgett, R.J., R. Shaye, and J.F. Fruge, Jr., *The effect of altered bone metabolism on orthodontic tooth movement*. Am J Orthod, 1981. **80**(3): p. 256-62.
13. Seow, W.K., et al., *Dental defects in the deciduous dentition of premature infants with low birth weight and neonatal rickets*. Pediatr Dent, 1984. **6**(2): p. 88-92.
14. Limeback, H., et al., *The effects of hypocalcemia/hypophosphatemia on porcine bone and dental hard tissues in an inherited form of type 1 pseudo-vitamin D deficiency rickets*. J Dent Res, 1992. **71**(2): p. 346-52.
15. Nikiforuk, G. and D. Fraser, *Chemical determinants of enamel hypoplasia in children with disorders of calcium and phosphate homeostasis*. J Dent Res, 1979. **58**(Spec Issue B): p. 1014-5.
16. Lv, H., et al., *PHEX neutralizing agent inhibits dentin formation in mouse tooth germ*. Tissue and Cell, 2011. **43**(2): p. 125-130.
17. Bailleul-Forestier, I., et al., *Immunolocalization of vitamin D receptor and calbindin-D28k in human tooth germ*. Pediatr Res, 1996. **39**(4 Pt 1): p. 636-42.
18. Descroix, V., et al., *Physiopathology of Dental Rickets in Vitamin D Receptor-ablated Mice*. J Dent Res, 2010. **89**(12): p. 1427-1432.

19. Zhang, X., et al., *Normalisation of calcium status reverses the phenotype in dentin, but not in enamel of VDR-deficient mice*. Archives of Oral Biology, 2009. **54**(12): p. 1105-1110.
20. Goepferd, S.J. and C.M. Flaitz, *Enamel hypoplasia associated with congenital hypoparathyroidism*. Pediatr Dent, 1981. **3**(2): p. 196-200.
21. Assif, D., *Dental changes in hypoparathyroidism*. Refuat Hapeh Vehashinayim, 1977. **26**(1): p. 13-9.
22. Calvi, L.M., et al., *Constitutively active PTH/PTHrP receptor in odontoblasts alters odontoblast and ameloblast function and maturation*. Mechanisms of Development, 2004. **121**(4): p. 397-408.
23. Hendy, G.N., et al., *Mutations of the calcium-sensing receptor (CASR) in familial hypocalciuric hypercalcemia, neonatal severe hyperparathyroidism, and autosomal dominant hypocalcemia*. Human Mutation, 2000. **16**(4): p. 281-296.
24. Quarles, L.D., *Extracellular calcium-sensing receptors in the parathyroid gland, kidney, and other tissues*. Current Opinion in Nephrology and Hypertension, 2003. **12**(4): p. 349-355.
25. Watanabe, S., et al., *Association between activating mutations of calcium-sensing receptor and Bartter's syndrome*. The Lancet, 2002. **360**(9334): p. 692-694.
26. Leach, E., W. John, and N. Thalange, *A lifetime of aches, pains, and hypocalcaemia*. Endocrine Abstracts, 2010. **24**(P44).
27. Mathias, R.S., et al., *Identification of the calcium-sensing receptor in the developing tooth organ*. J Bone Miner Res, 2001. **16**(12): p. 2238-44.

28. Moran, R.A., E.M. Brown, and J.W. Bawden, *Immunohistochemical localization of Galphaq, PLCbeta, Galphai1-2, PKA, and the endothelin B and extracellular Ca²⁺-sensing receptors during early amelogenesis*. J Dent Res, 2000. **79**(11): p. 1896-901.
29. Chen, J., et al., *Calcium-mediated differentiation of ameloblast lineage cells in vitro*. J Exp Zool B Mol Dev Evol, 2009. **312B**(5): p. 458-64.
30. Sun, W., et al., *Alterations in phosphorus, calcium and PTHrP contribute to defects in dental and dental alveolar bone formation in calcium-sensing receptor-deficient mice*. Development. **137**(6): p. 985-92.
31. Jernvall, J. and I. Thesleff, *Reiterative signaling and patterning during mammalian tooth morphogenesis*. Mech Dev, 2000. **92**(1): p. 19-29.
32. Thesleff, I., X.P. Wang, and M. Suomalainen, *Regulation of epithelial stem cells in tooth regeneration*. C R Biol, 2007. **330**(6-7): p. 561-4.
33. Vaahtokari, A., et al., *The enamel knot as a signaling center in the developing mouse tooth*. Mech Dev, 1996. **54**(1): p. 39-43.
34. Kratochwil, K., et al., *Lef1 expression is activated by BMP-4 and regulates inductive tissue interactions in tooth and hair development*. Genes Dev, 1996. **10**(11): p. 1382-94.
35. Bei, M. and R. Maas, *FGFs and BMP4 induce both Msx1-independent and Msx1-dependent signaling pathways in early tooth development*. Development, 1998. **125**(21): p. 4325-33.
36. Thesleff, I. and P. Nieminen, *Tooth morphogenesis and cell differentiation*. Curr Opin Cell Biol, 1996. **8**(6): p. 844-50.

37. Thesleff, I., S. Keranen, and J. Jernvall, *Enamel knots as signaling centers linking tooth morphogenesis and odontoblast differentiation*. *Adv Dent Res*, 2001. **15**: p. 14-8.
38. Tompkins, K., *Molecular mechanisms of cytodifferentiation in mammalian tooth development*. *Connect Tissue Res*, 2006. **47**(3): p. 111-8.
39. Fukumoto, S. and Y. Yamada, *Review: extracellular matrix regulates tooth morphogenesis*. *Connect Tissue Res*, 2005. **46**(4-5): p. 220-6.
40. Fukumoto, S., et al., *Ameloblastin is a cell adhesion molecule required for maintaining the differentiation state of ameloblasts*. *J Cell Biol*, 2004. **167**(5): p. 973-83.
41. Fukumoto, S., et al., *Essential roles of ameloblastin in maintaining ameloblast differentiation and enamel formation*. *Cells Tissues Organs*, 2005. **181**(3-4): p. 189-95.
42. Fincham, A.G., J. Moradian-Oldak, and J.P. Simmer, *The structural biology of the developing dental enamel matrix*. *J Struct Biol*, 1999. **126**(3): p. 270-99.
43. Le, T.Q., et al., *The effect of LRAP on enamel organ epithelial cell differentiation*. *J Dent Res*, 2007. **86**(11): p. 1095-9.
44. Xu, L., H. Harada, and A. Taniguchi, *The effects of LAMP1 and LAMP3 on M180 amelogenin uptake, localization and amelogenin mRNA induction by amelogenin protein*. *J Biochem*, 2008. **144**(4): p. 531-7.
45. Fukumoto, S., *Ameloblastin is a cell adhesion molecule required for maintaining the differentiation state of ameloblasts*. *J Cell Bio*, 2004. **167**(5): p. 973-983.

46. Hatakeyama, J., et al., *Synergistic roles of amelogenin and ameloblastin*. J Dent Res, 2009. **88**(4): p. 318-22.
47. Polakis, P., *Wnt signaling and cancer*. Genes Dev, 2000. **14**(15): p. 1837-51.
48. Bei, M., S. Stowell, and R. Maas, *Msx2 controls ameloblast terminal differentiation*. Dev Dyn, 2004. **231**(4): p. 758-65.
49. Kettunen, P. and I. Thesleff, *Expression and function of FGFs-4, -8, and -9 suggest functional redundancy and repetitive use as epithelial signals during tooth morphogenesis*. Dev Dyn, 1998. **211**(3): p. 256-68.
50. Tabata, M.J., et al., *Bone morphogenetic protein 4 is involved in cusp formation in molar tooth germ of mice*. Eur J Oral Sci, 2002. **110**(2): p. 114-20.
51. Yamaguti, P.M., V.E. Arana-Chavez, and A.C. Acevedo, *Changes in amelogenesis in the rat incisor following short-term hypocalcaemia*. Arch Oral Biol, 2005. **50**(2): p. 185-8.
52. Kukita, A., et al., *Primary and secondary culture of rat ameloblasts in serum-free medium*. Calcif Tissue Int, 1992. **51**(5): p. 393-8.
53. Woltgens, J.H., et al., *Biom mineralization during early stages of the developing tooth in vitro with special reference to secretory stage of amelogenesis*. Int J Dev Biol, 1995. **39**(1): p. 203-12.
54. Aoba, T. and E.C. Moreno, *The enamel fluid in the early secretory stage of porcine amelogenesis: chemical composition and saturation with respect to enamel mineral*. Calcif Tissue Int, 1987. **41**(2): p. 86-94.
55. Bawden, J.W., *Calcium transport during mineralization*. Anat Rec, 1989. **224**(2): p. 226-33.

56. Bawden, J.W., et al., *Distribution of protein kinase C alpha and accumulation of extracellular Ca²⁺ during early dentin and enamel formation*. J Dent Res, 1994. **73**(8): p. 1429-36.
57. Brown, E.M., *Extracellular calcium sensing and extracellular calcium signalling*. Physiological Reviews, 2001(81): p. 240-269.
58. Herbert, S., *Molecular cloning and functional expression of human parathyroid calcium sensing receptor*. Jour Bio Chem, 1995(270): p. 12919-12925.
59. Janicic, N., et al., *Mapping of the calcium-sensing receptor gene (CASR) to human chromosome 3q13.3-21 by fluorescence in situ hybridization, and localization to rat chromosome 11 and mouse chromosome 16*. Mamm Genome, 1995. **6**(11): p. 798-801.
60. Garrett, J.E., et al., *Molecular cloning and functional expression of human parathyroid calcium receptor cDNAs*. J Biol Chem, 1995. **270**(21): p. 12919-25.
61. Skelly, B.J. and R.J. Franklin, *Mutations in genes causing human familial isolated hyperparathyroidism do not account for hyperparathyroidism in Keeshond dogs*. Vet J, 2007. **174**(3): p. 652-4.
62. Riccardi, D., et al., *Cloning and functional expression of a rat kidney extracellular calcium/polyvalent cation-sensing receptor*. Proc Natl Acad Sci U S A, 1995. **92**(1): p. 131-5.
63. Butters, R.R., Jr., et al., *Cloning and characterization of a calcium-sensing receptor from the hypercalcemic New Zealand white rabbit reveals unaltered responsiveness to extracellular calcium*. J Bone Miner Res, 1997. **12**(4): p. 568-79.

64. Chikatsu, N., et al., *Cloning and characterization of two promoters for the human calcium-sensing receptor (CaSR) and changes of CaSR expression in parathyroid adenomas*. J Biol Chem, 2000. **275**(11): p. 7553-7.
65. Magno, A.L., B.K. Ward, and T. Ratajczak, *The calcium-sensing receptor: a molecular perspective*. Endocr Rev, 2011. **32**(1): p. 3-30.
66. Bradbury, R.A., et al., *Expression of the parathyroid Ca(2+)-sensing receptor in cytotrophoblasts from human term placenta*. J Endocrinol, 1998. **156**(3): p. 425-30.
67. Bikle, D.D., *Calcium- and vitamin D-regulated keratinocyte differentiation* Molecular Cell Endocrinology, 2001(177): p. 161-171.
68. Oda, Y., *The calcium sensing receptor and its alternatively spliced form in Murine Epidermal differentiation*. J Bio Chem, 2000 (275): p. 1183-1190.
69. Bai, M., et al., *Expression and characterization of inactivating and activating mutations in the human Ca²⁺-sensing receptor*. J Biol Chem, 1996. **271**(32): p. 19537-45.
70. Ray, K., et al., *Identification of the sites of N-linked glycosylation on the human calcium receptor and assessment of their role in cell surface expression and signal transduction*. J Biol Chem, 1998. **273**(51): p. 34558-67.
71. Bai, M., S. Trivedi, and E.M. Brown, *Dimerization of the extracellular calcium-sensing receptor (CaR) on the cell surface of CaR-transfected HEK293 cells*. J Biol Chem, 1998. **273**(36): p. 23605-10.
72. Ray, K., et al., *Identification of the cysteine residues in the amino-terminal extracellular domain of the human Ca(2+) receptor critical for dimerization*.

- Implications for function of monomeric Ca(2+) receptor.* J Biol Chem, 1999. **274**(39): p. 27642-50.
73. Quinn, S.J., M. Bai, and E.M. Brown, *pH Sensing by the calcium-sensing receptor.* J Biol Chem, 2004. **279**(36): p. 37241-9.
74. Huang, Y., et al., *Identification and dissection of Ca(2+)-binding sites in the extracellular domain of Ca(2+)-sensing receptor.* J Biol Chem, 2007. **282**(26): p. 19000-10.
75. Huang, Y., et al., *Multiple Ca(2+)-binding sites in the extracellular domain of the Ca(2+)-sensing receptor corresponding to cooperative Ca(2+) response.* Biochemistry, 2009. **48**(2): p. 388-98.
76. Silve, C., et al., *Delineating a Ca²⁺ binding pocket within the venus flytrap module of the human calcium-sensing receptor.* J Biol Chem, 2005. **280**(45): p. 37917-23.
77. Pace, A.J., L. Gama, and G.E. Breitwieser, *Dimerization of the calcium-sensing receptor occurs within the extracellular domain and is eliminated by Cys --> Ser mutations at Cys101 and Cys236.* J Biol Chem, 1999. **274**(17): p. 11629-34.
78. Zhao, X.M., et al., *A missense mutation in the seventh transmembrane domain constitutively activates the human Ca²⁺ receptor.* FEBS Lett, 1999. **448**(1): p. 180-4.
79. Zhang, Z., et al., *The extracellular calcium-sensing receptor dimerizes through multiple types of intermolecular interactions.* J Biol Chem, 2001. **276**(7): p. 5316-22.

80. Hu, J., et al., *A region in the seven-transmembrane domain of the human Ca²⁺ receptor critical for response to Ca²⁺*. J Biol Chem, 2005. **280**(6): p. 5113-20.
81. Ray, K., et al., *The carboxyl terminus of the human calcium receptor. Requirements for cell-surface expression and signal transduction*. J Biol Chem, 1997. **272**(50): p. 31355-61.
82. Chang, W., et al., *Amino acids in the cytoplasmic C terminus of the parathyroid Ca²⁺-sensing receptor mediate efficient cell-surface expression and phospholipase C activation*. J Biol Chem, 2001. **276**(47): p. 44129-36.
83. Bosel, J., et al., *Signaling of the human calcium-sensing receptor expressed in HEK293-cells is modulated by protein kinases A and C*. Exp Clin Endocrinol Diabetes, 2003. **111**(1): p. 21-6.
84. Bulenger, S., S. Marullo, and M. Bouvier, *Emerging role of homo- and heterodimerization in G-protein-coupled receptor biosynthesis and maturation*. Trends Pharmacol Sci, 2005. **26**(3): p. 131-7.
85. Huang, Y., et al., *Calcium-sensing receptor ubiquitination and degradation mediated by the E3 ubiquitin ligase dorfín*. J Biol Chem, 2006. **281**(17): p. 11610-7.
86. Breitwieser, G.E., S.U. Miedlich, and M. Zhang, *Calcium sensing receptors as integrators of multiple metabolic signals*. Cell Calcium, 2004. **35**(3): p. 209-16.
87. Cavanaugh, A., et al., *Calcium-sensing receptor biosynthesis includes a cotranslational conformational checkpoint and endoplasmic reticulum retention*. J Biol Chem, 2010. **285**(26): p. 19854-64.

88. Morfis, M., A. Christopoulos, and P.M. Sexton, *RAMPs: 5 years on, where to now?* Trends Pharmacol Sci, 2003. **24**(11): p. 596-601.
89. Bouschet, T., S. Martin, and J.M. Henley, *Receptor-activity-modifying proteins are required for forward trafficking of the calcium-sensing receptor to the plasma membrane.* J Cell Sci, 2005. **118**(Pt 20): p. 4709-20.
90. McCudden, C., *G-Protein signalling:back to the future.* Cell and Molecular Life Sciences, 2005. **62**(5): p. 551-577.
91. Parekh, B., *Cracking the calcium entry code.* Nature, 2006(132): p. 153-165.
92. Bhagathula, N., *Upregulation of calcium-sensing receptor and mitogen-activated protein kinase signaling in the regulation of growth and colon carcinoma.* British J Cancer, 2005(93): p. 1364-1371.
93. Bikle, D.D., *Calcium-induced human keratinocyte differentiation requires Src-Fyn-mediated PI3K dependent activation of PLC gamma.* Mol Bio Cell, 2005(16): p. 3236-3246.
94. Rodriguez, L., *Expression and Functional Assessment of an Alternatively Spliced Extracellular Ca sensing Receptor in Growth Plate Chondrocytes.* Endocrinology, 2005. **146**: p. 5294-5303.
95. Reddy, E., *Signalling by dual specificity kinases.* Oncogene, 1998. **17**: p. 1447-1455.
96. Wennerberg, K., *Rho and Rac take center stage.* Cell, 2004. **116**: p. 167-179.
97. Garrett, J.E., *Extracellular calcium receptor.* Curr Opin Cell Bio, 1995(7): p. 474-492.

98. Biz, M.T., et al., *GTPases RhoA and Rac1 are important for amelogenin and DSPP expression during differentiation of ameloblasts and odontoblasts*. Cell Tissue Res, 2010.
99. Zhang, Y., et al., *JNK/c-Jun signaling pathway mediates the fluoride-induced down-regulation of MMP-20 in vitro*. Matrix Biol, 2007. **26**(8): p. 633-41.

***CHAPTER 2-CALCIUM MEDIATED DIFFERENTIATION OF AMELOBLAST
LINEAGE CELLS IN VITRO***

Introduction-

Calcium is vital for mineralized tissues, in both structural and cellular functions. The relationship between calcium and enamel formation is clearly evident in patients suffering from compromised calcium homeostasis, particularly hypocalcemia. Whether the result of kidney failure, endocrine system malfunction, or even poor dietary intake, the ultimate result of hypocalcemia on enamel formation is seen as varying degrees of hypoplasia and hypomineralization. In an effort to better understand the effects of calcium on ameloblasts, I initiated studies of the effects of elevated calcium levels on ameloblast lineage cells. These studies lead to the following manuscript, which was published in *J Exp Zool*, 2009, where we describe the response of primary human ameloblast lineage cells to increased extracellular calcium. This is the first report of the effects of calcium on primary human ameloblast lineage cells.

These studies lead to me to additional questions including: 1) whether increasing calcium specifically upregulates the amelogenin gene; 2) what other genes does calcium upregulate in ameloblast lineage cells; 3) whether these effects can be identified in a pure ameloblast lineage cell which can be selected only by prolonging cell growth with SV40 transfection; 4) is the CaSR receptor a possible candidate for mediating calcium related cell changes. These questions were addressed by a series of additional studies that we have included as appendices 1-4 to this chapter, described as follows.

Appendix 1-We examined and confirmed that extracellular calcium regulates amelogenin expression specifically at the amelogenin promoter.

Appendix 2-We examined through microarray analysis, what other genes are regulated by extracellular calcium.

Appendix 3-We established and characterized a homogenous growth enhanced human ameloblast lineage cell line to address the question whether calcium specifically regulates ameloblast differentiation or whether this may be mediated through calcium effects on other cell types in the primary culture system.

Appendix 4-We examined the levels of CaSR expression in our human ameloblast lineage cells, and identified the cellular localization pattern of CaSR during human fetal tooth development.

**JOHN WILEY AND SONS LICENSE
TERMS AND CONDITIONS**

Feb 01, 2011

This is a License Agreement between James J Chen ("You") and John Wiley and Sons ("John Wiley and Sons") provided by Copyright Clearance Center ("CCC"). The license consists of your order details, the terms and conditions provided by John Wiley and Sons, and the payment terms and conditions.

All payments must be made in full to CCC. For payment instructions, please see information listed at the bottom of this form.

License Number	2600030120493
License date	Feb 01, 2011
Licensed content publisher	John Wiley and Sons
Licensed content publication	Journal of Experimental Zoology Part A: Ecological Genetics and Physiology
Licensed content title	Calcium-mediated differentiation of ameloblast lineage cells in vitro
Licensed content author	James Chen, Yan Zhang, Joseph Mendoza, Pamela DenBesten
Licensed content date	Jul 15, 2009
Start page	458
End page	464
Type of use	Dissertation/Thesis
Requestor type	Author of this Wiley article
Format	Print and electronic
Portion	Full article
Will you be translating?	No
Order reference number	
Total	0.00 USD

[Terms and Conditions](#)

TERMS AND CONDITIONS

This copyrighted material is owned by or exclusively licensed to John Wiley & Sons, Inc. or one of its group companies (each a "Wiley Company") or a society for whom a Wiley Company has exclusive publishing rights in relation to a particular journal (collectively "WILEY"). By clicking "accept" in connection with completing this licensing transaction, you agree that the following terms and conditions apply to this transaction (along with the billing and payment terms and conditions established by the Copyright Clearance Center Inc., ("CCC's Billing and Payment terms and conditions"), at the time that you opened your Rightslink account (these are available at any time at <http://myaccount.copyright.com>)

Terms and Conditions

1. The materials you have requested permission to reproduce (the "Materials") are protected by

copyright.

2. You are hereby granted a personal, non-exclusive, non-sublicensable, non-transferable, worldwide, limited license to reproduce the Materials for the purpose specified in the licensing process. This license is for a one-time use only with a maximum distribution equal to the number that you identified in the licensing process. Any form of republication granted by this licence must be completed within two years of the date of the grant of this licence (although copies prepared before may be distributed thereafter). The Materials shall not be used in any other manner or for any other purpose. Permission is granted subject to an appropriate acknowledgement given to the author, title of the material/book/journal and the publisher and on the understanding that nowhere in the text is a previously published source acknowledged for all or part of this Material. Any third party material is expressly excluded from this permission.

3. With respect to the Materials, all rights are reserved. Except as expressly granted by the terms of the license, no part of the Materials may be copied, modified, adapted (except for minor reformatting required by the new Publication), translated, reproduced, transferred or distributed, in any form or by any means, and no derivative works may be made based on the Materials without the prior permission of the respective copyright owner. You may not alter, remove or suppress in any manner any copyright, trademark or other notices displayed by the Materials. You may not license, rent, sell, loan, lease, pledge, offer as security, transfer or assign the Materials, or any of the rights granted to you hereunder to any other person.

4. The Materials and all of the intellectual property rights therein shall at all times remain the exclusive property of John Wiley & Sons Inc or one of its related companies (WILEY) or their respective licensors, and your interest therein is only that of having possession of and the right to reproduce the Materials pursuant to Section 2 herein during the continuance of this Agreement. You agree that you own no right, title or interest in or to the Materials or any of the intellectual property rights therein. You shall have no rights hereunder other than the license as provided for above in Section 2. No right, license or interest to any trademark, trade name, service mark or other branding ("Marks") of WILEY or its licensors is granted hereunder, and you agree that you shall not assert any such right, license or interest with respect thereto.

5. NEITHER WILEY NOR ITS LICENSORS MAKES ANY WARRANTY OR REPRESENTATION OF ANY KIND TO YOU OR ANY THIRD PARTY, EXPRESS, IMPLIED OR STATUTORY, WITH RESPECT TO THE MATERIALS OR THE ACCURACY OF ANY INFORMATION CONTAINED IN THE MATERIALS, INCLUDING, WITHOUT LIMITATION, ANY IMPLIED WARRANTY OF MERCHANTABILITY, ACCURACY, SATISFACTORY QUALITY, FITNESS FOR A PARTICULAR PURPOSE, USABILITY, INTEGRATION OR NON-INFRINGEMENT AND ALL SUCH WARRANTIES ARE HEREBY EXCLUDED BY WILEY AND ITS LICENSORS AND WAIVED BY YOU.

6. WILEY shall have the right to terminate this Agreement immediately upon breach of this Agreement by you.

7. You shall indemnify, defend and hold harmless WILEY, its Licensors and their respective directors, officers, agents and employees, from and against any actual or threatened claims, demands, causes of action or proceedings arising from any breach of this Agreement by you.

8. IN NO EVENT SHALL WILEY OR ITS LICENSORS BE LIABLE TO YOU OR ANY OTHER PARTY OR ANY OTHER PERSON OR ENTITY FOR ANY SPECIAL, CONSEQUENTIAL, INCIDENTAL, INDIRECT, EXEMPLARY OR PUNITIVE DAMAGES, HOWEVER CAUSED, ARISING OUT OF OR IN CONNECTION WITH THE DOWNLOADING, PROVISIONING, VIEWING OR USE OF THE MATERIALS REGARDLESS OF THE FORM OF ACTION, WHETHER FOR BREACH OF CONTRACT, BREACH OF WARRANTY, TORT, NEGLIGENCE, INFRINGEMENT OR OTHERWISE (INCLUDING, WITHOUT LIMITATION, DAMAGES BASED ON LOSS OF PROFITS, DATA, FILES, USE, BUSINESS OPPORTUNITY OR CLAIMS OF THIRD PARTIES), AND WHETHER OR NOT THE PARTY HAS BEEN ADVISED OF THE POSSIBILITY OF SUCH DAMAGES. THIS LIMITATION SHALL APPLY NOTWITHSTANDING ANY FAILURE OF ESSENTIAL PURPOSE OF ANY LIMITED REMEDY PROVIDED HEREIN.

or money order referencing your account number and this invoice number
RLNK10923401.

Once you receive your invoice for this order, you may pay your invoice by credit card.
Please follow instructions provided at that time.

Make Payment To:
Copyright Clearance Center
Dept 001
P.O. Box 843006
Boston, MA 02284-3006

If you find copyrighted material related to this license will not be used and wish to
cancel, please contact us referencing this license number 2600030120493 and noting
the reason for cancellation.

Questions? customercare@copyright.com or +1-877-622-5543 (toll free in the US) or
+1-978-646-2777.

The following manuscript was published in Journal of Experimental Zoology (Part 1, Molecular, Evolution, Development) 15;312B(5):458-464

**CALCIUM MEDIATED DIFFERENTIATION OF AMELOBLAST
LINEAGE CELLS *IN VITRO***

James Chen¹, Yan Zhang, Joseph Mendoza¹ and Pamela DenBesten¹

Department of Orofacial Sciences, University of California, San Francisco, CA, USA

Running title: Calcium mediated ameloblast differentiation

Key words: ameloblast, calcium, differentiation, enamel

Abstract:

Calcium is a key component of the mineralized enamel matrix, but may also have a role in ameloblast cell differentiation. In this study we used human ameloblast lineage cells to determine the effect of calcium on cell function. **Methods:** Primary human ameloblast lineage cells were isolated from human fetal tooth buds. Cells were treated with calcium ranging 0.05 to 1.8mM. Cell morphology was imaged by phase contrast microscopy, and amelogenin was immunolocalized. Proliferation of cells treated with calcium was measured by BrdU immunoassay. The effect of calcium on mRNA expression of amelogenin, Type 1 collagen, DSPP, amelotin and KLK-4 were compared by PCR analysis. Von Kossa staining was used to detect mineral formation after cells were pretreated with calcium. **Results:** Calcium induced cell organization and clustering at 0.1 and 0.3mM concentrations. Increasing concentrations of calcium significantly reduced ameloblast lineage cell proliferation. The addition of 0.1mM calcium to cultures

upregulated expression of amelogenin, Type I collagen, and amelotin. After pretreatment with 0.3mM calcium, the cells could form a mineralized matrix. **Conclusions:** These studies, which utilized human ameloblast lineage cells grown *in vitro*, showed that the addition of calcium at 0.1 and 0.3mM, induced cell differentiation and upregulation of amelogenin Type I collagen and amelotin.

Introduction:

Tooth enamel formation is initiated by differentiation of the ectodermally derived dental lamina. Epithelial cells from dental lamina then differentiate into inner enamel epithelial cells, pre-secretory, secretory, and transitional and then finally mature ameloblasts (Fig 1) (Matthiessen and Romert, 1980, Paine *et al.*, 2001, Simmer and Fincham, 1995).

Ameloblasts are highly specialized mineralizing epithelial cells, which regulate the production, resorption, ion transport and degradation of the protein enamel matrix (Fincham *et al.*, 1999, Paine *et al.*, 2001).

Enamel formation requires the deposition of free calcium and other ions into the developing proteinaceous enamel extracellular matrix. Calcium imbalance in humans can be associated with enamel hypoplasia, as seen in Enamel-renal syndrome (Fu *et al.*, 2006).

In rats that cannot absorb calcium due to a vitamin D deficiency, total enamel thickness and intraprismatic enamel were reduced compared to controls (Papagerakis *et al.*, 1999).

Further support that calcium homeostasis is critical for enamel formation can be seen when thyro-parathyroidectomized rats presented with enamel defects in the late and maturation stages (Yamaguti *et al.*, 2005).

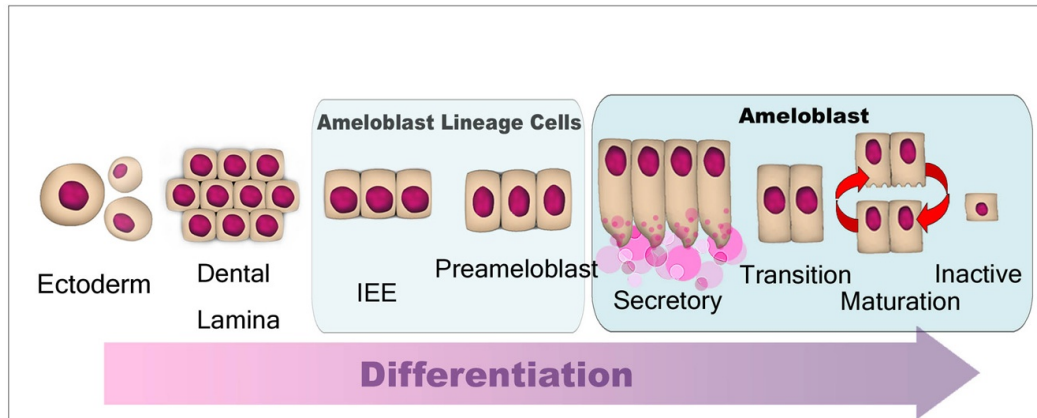


Figure 1. This is a diagram showing stages of ameloblast differentiation. Ameloblast terminal differentiation begins when inner enamel epithelial cells (IEE) differentiate into pre-secretory ameloblasts (PA). From the pre-secretory stage, ameloblasts continue to differentiate until they reach the maturation stage. Cells grown *in vitro* represent early stages of ameloblast differentiation.

In addition to its role as a vital component of mineralizing tissues, Ca^+ can regulate cellular functions in multiple cell types (Brown and MacLeod, 2001). At the molecular level, variations in extracellular calcium concentrations promote differentiation of epithelial derived cells, specifically keratinocytes (Oda *et al.*, 1998). Keratinocytes treated with calcium concentrations greater than 0.1mM alter their pattern of gene expression and differentiation (Oda *et al.*, 1998). In the environment directly surrounding immature enamel, calcium levels are higher than 0.1mM, the threshold necessary for keratinocyte differentiation (0.4mM-0.6mM) (Aoba and Moreno, 1987). However, this represents the average calcium concentration in the enamel fluid, and

calcium levels could be higher or lower in various microenvironments present at different stages of enamel maturation. Intracellular calcium regulation may be linked to expression of intracellular calcium binding proteins such as calbindin D 9kDa and calbindin D 28kDa (Berdal *et al.*, 1991, Sasaki and Garant, 1987), and the calcium sensing receptor (CaSR). These calcium binding proteins, as well as CaATPase have been implicated in intracellular calcium regulation (Bawden, 1989, Berdal *et al.*, 1991).

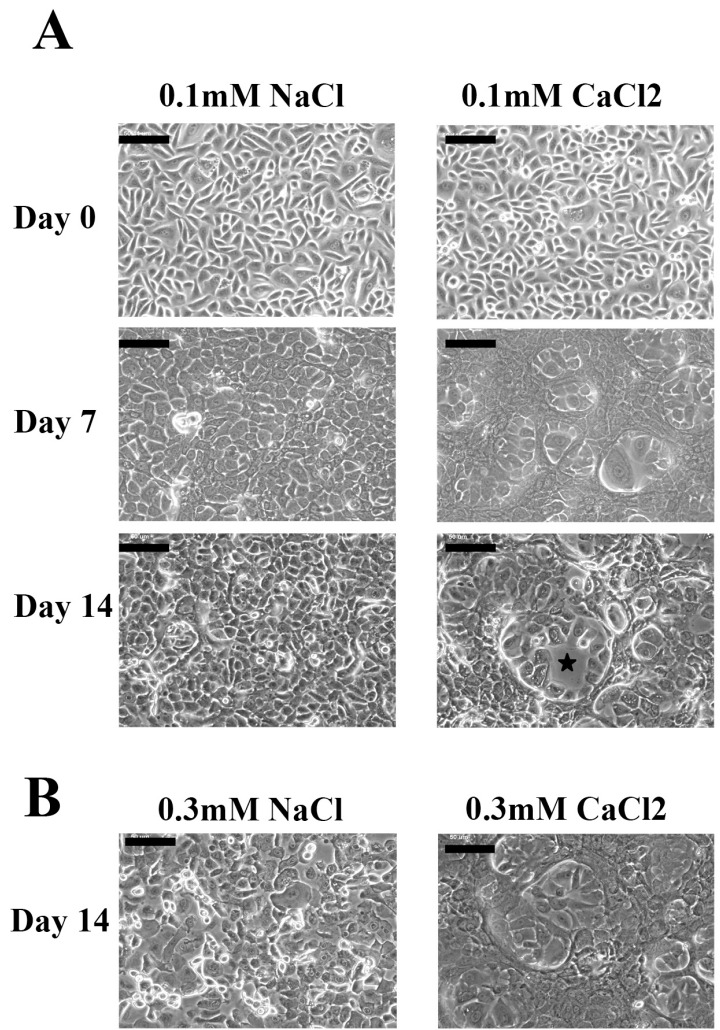
Currently, it is not well understood what role extracellular calcium variations play in enamel formation and ameloblast function. Enamel organ epithelial cells grown in culture respond to extracellular calcium with a spike in intracellular calcium (Mathias *et al.*, 2001), similar to keratinocytes (Bikle *et al.*, 1996). This suggests that, similar to keratinocytes, calcium may regulate differentiation and/or gene expression in ameloblasts. Woltgens and co-workers showed that in hamster molar organ culture, calcium is required for ameloblast differentiation (Woltgens *et al.*, 1995).

Studies of the specific role of calcium in ameloblast differentiation have been limited by the lack of a cell culture system. In these studies we used a human ameloblast lineage cell culture system to determine the effects of extracellular calcium on human ameloblast lineage cells *in vitro*.

Results:

Morphological changes in response to elevated calcium:

Primary ameloblast lineage cells treated with calcium showed a pronounced difference in cell morphology compared to control samples. The initial cell morphology was similar among all groups (Fig 2a). Cells in the calcium treated groups began to organize and arrange in specific cell clusters by day 7. By day 14, control cells began to lose cellular contact while the calcium treated cells maintained their cellular connections. Roughly 20-30% of the cells treated with calcium showed an organization of orderly columnar cells surrounding what appears to be a lumen (Fig 2a). These structures were present in



all triplicate samples at both calcium concentrations (Fig 2a, 2b) and were present throughout the plate.

Figure 2. Ameloblast lineage cell morphology in the presence of calcium show: A) Cells cultured in KGM-2 media at day 0 have a cobblestone appearance. When the calcium concentration in the

media is increased to 0.1mM CaCl₂, cells begin to organize after 7 days of culture. After 14 days calcium treated cells showed lumen (star) formation and columnar shaped cells. Control cells grown in the same concentration of NaCl, maintained their initial cobblestone shape morphology. B) This same cell organization also occurs at higher (0.3mM CaCl₂). Bar = 100 μm

Ameloblast proliferation:

Ameloblast lineage cell proliferation significantly decreased in the presence of 0.3mM and 1.8mM calcium as compared to controls (p<0.05 by ANVOA followed by Bonferroni post-test) (Fig 3). The proliferation rate of cells grown in calcium free media also decreased as compared to the 0.05mM calcium treated cells, confirming that a

minimum amount of calcium is needed for ameloblast lineage cells growth *in vitro*.

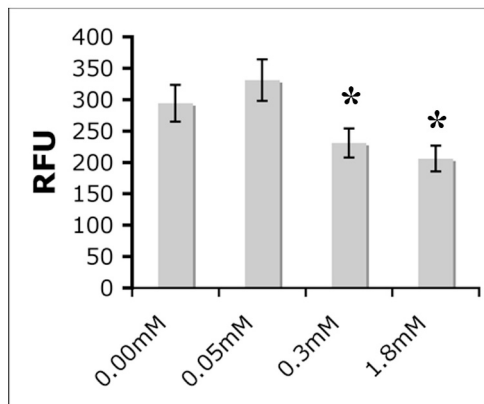


Figure 3. BrdU immunoassay showed a significant decrease in ameloblast lineage cell proliferation at 0.3mM and 1.8mM calcium. RFU = relative fluorescent unit. (ANOVA p<0.05 and multiple t-test

p<0.05)

Calcium induced Von Kossa positive foci:

Von Kossa positive foci were present in ameloblasts lineage cells that were first cultured in 0.3mM CaCl₂, followed by mineralization buffer (containing 3.0mM calcium).

Mineralized foci were not present in samples that were pre-treated with lower levels of calcium prior to incubation in mineralizing buffer (Fig 4), or in NaCl treated controls.

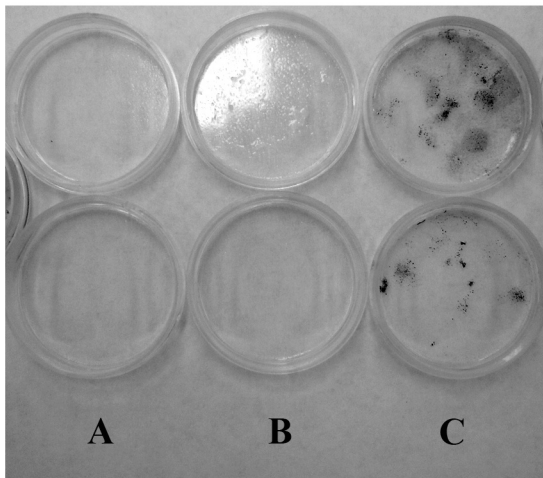


Figure 4. Von Kossa staining of ameloblast lineage cells grown in A) 0.00, B) 0.05, or C)

0.3mM calcium prior to addition of 3.0mM calcium for mineral induction. Mineral

formed when cells were pretreated with

0.3mM calcium. This suggests that calcium-induced cell differentiation is required for

mineral induction (all samples were completed

in duplicate, shown in the parallel upper and lower plates).

Calcium regulated gene expression:

RT-PCR analysis of control and calcium treated cells showed an increase in amelogenin expression when treated with calcium; concurrently, there was no detectable change in

GAPDH levels (Fig 5a). RT-PCR results were confirmed by immunofluorescent staining with antibodies specific for amelogenin, which showed intense cytoplasmic amelogenin

immunostaining in 0.1mM calcium treated as compared to control cells grown in

0.05mM calcium (Fig 5b). qPCR analysis showed that calcium induced a two-fold

increase in expression of both Type I collagen and amelotin. KLK4 and DSPP mRNA were detected by qPCR, though there were no detectable differences between control and treatment groups (Table 1). qPCR showed upregulation of amelogenin, though the lack of amelogenin expression at 0.05 mM calcium prevented a calculation of the fold increase in amelogenin upregulation by 0.1 mM calcium.

Table 1. *Markers of ameloblast differentiation*

Gene Name	0.1 mM Ca	Fold increase at 0.1mM Ca
Collagen I	+++	2.14*
DSPP	+	0
Amelotin	++	2.10*
Amelogenin	++	N/A
KLK4	++	0

+ the initial relative level of expression*P<0.02 (t-test)

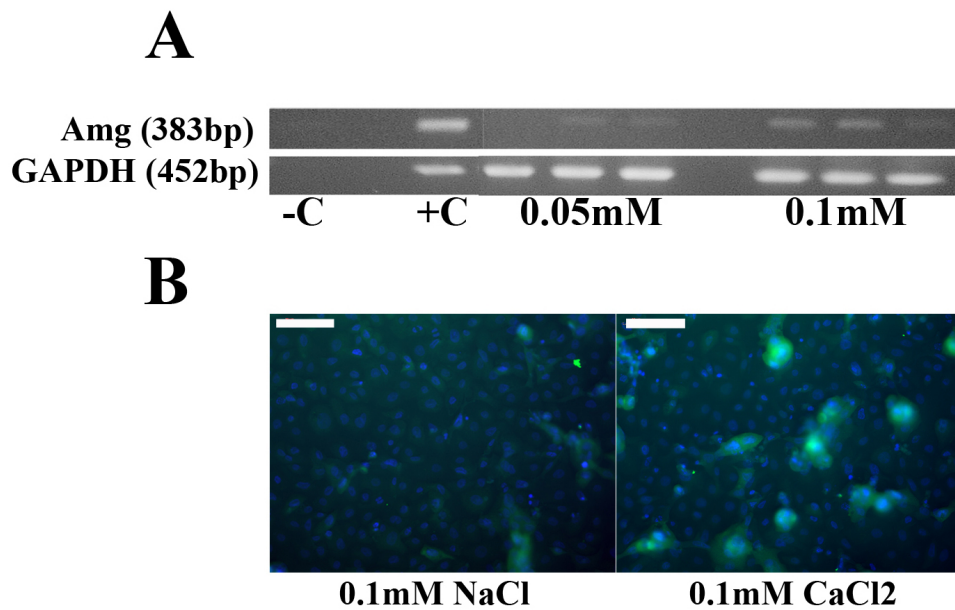


Figure 5. A) RT-PCR for amelogenin mRNA shows positive amelogenin expression in cells grown in media containing 0.05mM calcium, with more obvious expression at 0.1mM calcium (14 days in culture). Negative control (C-) is without DNA and positive control (C+) is amplified from a human fetal tooth bud cDNA library. B) Day 14 immunofluorescent staining for amelogenin shows positive immunostaining at 0.1mM calcium compared to very low levels of amelogenin expression in the control 0.1mM NaCl sample. (Blue-nuclear stain, Green-amelogenin). Bar=100 μ m

Discussion:

The role of calcium in tooth formation and in particular enamel development is not well understood. Most studies of calcium and ameloblasts have focused calcium transport into the mineralizing enamel matrix (Hubbard, 2000). Previously published tooth organ culture studies suggest that calcium has a role in early ameloblast differentiation (Woltgens *et al.*, 1995). Lyaruu *et al* used potassium pyrontimonate-osmium tetroxide

(PA) cytochemistry in developing hamster molar tooth germs, to show the presence of ionized calcium in various cellular regions of differentiating pre-secretory ameloblasts (Lyaruu *et al.*, 1985). After initiation of dentin mineralization calcium was localized on the plasma membrane and mitochondria of pre-secretory ameloblasts (Lyaruu *et al.*, 1985). Woltgens *et al* showed that low calcium concentrations in the medium of the hamster tooth germs grown in culture prevented initial dentin mineralization and enamel formation (Woltgens *et al.*, 1995).

We used human ameloblast lineage cells, derived from bell stage human tooth germs, and have identified these cells as derived from enamel organ epithelia, as including inner enamel epithelial cells or early and late pre-secretory cells (Fig 1) (DenBesten *et al.*, 2005, Le *et al.*, 2007, Zhang *et al.*, 2007, Zhang *et al.*, 2006). We used these cells to determine whether calcium has a role in ameloblast lineage cell differentiation.

We found that the rate of proliferation of primary ameloblast lineage cells was decreased as calcium concentrations increased. When calcium was increased from 0.05mM to either 0.1mM or 0.3mM, the cells organized, with changes in cell morphology. When the cells were grown in the presence of calcium for 14 days, the cells appeared to form columnar shapes surrounding a lumen. Further studies, including localization of cell adhesion molecules, will determine whether the calcium treated cells are polarized.

The morphology and mRNA expression in cells grown in 0.1mM calcium were similar to those grown in 0.3mM calcium. These levels of calcium were lower than the lowest levels used by Woltgens *et al* (Woltgens *et al.*, 1995). In the Woltgens study, neither enamel nor dentin formed at 0.9mM calcium, suggesting that higher calcium levels than the ones used in our study are required for tooth tissue mineralization. It may be that

lower levels of calcium will promote early ameloblast lineage cell differentiation, whereas higher calcium levels are required for matrix mineralization.

The effects of calcium on enamel matrix protein expression, showed specific rather than general effects. Amelogenin expression was upregulated by calcium at both the mRNA and protein levels. These results are consistent with those Bronckers *et al.*, who showed that calcium can, to some extent, rescue amelogenin expression in fluoride treated tooth organs, and calcium alone can increase amelogenin expression in organ culture (Bronckers *et al.*, 2006). Further studies are required to determine whether calcium acts directly on the amelogenin promoter, or indirectly to enhance amelogenin expression through other signaling pathways. Previous studies have shown that CaSR is expressed in both murine and porcine ameloblasts (Mathias *et al.*, 2001, Moran *et al.*, 2000). In our study we confirmed CaSR expression in our human ameloblast lineage cells (data not shown). The role of the CaSR in mediating amelogenin expression in ameloblasts remains to be determined.

Increased calcium also upregulated Type I collagen and amelotin expression in ameloblast lineage cells. Type I collagen has not generally been associated with genes normally expressed by ameloblasts during any stage of differentiation, and may suggest a heterogeneous cell population including some dental mesenchyme. However, we have routinely detected Type I collagen expression in our ameloblast lineage cells, and in developing primary human tooth matrix (data not shown), and may be a marker of early stage enamel organ epithelial cells. Further studies are in progress to determine the role of Type I collagen in enamel formation.

Amelotin is a relatively new matrix protein shown to be highly expressed during later stages of ameloblast differentiation in the mouse (Iwasaki *et al.*, 2005). We find amelotin in our ameloblast lineage cells, and suggest that amelotin is expressed at lower levels at early stages of enamel formation in humans.

There was no effect of calcium on KLK-4 and DSPP expression. Although, KLK-4 is shown to be upregulated later in enamel formation, at the maturation stage (Simmer and Hu, 2002) we have also shown that KLK-4 to be present in human ameloblast lineage cells (Yan *et al.*, 2006). DSPP expression can be detected in pre-secretory ameloblasts (Begue-Kirn *et al.*, 1998). The lack of an effect of calcium on DSPP and KLK-4 expression suggests a specific effect of calcium on regulation of amelogenin, Type I collagen, and amelotin, rather than simply a nonspecific effect on cell differentiation. It is plausible that regulatory elements for amelogenin, Type I collagen, and amelotin respond specifically to calcium, whereas DSPP and KLK-4 regulatory elements do not. However, the exact mechanism of such a response will need to be elucidated.

The addition of 3.0mM calcium into the mineralization buffer resulted in the formation of Von Kossa positive nodules. Von Kossa positive nodules were more evident when ameloblast lineage cells were pre-treated with calcium. These results further indicate that calcium alters expression of enamel matrix proteins, possibly related to mineral formation. These studies have utilized human ameloblast lineage cells, grown *in vitro* to investigate the role of calcium in ameloblast differentiation. Calcium promoted changes in cell morphology, decreased cell proliferation, and upregulated matrix proteins, including amelogenin, Type I collagen and amelotin. The specific signaling pathways used by calcium to regulate enamel formation remain to be identified.

Methods:*Materials:*

Rabbit anti-human amelogenin was made against recombinant full-length recombinant human amelogenin synthesized in our laboratory. Polyclonal antibodies against the CaSR were purchased from Santa Cruz Biotech (Santa Cruz, CA). Secondary antibodies were purchased from Sigma (St. Louis, MO) and Hoechst counterstain was purchased from Invitrogen (Carlsbad, CA). Primers specific for amelogenin were purchased from Elim Bio (Hayward, CA) (forward primer- GGCTGCACCACCAAATCATCC and reverse primer- CCCGCTTGGTCTTGTCTGTCG). Primers specific for GAPDH were also purchased from Elim Bio (forward primer- ACCACAGTCCATGCCATCAC and reverse primer- TCCACCACCCTGTTGCTGTA). All qPCR primers/probes were purchased from Applied Biosystems (Foster City, CA). Primers/probers are proprietary to Applied Biosystems, and therefore sequences are not available. Taqman master mixes for qPCR were purchased from Roche Applied Sciences (Indianapolis, IN). KGM-2 media was purchased from Lonza (Walkersville, MD).

Cell isolation and cell culture:

Primary ameloblast lineage cells were isolated from 18-23 week old fetal tooth buds, with permission obtained through the tissue-sharing program at UCSF, as previously described DenBesten *et al* in 2005 (DenBesten *et al.*, 2005, Le *et al.*, 2007, Yan *et al.*, 2006, Zhang *et al.*, 2007, Zhang *et al.*, 2006). Briefly, the tissue mass from these tooth buds was dispersed by the addition of 1 mg/ml collagenase/dispase mixture dissolved in PBS at 37°C for 2 hr. The tissue mass was further digested with 0.05% trypsin with EDTA for 5

min at 37°C. Ameloblast lineage cells were specifically selected for by keratinocyte selective media, KGM-2 w/o serum and supplemented with 0.05mM calcium (Fig 1). Passage one primary ameloblast lineage cells were plated on 10mm dishes and cultured in KGM-2 media. When cultures reached 70-80% confluence either CaCl₂ or NaCl was added to the culture media (0.05, 0.1mM, 0.3mM). Cells were cultured for 14 days and compared by phase contrast microscopy (Nikon TMS), immunofluorescent staining, and gene expression by PCR.

Ameloblast lineage cell proliferation assay:

Passage one primary ameloblast lineage cells were plated at 3X10⁵ cells/well in a 96 well plate. They were then cultured for 24hrs in KGM-2 and synchronized for 8 hrs using KBM/HBSS (no growth factors and no calcium). After synchronization the cells were treated with KGM-2 media plus calcium (0.00mM, 0.05mM, 0.3mM, and 1.8mM) for 8 hrs, during which, BrdU was added to the media (Roche Proliferation Assay Kit). BrdU incorporation was detected and analyzed by SpectraMax Gemini XS (Molecular Devices) and SoftMax Pro respectively.

Von Kossa staining:

Passage one primary human ameloblast lineage cells were grown in KGM-2 to a density of around 70-80%. Calcium, at a final concentration of 0.1mM and 0.3mM, was then added to the medium for 2 weeks to induce cell differentiation. Medium containing 0.1mM and 0.3 mM NaCl were used as control. The media was then changed to induce mineralization, and the cells were cultured for an additional 2 weeks, with media at 3.0mM calcium concentrations containing 10.0mM b-glycerolphosphate, and 50 mg/ml

L-ascorbic acid as optimized for other mineral assays (Maniatopoulos *et al.*, 1988). The cells were then stained by Von Kossa to detect mineral formation

RNA isolation and gene expression assays:

Total RNA was isolated from primary ameloblast cell cultures (control and 0.1mM calcium). Media was removed and plates were washed with PBS. Cells were scrapped from the plates following incubation in 0.05% trypsin for 5 min at 37°C, and total RNA was isolated using Qiagen's RNeasy Kit. Purified RNA was quantified by UV spectroscopy on a Nanodrop (Thermo Fisher Scientific, Waltham, MA) and equal amounts of RNA from control and test samples were converted to cDNA by Superscript III kit (Invitrogen). Aliquots of the resulting cDNA were used for gene expression assays. Expression of amelogenin and GAPDH were detected by PCR with gene specific primers. Conditions for PCR were: annealing temperature 56°C (1min) and extension temperature 72°C (1min), this was repeated for 30 cycles. Type I Collagen, Amelotin, DSPP, KLK4 expression were detected on a 7500 Real Time PCR machine from Applied Biosystems. Conditions for qPCR were as follows: 94°C (15sec), 60°C (1min), and 40 cycles.

Immunofluorescent staining:

Primary ameloblast lineage cells were washed three times with PBS and fixed with 4% PFA overnight. All samples were incubated with 5% BSA in PBS/0.1% Triton X-100 for 1 hr at room temperature to block non-specific binding. Samples were then incubated with primary antibodies against amelogenin (1mg/ml) and CaSR (4mg/ml) overnight at 4° C. Control cells were incubated with purified rabbit IgG. Cells were then washed three times with PBS and incubated with secondary antibodies (Goat Anti-rabbit FITC conjugated 1:40) for 1 hr at RT. Cells were washed three more times with PBS and

counterstained with Hoechst 1:10,000. Cells were then washed three times with PBS and mounted with permamount (Fisher). All samples were visualized by light microscopy under epifluorescence on a Nikon E800 system.

Acknowledgements: This grant was supported by funding from the National Institutes of Health Grant # R21DE13508 to PDB and a T32-DE07306 training grant. The authors gratefully acknowledge Dr. Bernhard Ganss for his helpful discussions on amelotin in enamel formation.

References

- AOBA, T. and MORENO, E.C. (1987). The enamel fluid in the early secretory stage of porcine amelogenesis: chemical composition and saturation with respect to enamel mineral. *Calcif Tissue Int* 41: 86-94.
- BAWDEN, J.W. (1989). Calcium transport during mineralization. *Anat Rec* 224: 226-33.
- BEGUE-KIRN, C., KREBSBACH, P.H., BARTLETT, J.D. and BUTLER, W.T. (1998). Dentin sialoprotein, dentin phosphoprotein, enamelysin and ameloblastin: tooth-specific molecules that are distinctively expressed during murine dental differentiation. *Eur J Oral Sci* 106: 963-70.
- BERDAL, A., NANJI, A., SMITH, C.E., AHLUWALIA, J.P., THOMASSET, M., CUISINIER-GLEIZES, P. and MATHIEU, H. (1991). Differential expression of calbindin-D 28 kDa in rat incisor ameloblasts throughout enamel development. *Anat Rec* 230: 149-63.

- BIKLE, D.D., RATNAM, A., MAURO, T., HARRIS, J. and PILLAI, S. (1996). Changes in calcium responsiveness and handling during keratinocyte differentiation. Potential role of the calcium receptor. *J Clin Invest* 97: 1085-93.
- BRONCKERS, A.L., BERVOETS, T.J., WOLTGENS, J.H. and LYARUU, D.M. (2006). Effect of calcium, given before or after a fluoride insult, on hamster secretory amelogenesis in vitro. *Eur J Oral Sci* 114 Suppl 1: 116-22; discussion 127-9, 380.
- BROWN, E.M. and MACLEOD, R.J. (2001). Extracellular calcium sensing and extracellular calcium signaling. *Physiol Rev* 81: 239-297.
- DENBESTEN, P.K., MACHULE, D., ZHANG, Y., YAN, Q. and LI, W. (2005). Characterization of human primary enamel organ epithelial cells in vitro. *Arch Oral Biol* 50: 689-94.
- FINCHAM, A.G., MORADIAN-OLDAK, J. and SIMMER, J.P. (1999). The structural biology of the developing dental enamel matrix. *J Struct Biol* 126: 270-99.
- FU, X.J., NOZU, K., GOJI, K., IKEDA, K., KAMIOKA, I., FUJITA, T., KAITO, H., NISHIO, H., IIJIMA, K. and MATSUO, M. (2006). Enamel-renal syndrome associated with hypokalaemic metabolic alkalosis and impaired renal concentration: a novel syndrome? *Nephrol Dial Transplant* 21: 2959-62.
- HUBBARD, M.J. (2000). Calcium transport across the dental enamel epithelium. *Crit Rev Oral Biol Med* 11: 437-66.
- IWASAKI, K., BAJENOVA, E., SOMOGYI-GANSS, E., MILLER, M., NGUYEN, V., NOURKEYHANI, H., GAO, Y., WENDEL, M. and GANSS, B. (2005). Amelotin--a Novel Secreted, Ameloblast-specific Protein. *J Dent Res* 84: 1127-32.

LE, T.Q., ZHANG, Y., LI, W. and DENBESTEN, P.K. (2007). The effect of LRAP on enamel organ epithelial cell differentiation. *J Dent Res* 86: 1095-9.

LYARUU, D.M., BRONCKERS, A.L., BURGER, E.H. and WOLTGENS, J.H. (1985). Localization of calcium in differentiating odontoblasts and ameloblasts before and during early dentinogenesis and amelogenesis in hamster tooth germs. *J Histochem Cytochem* 33: 595-603.

MANIATOPOULOS, C., SODEK, J. and MELCHER, A.H. (1988). Bone formation in vitro by stromal cells obtained from bone marrow of young adult rats. *Cell Tissue Res* 254: 317-30.

MATHIAS, R.S., MATHEWS, C.H., MACHULE, C., GAO, D., LI, W. and DENBESTEN, P.K. (2001). Identification of the calcium-sensing receptor in the developing tooth organ. *J Bone Miner Res* 16: 2238-44.

MATTHIESSEN, M.E. and ROMERT, P. (1980). Ultrastructure of the human enamel organ. II. Internal enamel epithelium, preameloblasts, and secretory ameloblasts. *Cell Tissue Res* 205: 371-82.

MORAN, R.A., BROWN, E.M. and BAWDEN, J.W. (2000). Immunohistochemical localization of Galphaq, PLCbeta, Galphai1-2, PKA, and the endothelin B and extracellular Ca²⁺-sensing receptors during early amelogenesis. *J Dent Res* 79: 1896-901.

ODA, Y., TU, C.L., PILLAI, S. and BIKLE, D.D. (1998). The calcium sensing receptor and its alternatively spliced form in keratinocyte differentiation. *J Biol Chem* 273: 23344-52.

PAINE, M.L., WHITE, S.N., LUO, W., FONG, H., SARIKAYA, M. and SNEAD, M.L. (2001). Regulated gene expression dictates enamel structure and tooth function. *Matrix Biol* 20: 273-92.

PAPAGERAKIS, P., HOTTON, D., LEZOT, F., BROOKES, S., BONASS, W., ROBINSON, C., FOREST, N. and BERDAL, A. (1999). Evidence for regulation of amelogenin gene expression by 1,25-dihydroxyvitamin D(3) in vivo. *J Cell Biochem* 76: 194-205.

SASAKI, T. and GARANT, P.R. (1987). Mitochondrial migration and Ca-ATPase modulation in secretory ameloblasts of fasted and calcium-loaded rats. *Am J Anat* 179: 116-30.

SIMMER, J.P. and FINCHAM, A.G. (1995). Molecular mechanisms of dental enamel formation. *Crit Rev Oral Biol Med* 6: 84-108.

SIMMER, J.P. and HU, J.C. (2002). Expression, structure, and function of enamel proteinases. *Connect Tissue Res* 43: 441-9.

WOLTGENS, J.H., LYARUU, D.M., BRONCKERS, A.L., BERVOETS, T.J. and VAN DUIN, M. (1995). Biomineralization during early stages of the developing tooth in vitro with special reference to secretory stage of amelogenesis. *Int J Dev Biol* 39: 203-12.

YAMAGUTI, P.M., ARANA-CHAVEZ, V.E. and ACEVEDO, A.C. (2005). Changes in amelogenesis in the rat incisor following short-term hypocalcaemia. *Arch Oral Biol* 50: 185-8.

YAN, Q., ZHANG, Y., LI, W. and DENBESTEN, P.K. (2006). Differentiation of human ameloblast-lineage cells in vitro. *Eur J Oral Sci* 114 Suppl 1: 154-8; discussion 164-5, 380-1.

ZHANG, Y., LI, W., CHI, H.S., CHEN, J. and DENBESTEN, P.K. (2007). JNK/c-Jun signaling pathway mediates the fluoride-induced down-regulation of MMP-20 in vitro. *Matrix Biol* 26: 633-41.

ZHANG, Y., YAN, Q., LI, W. and DENBESTEN, P.K. (2006). Fluoride down-regulates the expression of matrix metalloproteinase-20 in human fetal tooth ameloblast-lineage cells in vitro. *Eur J Oral Sci* 114 Suppl 1: 105-10; discussion 127-9, 380.

Appendix 1-Calcium mediated activation of the human amelogenin promoter

Rationale:

Our publication describing the effects of extracellular calcium on ameloblast differentiation showed upregulation of amelogenin expression both at protein and mRNA levels. In the studies described in this appendix, we further determined the direct effect of calcium on amelogenin expression by monitoring expression of the human amelogenin promoter in the presence of calcium. A study of the relationship between levels of calcium required to upregulated amelogenin in a 24hr time period were needed to determine the calcium levels used in these studies. This calcium level was then used to assess amelogenin promoter activity in response to calcium.

Materials:

The amelogenin qPCR primer/probe was purchased from Applied Biosystems (Foster City, CA). Primer/probes are proprietary to Applied Biosystems, and therefore sequences are not available. qPCR experiments were conducted using a 7500 Real Time PCR machine (Applied Biosystems, Redwood City, CA). Taqman master mixes for qPCR were purchased from Roche Applied Sciences (Indianapolis, IN). KGM-2 media was purchased from Lonza (Walkersville, MD). Cellular imaging and immunofluorescent imaging were conducted using Nikon E800 system (Nikon TMS, Melville, NY, USA) and SimplePCI imaging software version 5.3.1.

Methods:

Full-length amelogenin promoter driven GFP cloning:

Primers were designed to amplify the full 2.2kb human amelogenin promoter for the purposes of cloning the full 2.2kb fragment into a GFP reporting vector (FUGW) (Fig 1). The forward primer sequence included a PstI restriction enzyme cutting site, while the reverse primer included a BamHI restriction enzyme cutting site. The 2.2kb amelogenin promoter was amplified by PCR from a commercially available human genome library (Clontech, Mountain View, Ca) under the following conditions: annealing temperature 56°C (30 sec) and extension temperature 72°C (3 min), this was repeated for 35 cycles. The resulting PCR product was then subcloned into pCR-Blunt II-TOPO shuttle vector via blunted ended recombination (Invitrogen, Carlsbad CA). The 2.2kb-AmgPromoter-pCR-Blunt II vector was amplified by using OneShot TOP10 chemically competent DH5 α cells (Invitrogen, Carlsbad, CA). The full 2.2kb fragment was then sequenced to assure fidelity during amplification (Elimbio, Hayward, Ca). From the shuttle vector the 2.2kb amelogenin promoter was subcloned into FUGW via PstI and BamHI digestion followed by T4-Ligase recombination (NEB, Ipswich, MA). After subcloning, the 2.2kb-FUGW was amplified by transformation into DH5 α cells. DNA was purified by using Qiagen's Maxiprep kit under sterile conditions to a final concentration of 1mg/ml (Valencia, Ca).

FIG 1:

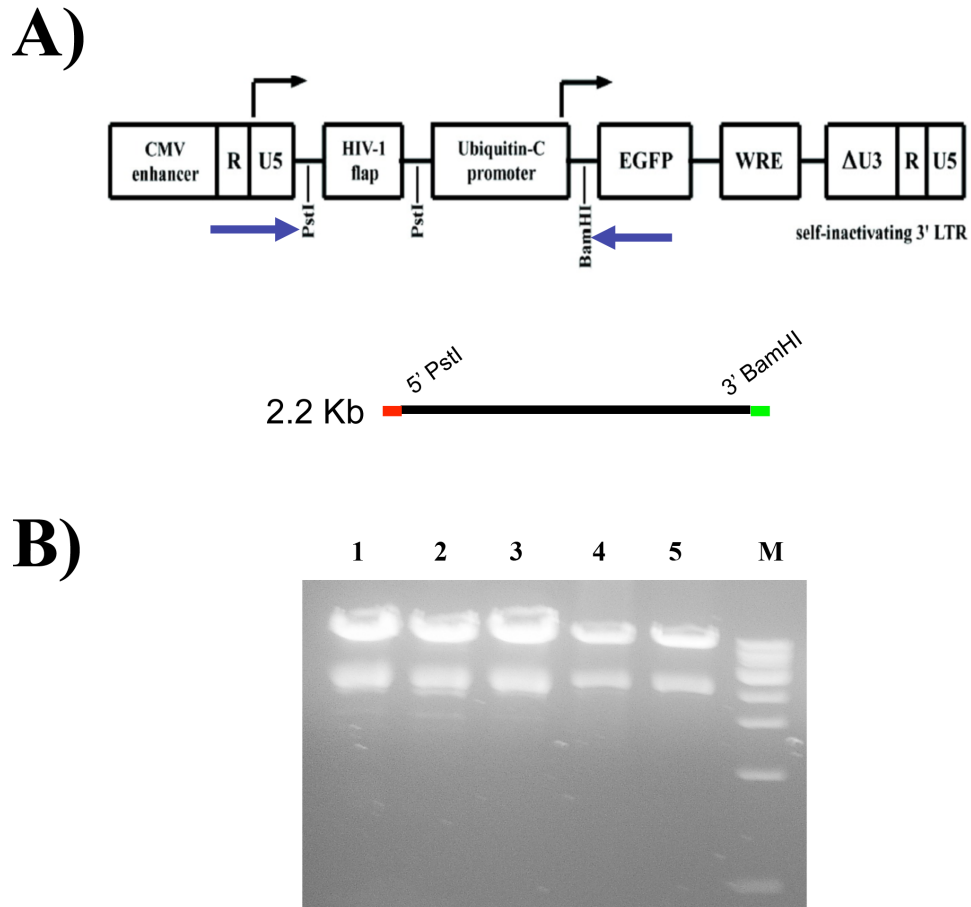


Figure 1-Construction of human amelogenin promoter driven GFP reporter vector

A) Linear diagram of FUGW vector where the arrow indicates the insertion plus the location of both restriction enzyme sites (arrow). Linear diagram of the restriction enzyme sites engineered in the 2.2kb amelogenin promoter insert, PstI at the 5' end and BamHI at the 3' end.

B) PstI/BamHI digestion of five (1-5) different bacterial clones containing 2.2kb amelogenin promoter-FUGW. The lower band indicates the 2.2kb amelogenin promoter fragment.

Human ameloblast lineage cell isolation and transfection:

Primary ameloblast lineage cells were isolated from 18-23 week old fetal tooth buds, with permission obtained through the tissue-sharing program at UCSF, as previously described [1-5]. Briefly, the tissue mass from these tooth buds was dispersed by the addition of 1 mg/ml collagenase/dispase mixture dissolved in PBS at 37°C for 2 hr. The tissue mass was further digested with 0.05% trypsin with EDTA for 5 min at 37°C. Ameloblast lineage cells were selected in keratinocyte selective media, KGM-2 w/o serum and supplemented with 0.05mM calcium.

Passage one primary human ameloblasts were cultured to 50% confluency prior to transfection. The 2.2kb-FUGW vector (described above) was transfected into primary cells using a Roche's Fugene HD transfection kit (Mountain View, Ca). The ratio of transfection agent to DNA was 4ml:2mg for one well of a six well plate. After 24hrs the media was changed and either 3.0mM NaCl or CaCl₂ was added to culture media. After 24hr treatment, GFP signal was detected by light microscopy under epifluorescence on a Nikon E800 system (Nikon TMS, Melville, NY, USA) and SimplePCI imaging software version 5.3.1.

RNA isolation and gene expression assays:

Total RNA was isolated from primary ameloblast cell cultures (control and 0.1mM calcium). Media was removed and the plates were washed with PBS. Cells were scrapped from the plates following incubation in 0.05% trypsin for 5 min at 37°C, and

total RNA was isolated using Qiagen's RNAeasy Kit (Valencia, Ca). Purified RNA was quantified by UV spectroscopy on a Nanodrop (Thermo Fisher Scientific, Waltham, MA) and equal amounts of RNA from control and test samples were converted to cDNA by Superscript III kit (Invitrogen, Carlsbad, Ca). Aliquots of the resulting cDNA were used for gene expression assays. qPCR using amelogenin specific probes (Applied Biosystems, Redwood City, CA) were conducted using Applied Systems' 7500 Real Time PCR machine.

Results:

In our published paper, we reported that amelogenin was upregulated by the addition of 0.1mM calcium after 2 weeks exposure time. Here we determined the short-term effect of calcium (24hr) on our primary human ameloblast cells. At low concentrations of calcium, less than 0.5mM, there was little to no change in amelogenin expression as measured by qPCR (Fig 2). However, this increased to an over 4 fold response at 1.5 mM calcium and an over 6 fold increase at 3.0 mM calcium

FIG 2:

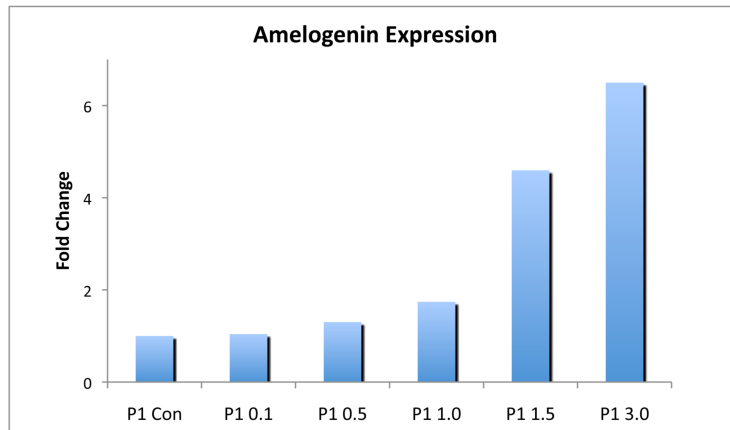


Figure 2-Calcium dose dependent amelogenin expression

Passage one primary ameloblasts treated for 24hr with calcium concentrations ranging from 0.05mM (Con) to 3.0mM showed increased amelogenin expression as calcium concentration increased. Y-axis is fold change and x-axis is concentration of CaCl₂ in mM. The level of amelogenin expression is recorded as fold change relative to the passage one control cells.

Transfection of passage one primary human ameloblasts with a GFP reporter vector, under the control of the full human 2.2kb amelogenin promoter, resulted in a significant increase in GFP fluorescence in cells treated with 3.0mM calcium compared to 3.0mM NaCl. This effect was seen in all triplicate samples (Fig 3). Phase contrast microscopic evaluation showed similar cellular organization in the 3.0mM treated group as those seen in 0.1mM calcium treatment (Fig 3)

FIG 3:

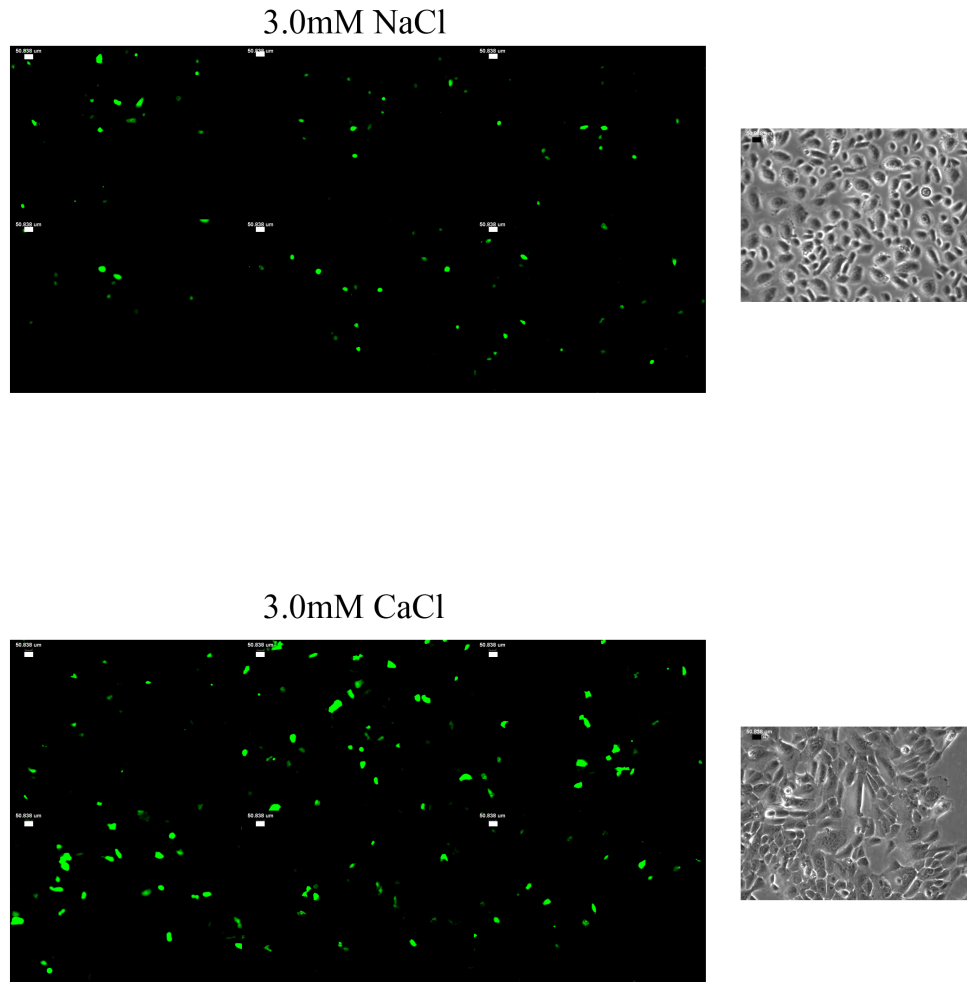


Figure 3. Human amelogenin promoter activity in response to increased dose of calcium. 24hr calcium treatment showed significantly higher level of positive GFP fluorescence in 3.0mM CaCl₂ compared to 3.0mM NaCl (Green-positive GFP signal). Triplicate samples are seen in each column, and each row represents images from different regions of the culture dish. Phase contrast images of the samples showed consistent changes in cellular organization in calcium treatment group only. Bar=50 μ m

Discussion:

Our published manuscript showed an enhanced expression of amelogenin in the presence of increased calcium [6]. Amelogenin mRNA levels are controlled both at the transcriptional as well as at the post-transcriptional levels. Post-transcriptional control of amelogenin mRNA has been shown to occur in the form of a positive feedback mechanism involving reuptake of secreted amelogenin proteins [7]. *In vivo*, a small portion of amelogenins are taken in by secretory ameloblasts, and it is thought that the internalized amelogenin proteins act to protect amelogenin mRNA from degradation [7]. The precise mechanism for this regulation is not well understood, but it appears that a region in exon 6 of the full length amelogenin messenger RNA is important for mediating the interaction with amelogenin protein [8]. Other than the aforementioned interaction between amelogenin protein and mRNA, no other evidence exists regarding post-transcriptional regulation of amelogenin.

Transcriptional regulation of amelogenin expression has been well examined, unlike that of post-transcriptional regulation, but there exists some debate as to which regions of the amelogenin promoter are essential for expression. Zhou *et al* cloned different lengths of the mouse amelogenin promoter into a luciferase reporter vector and showed the region between -70bp/-51bp were absolutely essential for promoter activity [9]. This region between -70bp/-51bp includes a binding region for CCAAT/enhancer-binding protein alpha (C/EBP α) [9]. In a follow-up report, Zhou *et al* found the region between -70bp/-51bp shared a high level of homology among multiple species, indicating the importance of this region for tooth formation [10]. The results reported by Zhou *et al*

were in stark contrast to reports by Suzawa *et al* and Xu *et al*. [7, 9, 11]. Xu *et al* identified suppressor elements in the region between -464bp and -74bp [12]. Whereas Suzawa *et al* found the region between -1102bp and -261bp to be required for minimal amelogenin expression [11].

To explore the possible role of calcium amelogenin transcription regulation, we cloned the entire 2.2kb human amelogenin promoter fragment into a GFP reporter vector. The enhanced GFP activity in the presence of calcium, confirmed our previous PCR result, and indicated the calcium is involved in transcriptional regulation of amelogenin expression, as opposed to post-transcriptional instability.

C/EBP α is a likely candidate as a mediator for this effect of calcium in upregulating amelogenin expression. Keratinocytes grown in culture show increased C/EBP α levels in response to elevated extracellular calcium levels [13], and the combination of elevated calcium and C/EBP α levels cue keratinocyte differentiation [13, 14]. Based on our studies, ameloblasts respond in a similar fashion to calcium as their embryological counterparts, keratinocytes, and thus suggesting an interesting possibility of calcium and C/EBP α promoting ameloblast differentiation.

In summary, these studies showed that extracellular calcium regulates amelogenin expression directly at the promoter level. The cellular response to extracellular calcium is dependent on the level and duration of calcium exposure. These results suggest that calcium accumulation or excess may be the signal to induce secretory ameloblast up-regulation of amelogenin. As ameloblast maturation continues and as the enamel matrix mineralizes, the decrease in free calcium could be responsible for the decrease in amelogenin expression as seen during the maturation stage. Future studies will be needed

to determine which specific region of the amelogenin promoter and possibly other transcription factors are responsible for mediating the effects of elevated extracellular calcium.

References:

1. DenBesten, P.K., et al., *Characterization of human primary enamel organ epithelial cells in vitro*. Arch Oral Biol, 2005. **50**(8): p. 689-94.
2. Le, T.Q., et al., *The effect of LRAP on enamel organ epithelial cell differentiation*. J Dent Res, 2007. **86**(11): p. 1095-9.
3. Yan, Q., et al., *Differentiation of human ameloblast-lineage cells in vitro*. Eur J Oral Sci, 2006. **114 Suppl 1**: p. 154-8; discussion 164-5, 380-1.
4. Zhang, Y., et al., *JNK/c-Jun signaling pathway mediates the fluoride-induced down-regulation of MMP-20 in vitro*. Matrix Biol, 2007. **26**(8): p. 633-41.
5. Zhang, Y., et al., *Fluoride down-regulates the expression of matrix metalloproteinase-20 in human fetal tooth ameloblast-lineage cells in vitro*. Eur J Oral Sci, 2006. **114 Suppl 1**: p. 105-10; discussion 127-9, 380.
6. Chen, J., et al., *Calcium-mediated differentiation of ameloblast lineage cells in vitro*. J Exp Zool B Mol Dev Evol, 2009. **312B**(5): p. 458-64.
7. Xu, L., et al., *Reuptake of extracellular amelogenin by dental epithelial cells results in increased levels of amelogenin mRNA through enhanced mRNA stabilization*. J Biol Chem, 2006. **281**(4): p. 2257-62.

8. Xu, L., H. Harada, and A. Taniguchi, *The exon 6ABC region of amelogenin mRNA contribute to increased levels of amelogenin mRNA through amelogenin protein-enhanced mRNA stabilization.* J Biol Chem, 2006. **281**(43): p. 32439-44.
9. Zhou, Y.L. and M.L. Snead, *Identification of CCAAT/enhancer-binding protein alpha as a transactivator of the mouse amelogenin gene.* J Biol Chem, 2000. **275**(16): p. 12273-80.
10. Xu, Y., et al., *NF-Y and CCAAT/enhancer-binding protein alpha synergistically activate the mouse amelogenin gene.* J Biol Chem, 2006. **281**(23): p. 16090-8.
11. Suzawa, T., et al., *Establishment of primary cultures for mouse ameloblasts as a model of their lifetime.* Biochem Biophys Res Commun, 2006. **345**(3): p. 1247-53.
12. Xu, L., et al., *Identification of a suppressor element in the amelogenin promoter.* J Dent Res, 2010. **89**(3): p. 246-51.
13. Oh, H.-S. and R.C. Smart, *Expression of CCAAT//Enhancer Binding Proteins (C//EBP) is Associated with Squamous Differentiation in Epidermis and Isolated Primary Keratinocytes and is Altered in Skin Neoplasms.* 1998. **110**(6): p. 939-945.
14. Bikle, D.D., et al., *Calcium- and vitamin D-regulated keratinocyte differentiation.* Mol Cell Endocrinol, 2001. **177**(1-2): p. 161-71.

Appendix 2-Extracellular calcium induced gene expression.

Rationale:

Calcium is incorporated into the mineralizing extracellular matrix and is obviously critical for hydroxyapatite formation. However few studies have determined whether calcium has additional functions in regulating ameloblast differentiation, similar to the effects of calcium in other epithelially derived cells. In large part, the lack of appropriate cell culture systems has limited these studies. As described above, we found that, extracellular calcium regulates gene expression, specifically amelogenin. However, it is possible that other genes expressed by human primary ameloblasts could also be regulated by extracellular calcium. This possibility was explored through microarray analyses comparing gene expression in ameloblast lineage cells exposed to either 0.3mM calcium for 30 minutes or 24 hrs. We chose these two particular time points to address early and late calcium response genes. Below is a summary of the results along with an extended discussion of the functions of the genes influenced by calcium, with their potential relationship to ameloblast differentiation.

Materials and Methods:

Cell isolation:

In collaboration with the tissue-sharing program at UCSF, human fetal maxillas and mandibles were isolated from 18-23 week old fetuses at San Francisco General Hospital. Primary tooth buds were microdisected from the mandibles under sterile conditions. All the primary tooth buds were pooled together, and extracellular tissue was dispersed with a combination of collagenase and dispase (1mg/ml diluted in tissue culture grade PBS w/o calcium) for 4 hours at 37°C. After collagenase/dispase treatment,

partially digested tooth buds were washed with PBS w/o calcium (tissue culture grade), and further digested with 0.05% trypsin and EDTA for 5 min at 37°C. Digested tooth buds were washed again with PBS w/o calcium and plated for expansion. Ameloblast lineage cells were selected by culture in a keratinocyte selective media, KGM-2 from Cambrex (Walkersville, VA, USA) w/o serum and supplemented with 0.05mM calcium [4,10].

Cell Culture and RNA preparation:

Passage zero primary ameloblast lineage cells were cultured to 50-60% confluence and then split to eight 100mm dishes (two plates each for 30 min w/ and w/o calcium and 24hr w/ and w/o calcium) at a cell density of 2×10^6 cells/plate. Cells were grown overnight, and then synchronized using KBM/HBSS (Cambrex, Walkersville, VA, USA). The following morning, the media was replaced by KGM-2 supplemented with 0.3mM calcium for either 30 minutes or 24 hr. Controls were subjected to the same conditions without calcium. Primary ameloblast lineage cells were collected at the same time and the total RNA was isolated from ameloblast using Qiagen's RNeasy RNA extraction kit (Valencia, CA, USA). Ambion's MessageAmp II (Austin, TX, USA) was used to amplify and convert total RNA, isolated from primary ameloblasts, to biotin labeled aRNA. Purified aRNA was then fragmented using an acetate buffer to increase hybridization to Affymetrix Human Genome 1.33 Plus 2 chips (Foster City, CA, USA). RNA quality control was monitored using Affymetrix Bioanalyzer.

Microarray analysis:

Genes significantly upregulated were analyzed to identify the top 100 genes significantly up or down regulated. Statistical analyses were completed through biostatistics services in the UCSF Genomics Core Facility. A Linear model was used to fit the array data to derive estimates and draw inference of the following comparisons: (i) CA30m vs. CO30m; (ii) CA24h vs. CO24h. Moderated *t*-statistics were derived and different significance criteria were explored for differential expression (DE) declaration. The number of DE genes at each time point are listed in the table below (TABLE 1).

TABLE 1:

Comparisons	fdr < 0.05	B > 0	Adjusted p < 0.05	Result Files
CA30m vs. CO30m	0	0	0	Mtop100list.CA30mvsCO30m.html Top 100 up-regulated genes & Top 100 down-regulated genes
CA24h vs. CO24h	1597	986	226	DElist.CA24hvsCO24h.html B>0 & abs(M)>0.58

Table 1: Derivation of significantly up or down regulated genes.

There were no significant differences in gene expression after 30 minutes in cells treated with 0.3mM calcium in two samples that were analyzed. However, we did generate a list of the top 100 up-regulated and top 100 down-regulated (compared to controls) genes as a reference for future studies. For the comparison CA24h vs.

C024h, we selected the 508 DE genes that had $(B > 0 \text{ AND } \text{abs}(M) > 0.58)$ (1.5-fold change) for more detailed annotations. ($B = \log$ posterior odds ratios, ratio between the probability that a given gene is differentially expressed over the probability that a given gene is not differentially, $M = \log$ fold change, 2 based. $M = 1$ means two-fold increase. $M = 0$ means equal expression)

A GO analysis was then completed by Creative Dynamics, (Port Jefferson, NY) where all 54,675 features (probe sets) interrogated on Affymetrix Human Genome U133 Plus 2.0 Array were mapped to biological process (BP), molecular function (MF) and cell component (CC) GO terms [1, 2]. For a set of interesting genes such as those which were identified as differently expressed between specific conditions, enrichment of GO terms was evaluated using the Fisher's exact statistical test, which is available in the topGO package [1].

Results:

Significant upregulation of genes occurred after 24 hr exposures, and included both ameloblast and odontoblast related genes.

The addition of 0.3mM calcium for 24 hrs to ameloblast lineage cells upregulated a number of extracellular matrix proteins; whereas, in the 30 min group there were no statistically significant alterations in gene expression, though GO analysis indicated enrichment of gene families (data not shown). Keratin 13 was most highly upregulated of all genes, though the majority of upregulated genes were members of the collagen family (TABLE 2), with two to five fold increased expression (collagen Type I, collagen type IV alpha 1, and collagen Type IV). Additionally, several other extracellular matrix

proteins including periostin and decorin were also significantly upregulated. Other genes significantly upregulated in response to 0.3mM calcium treatment included calcium binding proteins (CALB1), signaling molecules (WISP1), and cell growth regulators (GAS1). Amelogenin could be detected in the array, but was not identified as significantly upregulated by 0.3mM calcium at either 30 min or 24 hours.

TABLE 2:

<i>Name</i>	<i>Symbol</i>	<i>Fold Change</i>
Extracellular Matrix		
Collagen III alpha 1	COL3A1	4.96
Collagen IV type 1	COL4A1	2.57
Collagen V alpha 1	COL5A1	2.49
Collagen V alpha3	COL5A3	3.19
Collagen VI alpha 1	COL6A1	2.52
Collagen type VI, alpha 3	COL6A3	3.05
Collagen Type VIII alpha1	COL8A1	2.11
Collagen type XV, alpha 1	COL15A1	4.21
Keratin 13	KRT 13	7.06
Laminin alpha 4	LAMA4	4.26
Hyaluronan synthase 2	HAS2	4.21
Lumican	LUM	4.06
Nidogen 1	NID1	3.93
Involucrin	IVL	2.95
Periostin	PSTN	2.67
Decorin	DCN	2.36
Calbindin 1 28kDa	CALB1	2.05
Cell Signaling		
WNT1 inducible signaling protein 1	WISP1	3.85
Cell Growth		
Growth Arrest 1	GAS1	4.51

Table 2-Significantly upregulated genes

The most significantly upregulated genes are listed in groupings based on function. The handful of genes that were down regulated showed only minimal fold difference (< 1,

data not shown). The fold change is reported as the difference between the 24hr calcium treated group vs. the control group. Several additional genes were significantly up or down regulated at a p value of $p < 0.05$ (supplemental data 1). We chose to present the genes with a significant relationship to tooth formation, the genes specifically not addressed here were either of unknown function or presumed not relevant to tooth formation.

GO analysis suggested different effects of calcium after 30 minutes as compared to 24 hr calcium exposure in vitro:

Although only genes in the 24 hr calcium exposure group were significantly upregulated, GO analysis indicating differential enrichment of gene family expression at 30 min as compared to 24 hr calcium exposure. In the 24 hr group, the genes that were enriched were those relating to epidermal development, extracellular matrices, and ion transport (data not shown), whereas in the 30 min calcium exposure group the enriched genes were related to blood vessel remodeling, tissue remodeling, AP-2 adaptor complex (specifically clathrin coated endocytosis), MAP/ERK kinase, and epidermal growth factors (data not shown).

Discussion:

Studies in humans and mice have implicated calcium as a regulator of enamel formation and ameloblast differentiation. Both *in vitro* and *in vivo* studies have shown that calcium functions to promote enamel matrix formation, specifically, the production of amelogenins [3, 4]. Although, amelogenins comprise the largest portion of secretory

enamel matrix proteins, there are a host of other proteins found in the enamel matrix that are important for enamel formation. Ameloblasts are exposed to three different matrices; the basement membrane at the basolateral border of ameloblasts at the presecretory stage, the dentin matrix immediately after the dissolution of the basement membrane and prior to secretion of the enamel protein matrix, and the enamel matrix at the apical border beginning at the secretory stage [5, 6]. Each of these extracellular matrices seems to have a role in ameloblast differentiation [33]. The results of our microarray analysis point to an effect of calcium in up regulating extracellular matrix proteins, with most of the statistically significant upregulated genes being extracellular matrix components.

Upregulation of extracellular matrix proteins-

We found that 0.3mM calcium for 24 hrs resulted in up-regulation of genes involved in basement membrane formation, intercellular adhesion, and connective tissue development, such as: collagen Type IV, collagen Type VI, laminin, and nidogen. These components of the basement membrane are structurally important not only as a separation between epithelial and mesenchymal cells, but also some of these components are involved in anchoring epithelial cells to the underlying connective tissue. Pre-ameloblasts are situated on top of a basement membrane, which separates the future dentin forming odontoblasts and the enamel forming ameloblasts [6]. At this stage of development, both cell types are immature, and as they begin to differentiate, the basement membrane disappears[6]. Prior to this switch, the basement membrane must be maintained for correct compartmentalization of the two mineralizing cell types, where Collagen Type IV, collagen Type VI, laminin, and nidogen are components of this basement membrane in the developing tooth germ [7, 8]. In the early stages of

ameloblast differentiation, the basement membrane can provide support and coordination of the initial differentiation process, but in later stages, the proteins in the enamel matrix maintain what the original basement membrane had established [5, 9]. What is also intriguing is that cultured differentiated ameloblasts adhere to enamel matrix proteins, but do not adhere to basement membrane proteins, while opposite is true for preameloblasts, which can adhere to basement membrane proteins but not enamel matrix proteins [5, 9]. More recent studies have shown human ameloblast lineage cells grown on basement membrane like components showed increased amelogenin expression, indicating increased differentiation [10]. Therefore it is possible that, calcium can upregulate the formation of basement membrane proteins, required for further ameloblast differentiation.

In addition to basement membrane components promoting ameloblast differentiation, intercellular adhesion molecules also appear to be important for ameloblast differentiation. We found one particular intercellular adhesion molecule, periostin, to be upregulated in response to calcium. Periostin, an extracellular matrix protein found specifically at epithelial-mesenchymal interfaces, was also found to be significantly upregulated in response to elevated extracellular calcium levels. The exact function of periostin is not clear, but it is thought to function as a homophilic adhesion molecule involved in cell migration [11]. Purified recombinant periostin can bind to alpha 5 beta 3 and alpha 5 beta 5 integrin, and in doing so promote cell adhesion and motility [12]. Periostin is expressed at sites of epithelial and mesenchymal interaction in the developing tooth bud, more specifically in the PDL and cervical loop of developing molars [13]. Periostin null mice show no major enamel defects at birth, but as periostin null mice age and eat the continuously growing lower incisors began to show severe

enamel clefting [14]. On closer examination of the cervical loop region of the developing incisor of periostin null mice have a completely disorganized and pseudostratified dental epithelium [14]. The islands of pseudostratified ameloblasts are amelogenin positive, with similar amounts of amelogenin proteins as compared to wild-type controls [14]. Periostin appears to maintain the integrity of the ameloblast layer under normal function, and mice lacking periostin are born with normal enamel because *in utero* embryos are not subjected to occlusal forces. No study has identified at which stage of ameloblast differentiation periostin is expressed, but based on our study and the periostin null mouse, it does appear that periostin is expressed early in ameloblast differentiation, and may be regulated by calcium.

Our results turned up two other extracellular matrix proteins, whose association with ameloblasts and ameloblast differentiation has yet to be established. These two extracellular matrix proteins are collagen Type I alpha 1 and decorin. These two proteins are expressed by odontoblasts, but currently no evidence exists showing expression in ameloblasts [15]. Expression of collagen Type I was validated by real time PCR both from human ameloblast lineage cell lysates and mRNA isolated from ameloblasts by laser capture microscopy of human tooth fetal tooth buds (data not shown). In spite of this, *in situ* hybridization experiments were negative for collagen Type I expression by ameloblasts (data not shown). One possible explanation for the difference in our results is the fact that our primary human ameloblast lineage cells are heterogeneous and do contain small numbers of mesenchymally derived cells. It is therefore possible that calcium also has a major role in odontoblast differentiation, including the upregulation of collagen I type 1 and decorin, and that these

mesenchymally derived extracellular matrix molecules further direct ameloblast differentiation.

Cell regulatory molecules:

Although the majority of the upregulated genes in our microarray were related to extracellular matrices, there were some upregulated genes that are involved in cell signaling and cell growth. Both WISP-1 (WNT inducible signaling protein 1) and GAS-1 (growth arrest-1) were upregulated 4-fold in response to 0.3mM calcium compared to controls. GAS-1 was originally identified as a gene whose expression controls proliferation of cultured fibroblasts [16]. GAS-1 gene encodes a member of the glial cell-derived neurotrophic factor receptor a (GFRa) family of glycosyl phosphatidylinositol anchored surface antigens [17]. It was later discovered to be a Shh-binding factor that positively regulates the hedgehog signaling pathway [18]. GAS-1 and Shh interaction strongly affects limb and craniofacial development, such that GAS-1 null mice present with truncated maxillas and what appears to be poorly mineralized craniofacial structures (including teeth) [19].

Although tooth related defects in GAS-1 null mice were not mentioned, reports on the role of Shh signaling on tooth development [32] indicate that altered GAS-1 would affect enamel formation. Shh has long been implicated as a major factor in tooth development. In mice lacking Shh expression, tooth buds form, but their size and shape are vastly different from that of wild-type mice [20]. Dassule *et al* showed that in the absence of Shh, both odontoblast and ameloblast morphology was disorganized and lacked adequate polarization, though in later stages of tooth formation the absence of Shh does not alter matrix deposition. They proposed that Shh controls odontoblast

organization, therefore indirectly controls pre-ameloblast polarization [20]. However, contrary to the results of the Dassule study, Gritli-Linde *et al* showed Shh signaling was required for dental epithelial cell proliferation, growth, differentiation, and polarization [21]. Shh perpetuated pre-ameloblast cell proliferation and was required for secretory ameloblast differentiation [21]. Shh induced ameloblast differentiation via increased amelogenin and ameloblastin expression in ameloblast lineage cells *in vitro* [22].

Though there are no studies directly examining the role of GAS-1 on tooth development, the importance of Shh in tooth formation suggests that GAS-1 would similarly affect tooth development.

WISP-1, Wnt induced secreted protein-1 or CCN-4, was the other signaling protein that was upregulated in 0.3mM calcium treated ameloblast lineage cells. WISP-1 is a member of the CCN family, which also includes WISP-2/CCN5, WISP-3/CCN6, and CTGF [23]. Members of the CCN family share a similar modular structure consisting of an IGF binding domain, von Willenbrand type C binding domain, thrombospondin-1 domain, and a domain containing a putative cysteine knot [23]. Of those four binding domains, IGF binding domains offers the most intriguing relationship, because IGF-1 and IGFR-1 are both expressed by ameloblasts. The addition of IGF to ameloblast lineage cells increases amelogenin and ameloblastin expression [24, 25]. There have been no established links between CCN family members and IGF in ameloblast differentiation; however, it is plausible that an interaction between the two molecules could offer a mechanism for IGF induced amelogenin and ameloblastin expression. Members of the CCN family have important roles in a variety of developmental processes, especially in epithelial-mesenchymal interactions and cell proliferation [26]. Similar to GAS-1, there

have been no specific studies focusing on WISP-1 and amelogenesis, but the relationship between CTGF and amelogenesis has not been investigated.

CTGF is probably the more thoroughly studied member of CCN. CTGF was expressed by the dental lamina, invaginating epithelium, condensing mesenchyme, and lastly abundant expression was seen in the enamel knot and pre-ameloblasts [27, 28]. Loss of function studies using CTGF neutralizing antibodies revealed severe inhibition of proliferation in both the epithelium and mesenchyme [28]. Conversely, increased cell proliferation is seen when cultured dental epithelial and mesenchymal cells are treated with recombinant CTGF [28]. Further studies on CCN family members, especially WISP-1, and the role of calcium in their upregulation, will further enhance our understanding these signaling molecules in amelogenesis.

Calcium interacting proteins-

We found increased expression of calbindin D28K in our 0.3mM calcium treatment group. Calbindin D28K is neither a calcium buffering protein nor a calcium sensor, but in fact appears to act as both. Calcium buffering proteins like calbindin D9k can bind more calcium at a faster rate than calcium sensing proteins. The current hypothesis on the role of calcium buffering proteins is that they are required to dampen the calcium signal intracellularly [29]. On the other hand, calcium sensors, such as calmodulin, bind less calcium and upon binding to calcium, structural changes occur which lead to exposed sites of protein interaction.

Calbindin D28K can change its conformation upon calcium binding, and in doing so exposes proteolytic domains that were not present prior to calcium binding [30]. What purpose calbindin D28K and calbindin D9K serves in ameloblast and amelogenesis is

unclear, but an *in vivo* mouse study found no phenotype associated with calbindin D9K null mice [31]. This suggests that even though extracellular calcium could upregulate calbindin D28K, this effect has minimal impact on ameloblast differentiation and enamel formation.

Enamel matrix proteins:

Our microarray showed that human ameloblast lineage cells respond to elevated extracellular calcium levels. The lack of a significant upregulation in amelogenin expression in this microarray appears to be related to the calcium dose and time of exposure. As seen when ameloblasts exposed to low calcium levels 0.1mM for a prolonged period of time, two weeks, showed increased amelogenin expression compared to the same calcium concentration for 24hr [4]. In order to increase amelogenin expression rapidly, 24hrs, calcium levels of 1.5mM and higher are needed (appendix 1). The response of the amelogenin gene expression to increased calcium concentration and exposure times is consistent with a stage specific effect of calcium regulation on amelogenin expression. Similarly at these lower levels of calcium exposure, expression of other key enamel matrix proteins including MMP-20, amelotin, and ameloblastin were not upregulated. It is possible, that similar to amelogenin, with increased time or concentration of calcium, that these matrix proteins would also be upregulated.

Conclusion:

In conclusion these studies showed extracellular calcium can regulate expression of genes in ameloblast lineage cells. Many of those gene products are important components of the underlying supportive extracellular matrix. Our results also point toward a dose dependence, which in this study is reflected in the time of exposure) of

calcium mediated amelogenin expression for amelogenin and potentially other enamel matrix proteins. The genes upregulated in our current study may represent the early responders to changes in calcium levels, with the potential that prolonged exposure to calcium would eventually lead to a switch in gene expression from basement membrane components to enamel matrix components. Further studies will be needed to determine if such calcium dependence is present, and to determine the ameloblast differentiation stage-specific effects of calcium on gene expression.

Lastly, we identified upregulation of collagen Type 1 in our primary cultured cells. This was a surprising finding and led to further analysis in order to determine the origin of these changes in collagen Type I expression. We addressed this heterogeneity issue by deriving an immortalized ameloblast lineage cell line, reported in Appendix 3.

SUPPLEMENTAL DATA 1:

Num	Symbol	Fold increase	Adj-p	AccNum	Description
1	KRT13	7.06	0	3860	keratin 13
2	SLC6A14	5.52	0	11254	solute carrier family 6 (amino acid transporter), member 14
3	COL3A1	4.96	0	1281	collagen, type III, alpha 1 (Ehlers-Danlos syndrome type IV, autosomal dominant)
4	C1orf42	4.77	0	54544	chromosome 1 open reading frame 42
5	SPRR3	4.77	0	6707	small proline-rich protein 3
6	GAS1	4.51	0	2619	growth arrest-specific 1
7	LAMA4	4.26	0.001	3910	laminin, alpha 4
8	HAS2	4.21	0	3037	hyaluronan synthase 2
9	COL15A1	4.21	0.003	1306	collagen, type XV, alpha 1
10	OVOS2	4.1	0	144203	ovostatin 2
11	LUM	4.06	0	4060	lumican
12	NID1	3.93	0	4811	nidogen 1
13	WISP1	3.85	0.001	8840	WNT1 inducible signaling pathway protein 1
14	COL3A1	3.67	0	1281	collagen, type III, alpha 1 (Ehlers-Danlos syndrome type IV, autosomal dominant)
15	COL5A3	3.58	0	50509	collagen, type V, alpha 3
16	COL3A1	3.57	0	1281	collagen, type III, alpha 1 (Ehlers-Danlos syndrome type IV, autosomal dominant)

17	ADAMTS2	3.44	0	9509	MRNA; cDNA DKFZp686F12218 (from clone DKFZp686F12218) /// ADAM metallopeptidase with thrombospondin type 1 motif, 2
18	SPRR1A	3.4	0.006	6698	small proline-rich protein 1A
19	COL1A1	3.38	0.019	1277	collagen, type I, alpha 1
20	APCDD1	3.33	0.001	147495	adenomatosis polyposis coli down-regulated 1
21	KLK10	3.29	0	5655	kallikrein 10
22	HAS2	3.29	0	3037	Hyaluronan synthase 2
23	ENPP2	3.24	0	5168	ectonucleotide pyrophosphatase/phosphodiesterase 2 (autotaxin)
24	SPRR2B	3.23	0	6701	small proline-rich protein 2B
25	PAG1	3.23	0	55824	phosphoprotein associated with glycosphingolipid microdomains 1
26	EBF	3.22	0	1879	Early B-cell factor
27	COL5A3	3.19	0	50509	collagen, type V, alpha 3
28	ABI3BP	3.18	0.001	25890	ABI gene family, member 3 (NESH) binding protein
29	HOP	3.18	0	84525	homeodomain-only protein /// homeodomain-only protein
30	TNFRSF19	3.17	0	55504	tumor necrosis factor receptor superfamily, member 19
31	COL1A2	3.15	0	1278	collagen, type I, alpha 2
32	C5orf13	3.09	0	9315	chromosome 5 open reading frame 13
33	GPM6B	3.09	0	2824	glycoprotein M6B

34	COL6A3	3.05	0	1293	collagen, type VI, alpha 3
35	IVL	2.95	0	3713	involucrin
36	EPS8	2.94	0	2059	epidermal growth factor receptor pathway substrate 8
37	GPM6B	2.91	0.011	2824	glycoprotein M6B
38	GREM1	2.91	0.001	26585	gremlin 1, cysteine knot superfamily, homolog (Xenopus laevis)
39	PAG1	2.88	0	55824	phosphoprotein associated with glycosphingolipid microdomains 1
40	EDNRA	2.87	1	1909	endothelin receptor type A
41	ECG2	2.86	0	84651	esophagus cancer-related gene-2
42	COL1A1	2.85	0	1277	collagen, type I, alpha 1
43	PAPPA	2.83	0	5069	pregnancy-associated plasma protein A, pappalysin 1
44	ADAM12	2.82	0.002	8038	ADAM metallopeptidase domain 12 (meltrin alpha)
45	THY1	2.81	0	7070	Thy-1 cell surface antigen
46	SBSN	2.8	0	374897	suprabasin
47	CTGF	2.8	0	1490	connective tissue growth factor
48	ZFHX1B	2.8	0.01	9839	zinc finger homeobox 1b
49	SULT2B1	2.79	0	6820	sulfotransferase family, cytosolic, 2B, member 1
50	ID4	2.79	0	3400	inhibitor of DNA binding 4, dominant negative helix-loop-helix protein
51	SPON2	2.71	0	10417	spondin 2, extracellular matrix protein

52	GREM1	2.71	0.001	26585	gremlin 1, cysteine knot superfamily, homolog (Xenopus laevis)
53	IL8	2.7	0.026	3576	interleukin 8
54	POSTN	2.67	0.001	10631	periostin, osteoblast specific factor
55	PI3	2.67	0.022	5266	peptidase inhibitor 3, skin-derived (SKALP)
56	AKAP12	2.64	0.001	9590	A kinase (PRKA) anchor protein (gravin) 12
57	PAPPA	2.62	0.001	5069	pregnancy-associated plasma protein A, pappalysin 1
58	CLIC3	2.62	0	9022	chloride intracellular channel 3
59	IL1F9	2.6	0	56300	interleukin 1 family, member 9
60	PAPPA	2.6	0	5069	pregnancy-associated plasma protein A, pappalysin 1
61	EPB41L3	2.57	0.004	23136	erythrocyte membrane protein band 4.1-like 3
62	COL4A1	2.57	0	1282	collagen, type IV, alpha 1
63	PI3	2.57	0.02	5266	peptidase inhibitor 3, skin-derived (SKALP) /// peptidase inhibitor 3, skin-derived (SKALP)
64	SPRR1A	2.56	0.002	6698	small proline-rich protein 1A
65	WISP1	2.55	0.002	8840	WNT1 inducible signaling pathway protein 1
66	EDNRA	2.55	0.001	1909	endothelin receptor type A
67	EBF	2.55	0	1879	early B-cell factor
68	COL6A1	2.52	0.055	1291	collagen, type VI, alpha 1

69	COL5A1	2.49	0	1289	collagen, type V, alpha 1
70	SDC2	2.49	0	6383	syndecan 2 (heparan sulfate proteoglycan 1, cell surface-associated, fibroglycan)
71	HS3ST1	2.48	0	9957	heparan sulfate (glucosamine) 3-O-sulfotransferase 1
72	COL6A2	2.48	0.006	1292	collagen, type VI, alpha 2
73	EPB41L3	2.47	0.011	23136	erythrocyte membrane protein band 4.1-like 3
74	SPRR3	2.47	0	6707	small proline-rich protein 3
75	PAPPA	2.45	0.001	5069	pregnancy-associated plasma protein A, pappalysin 1
76	CCL2	2.44	0.716	6347	chemokine (C-C motif) ligand 2
77	CRABP2	2.43	0	1382	cellular retinoic acid binding protein 2
78	C5orf13	2.43	0	9315	chromosome 5 open reading frame 13
79	PAG1	2.43	0.004	55824	phosphoprotein associated with glycosphingolipid microdomains 1
80	FLJ13841	2.42	0.003	79755	hypothetical protein FLJ13841
81	COL1A2	2.41	0.005	1278	collagen, type I, alpha 2
82	AKAP12	2.4	0.006	9590	A kinase (PRKA) anchor protein (gravin) 12
83	EPB41L3	2.4	0.001	23136	erythrocyte membrane protein band 4.1-like 3 /// erythrocyte membrane protein band 4.1-like 3
84	COL5A1	2.4	0	1289	collagen, type V, alpha 1
85	THY1	2.39	0.002	7070	Thy-1 cell surface antigen

86	RHCG	2.39	0	51458	Rhesus blood group, C glycoprotein
87	OLFML2B	2.39	0.001	25903	olfactomedin-like 2B
88	ENPP2	2.39	0.002	5168	ectonucleotide pyrophosphatase/phosphodiesterase 2 (autotaxin)
89	212764_at	2.38	0.139	---	---
90	MYL9	2.38	0.003	10398	myosin, light polypeptide 9, regulatory
91	AKAP12	2.38	0	9590	A kinase (PRKA) anchor protein (gravin) 12
92	225728_at	2.37	0	---	---
93	226997_at	2.36	0.009	---	CDNA FLJ10196 fis, clone HEMBA1004776
94	DCN	2.36	0.008	1634	decorin
95	SHOX2	2.35	0.003	6474	short stature homeobox 2
96	TGM1	2.33	0	7051	transglutaminase 1 (K polypeptide epidermal type I, protein-glutamine-gamma-glutamyltransferase)
97	SFRP2	2.33	0.029	6423	secreted frizzled-related protein 2
98	SDC2	2.32	0.003	6383	syndecan 2 (heparan sulfate proteoglycan 1, cell surface-associated, fibroglycan)
99	PDGFRB	2.32	0	5159	platelet-derived growth factor receptor, beta polypeptide
100	PAPPA	2.32	1	5069	pregnancy-associated plasma protein A, pappalysin 1
101	SFRP2	2.31	0.016	6423	secreted frizzled-related protein 2
102	NID2	2.31	0	22795	nidogen 2 (osteonidogen)

103	COL5A1	2.3	0.001	1289	collagen, type V, alpha 1
104	SPRR2C	2.3	0	6702	small proline-rich protein 2C
105	EMP1	2.28	0	2012	epithelial membrane protein 1
106	NRP1	2.28	0.046	8829	neuropilin 1
107	COL4A1	2.27	0.001	1282	collagen, type IV, alpha 1
108	IGFBP4	2.26	0.046	3487	insulin-like growth factor binding protein 4
109	BGN /// SDCCAG33	2.26	0.006	10194 /// 633	biglycan /// serologically defined colon cancer antigen 33
110	TMEM47	2.25	0.708	83604	transmembrane protein 47
111	TCF8	2.23	0.012	6935	transcription factor 8 (represses interleukin 2 expression)
112	NID1	2.22	0.026	4811	nidogen 1
113	TWIST1	2.21	0.288	7291	twist homolog 1 (acrocephalosyndactyly 3; Saethre-Chotzen syndrome) (Drosophila)
114	POSTN	2.2	0.001	10631	periostin, osteoblast specific factor
115	MALL	2.2	0	7851	mal, T-cell differentiation protein-like
116	RCN3	2.19	0.001	57333	reticulocalbin 3, EF-hand calcium binding domain
117	PMP22	2.18	0.028	5376	peripheral myelin protein 22
118	S100A7	2.17	0.048	6278	S100 calcium binding protein A7 (psoriasin 1)
119	213258_at	2.17	0.009	---	CDNA FLJ26796 fis, clone PRS05079
120	ADAMTS2	2.16	0.012	9509	ADAM metallopeptidase with thrombospondin type 1 motif,

					2
121	IL1R1	2.16	0	3554	interleukin 1 receptor, type I
122	EMP1	2.16	0.064	2012	epithelial membrane protein 1
123	LOC51334	2.15	1	51334	mesenchymal stem cell protein DSC54
124	FGF2	2.15	1	2247	fibroblast growth factor 2 (basic)
125	MAP2	2.14	0.001	4133	Microtubule-associated protein 2
126	NEBL	2.14	0	10529	nebulette
127	CREB3L1	2.14	0.034	90993	cAMP responsive element binding protein 3-like 1
128	CD248	2.13	0.003	57124	CD248 antigen, endosialin
129	KLK11	2.13	0.001	11012	kallikrein 11
130	COLEC12	2.12	0.037	81035	collectin sub-family member 12 /// collectin sub-family member 12
131	SCEL	2.12	1	8796	sciellin
132	DCAMKL1	2.12	0.005	9201	Doublecortin and CaM kinase-like 1
133	DCN	2.12	0.013	1634	decorin
134	WASPIP	2.11	0.091	7456	Wiskott-Aldrich syndrome protein interacting protein
135	GPR124	2.11	0.005	25960	G protein-coupled receptor 124
136	COL8A1	2.11	0.087	1295	Collagen, type VIII, alpha 1
137	EMP1	2.11	0	2012	epithelial membrane protein 1
138	LOX	2.1	0.038	4015	lysyl oxidase
139	DCN	2.1	0.004	1634	decorin

140	PRRX1	2.1	0.001	5396	paired related homeobox 1
141	PPL	2.09	0.026	5493	periplakin
142	LCN2	2.07	0.002	3934	lipocalin 2 (oncogene 24p3)
143	SPARC	2.07	0.056	6678	secreted protein, acidic, cysteine-rich (osteonectin)
144	THY1	2.07	0.003	7070	Thy-1 cell surface antigen
145	CDH11	2.07	0.006	1009	cadherin 11, type 2, OB-cadherin (osteoblast)
146	SCEL	2.07	0.028	8796	sciellin
147	HEYL	2.06	0	26508	hairy/enhancer-of-split related with YRPW motif-like
148	UPK1B	2.06	0.01	7348	uroplakin 1B
149	PCDH18	2.06	0.014	54510	protocadherin 18
150	ADAMTS5	2.05	0.068	11096	ADAM metallopeptidase with thrombospondin type 1 motif, 5 (aggrecanase-2)
151	CALB1	2.05	0.018	793	calbindin 1, 28kDa
152	DDR2	2.05	0.014	4921	Discoidin domain receptor family, member 2
153	SCEL	2.04	0.013	8796	sciellin
154	A2ML1	2.04	0.048	144568	alpha-2-macroglobulin-like 1
155	COL4A2	2.04	0.07	1284	collagen, type IV, alpha 2
156	ChGn	2.04	0.129	55790	chondroitin beta1,4 N-acetylgalactosaminyltransferase
157	MSX2	2.03	0.002	4488	msh homeo box homolog 2 (Drosophila)
158	LOC492304	2.03	0.064	492304	putative insulin-like growth factor II associated protein

159	PRRX1	2.03	1	5396	Paired related homeobox 1
160	LOXL2	2.02	0.002	4017	lysyl oxidase-like 2
161	CLDN4	2.02	0.001	1364	claudin 4
162	PRRX1	2.01	0.013	5396	paired related homeobox 1
163	SERPINB9	2.01	0.608	5272	Serpin peptidase inhibitor, clade B (ovalbumin), member 9
164	COL6A1	2.01	0.004	1291	collagen, type VI, alpha 1
165	CACNA2D3	2	0.003	55799	calcium channel, voltage-dependent, alpha 2/delta 3 subunit
166	UNQ467	1.99	1	388533	KIPV467
167	DLC1	1.99	0.087	10395	deleted in liver cancer 1
168	CHN1	1.98	0.054	1123	chimerin (chimaerin) 1
169	CTHRC1	1.98	0.26	115908	collagen triple helix repeat containing 1
170	CXCL6	1.98	0.379	6372	chemokine (C-X-C motif) ligand 6 (granulocyte chemotactic protein 2)
171	NPTX2	1.98	0.348	4885	neuronal pentraxin II
172	INSIG1	1.98	0.01	3638	insulin induced gene 1
173	MSX2	1.98	0.007	4488	msh homeo box homolog 2 (Drosophila)
174	C2orf32	1.97	0.044	25927	chromosome 2 open reading frame 32
175	CPM	1.97	0.458	1368	carboxypeptidase M
176	COL13A1	1.96	0.026	1305	collagen, type XIII, alpha 1
177	INSIG1	1.96	0.002	3638	insulin induced gene 1
178	TRIB2	1.96	0.026	28951	tribbles homolog 2

					(Drosophila)
179	PDCD6 /// AHRR	1.96	0.218	10016 /// 57491	programmed cell death 6 /// aryl-hydrocarbon receptor repressor
180	RGS4	1.96	0.028	5999	regulator of G-protein signalling 4
181	SERPINB1	1.96	0.001	1992	serpin peptidase inhibitor, clade B (ovalbumin), member 1
182	IL8	1.95	0.007	3576	interleukin 8
183	PAPPA	1.94	0.21	5069	pregnancy-associated plasma protein A, pappalysin 1
184	TMPRSS11 E	1.94	0.013	28983	transmembrane protease, serine 11E
185	FBN1	1.94	0.027	2200	fibrillin 1 (Marfan syndrome)
186	FBLN1	1.94	0.02	2192	fibulin 1
187	GRHL1	1.94	0.157	29841	grainyhead-like 1 (Drosophila)
188	DCN	1.94	0.1	1634	decorin
189	WNT5A	1.93	0.002	7474	wingless-type MMTV integration site family, member 5A /// wingless-type MMTV integration site family, member 5A
190	SERPINB1	1.93	0.011	1992	serpin peptidase inhibitor, clade B (ovalbumin), member 1
191	C16orf30	1.93	0.005	79652	chromosome 16 open reading frame 30
192	UPK1B	1.93	0.048	7348	uroplakin 1B
193	DLC1	1.92	0.007	10395	deleted in liver cancer 1
194	BGN	1.92	0.013	633	biglycan

195	PLSCR4	1.92	1	57088	phospholipid scramblase 4
196	SERPINB4	1.91	0	6318	serpin peptidase inhibitor, clade B (ovalbumin), member 4 /// serpin peptidase inhibitor, clade B (ovalbumin), member 4
197	ALDH3B2	1.91	0.002	222	aldehyde dehydrogenase 3 family, member B2
198	SPINK5	1.91	0	11005	serine peptidase inhibitor, Kazal type 5
199	FLJ10159	1.91	1	55084	hypothetical protein FLJ10159
200	TMPRSS11B	1.91	0.01	132724	transmembrane protease, serine 11B
201	NEBL	1.89	0.01	10529	nebulette
202	COL4A2	1.89	0.01	1284	collagen, type IV, alpha 2
203	FLJ21511	1.89	0.001	80157	hypothetical protein FLJ21511
204	FLJ21511	1.89	0.015	80157	hypothetical protein FLJ21511
205	CLDN11	1.88	1	5010	claudin 11 (oligodendrocyte transmembrane protein)
206	PDZRN3	1.88	0.053	23024	PDZ domain containing RING finger 3
207	RCN3	1.87	0.006	57333	reticulocalbin 3, EF-hand calcium binding domain
208	ANKRD22	1.87	0.052	118932	ankyrin repeat domain 22
209	RRAD	1.87	0.005	6236	Ras-related associated with diabetes
210	SPARC	1.87	0.005	6678	secreted protein, acidic, cysteine-rich (osteonectin) /// secreted protein, acidic, cysteine-rich (osteonectin)
211	CCNE2	1.87	0.015	9134	cyclin E2

212	ADAMTS5	1.86	0.083	11096	ADAM metallopeptidase with thrombospondin type 1 motif, 5 (aggrecanase-2)
213	STEAP4	1.86	0.065	79689	STEAP family member 4
214	RRAD	1.86	0.017	6236	Ras-related associated with diabetes
215	SLC39A8	1.86	0.028	64116	solute carrier family 39 (zinc transporter), member 8
216	NEXN	1.86	1	91624	nexilin (F actin binding protein)
217	AQP3	1.85	0.001	360	aquaporin 3
218	TIMP2	1.85	0.015	7077	TIMP metallopeptidase inhibitor 2
219	WISP1	1.85	0.004	8840	WNT1 inducible signaling pathway protein 1
220	ADAM12	1.85	0.359	8038	ADAM metallopeptidase domain 12 (meltrin alpha)
221	SLC39A8	1.85	0.025	64116	solute carrier family 39 (zinc transporter), member 8
222	232060_at	1.85	1	---	Full-length cDNA clone CS0DD009YB17 of Neuroblastoma Cot 50-normalized of Homo sapiens (human)
223	ADAM12	1.85	0.469	8038	ADAM metallopeptidase domain 12 (meltrin alpha)
224	DDAH1	1.85	0.014	23576	dimethylarginine dimethylaminohydrolase 1
225	NOPE	1.84	1	57722	likely ortholog of mouse neighbor of Punc E11
226	FLT1	1.84	0.007	2321	Fms-related tyrosine kinase 1 (vascular endothelial growth factor/vascular permeability factor receptor)

227	COL6A1	1.84	0.742	1291	collagen, type VI, alpha 1
228	IGFL1	1.84	0.011	374918	insulin growth factor-like family member 1
229	LY6D	1.83	0.009	8581	lymphocyte antigen 6 complex, locus D
230	RUNX1T1	1.82	0.119	862	runt-related transcription factor 1; translocated to, 1 (cyclin D-related)
231	TCEAL7	1.82	1	56849	transcription elongation factor A (SII)-like 7
232	EDG3	1.82	0.336	1903	endothelial differentiation, sphingolipid G-protein-coupled receptor, 3
233	CST6	1.81	0.076	1474	cystatin E/M
234	FLJ21986	1.81	1	79974	hypothetical protein FLJ21986
235	KLK5	1.81	0.131	25818	kallikrein 5
236	FLJ37034	1.81	0.002	151176	hypothetical protein FLJ37034
237	FLJ90086	1.81	0.857	389389	Similar to AI661453 protein
238	PLEKHC1	1.81	0.525	10979	pleckstrin homology domain containing, family C (with FERM domain) member 1
239	COL6A2	1.81	0.066	1292	collagen, type VI, alpha 2
240	OCLN	1.81	0.03	4950	Occludin
241	SERPINB3	1.8	0.005	6317	serpin peptidase inhibitor, clade B (ovalbumin), member 3
242	EMP1	1.8	0.019	2012	Epithelial membrane protein 1
243	FBN1	1.8	0.734	2200	fibrillin 1 (Marfan syndrome)
244	LOX	1.8	0.291	4015	lysyl oxidase
245	TNFAIP6	1.8	0.6	7130	tumor necrosis factor, alpha-

					induced protein 6
246	SERPINB3	1.8	0.005	6317	serpin peptidase inhibitor, clade B (ovalbumin), member 3
247	SPRR1B	1.79	0.741	6699	small proline-rich protein 1B (cornifin)
248	HSPC159	1.79	0.017	29094	HSPC159 protein
249	203817_at	1.78	0.067	---	---
250	IGFL2	1.78	0.005	147920	insulin growth factor-like family member 2
251	GLTP	1.78	0.703	51228	glycolipid transfer protein
252	C5orf13	1.77	0.008	9315	Chromosome 5 open reading frame 13
253	SORBS2	1.77	0.01	8470	sorbin and SH3 domain containing 2
254	TFPI	1.77	1	7035	tissue factor pathway inhibitor (lipoprotein-associated coagulation inhibitor)
255	COL18A1	1.77	0.009	80781	collagen, type XVIII, alpha 1
256	DDR2	1.77	0.099	4921	Discoidin domain receptor family, member 2
257	KLK7	1.77	0.021	5650	kallikrein 7 (chymotryptic, stratum corneum)
258	SLPI	1.77	1	6590	secretory leukocyte peptidase inhibitor
259	HSPC159	1.77	0.005	29094	HSPC159 protein
260	FLT1	1.76	0.445	2321	Fms-related tyrosine kinase 1 (vascular endothelial growth factor/vascular permeability factor receptor)
261	SERPINB1	1.76	0.004	1992	Serpin peptidase inhibitor, clade B (ovalbumin), member

					1
262	EMILIN2	1.76	0.016	84034	elastin microfibril interfacier 2 /// elastin microfibril interfacier 2
263	PLEKHC1	1.76	0.008	10979	pleckstrin homology domain containing, family C (with FERM domain) member 1
264	TMEM45B	1.76	0.014	120224	transmembrane protein 45B
265	ACTA2	1.76	0.004	59	actin, alpha 2, smooth muscle, aorta
266	TIMP2	1.75	0.093	7077	TIMP metallopeptidase inhibitor 2
267	GPR124	1.75	0.11	25960	G protein-coupled receptor 124
268	SERPINB7	1.75	0.016	8710	serpin peptidase inhibitor, clade B (ovalbumin), member 7
269	GAS1	1.75	1	2619	growth arrest-specific 1
270	LYPD3	1.75	0.013	27076	LY6/PLAUR domain containing 3
271	CFL2	1.74	0.718	1073	cofilin 2 (muscle) /// cofilin 2 (muscle)
272	KRT19	1.73	0.085	3880	keratin 19
273	SERPINF1	1.73	0.068	5176	serpin peptidase inhibitor, clade F (alpha-2 antiplasmin, pigment epithelium derived factor), member 1
274	H19	1.73	0.259	283120	H19, imprinted maternally expressed untranslated mRNA
275	AK5	1.72	0.057	26289	adenylate kinase 5
276	MUC15	1.72	0.118	143662	mucin 15
277	236335_at	1.72	0.233	---	CDNA: FLJ21462 fis, clone

					COL04744
278	GLTP	1.72	0.057	51228	glycolipid transfer protein
279	EFEMP2	1.72	0.075	30008	EGF-containing fibulin-like extracellular matrix protein 2
280	CCBE1	1.72	0.057	147372	collagen and calcium binding EGF domains 1
281	COL1A2	1.72	1	1278	Collagen, type I, alpha 2
282	MAL2	1.72	0.044	114569	mal, T-cell differentiation protein 2
283	TWIST2	1.71	0.419	117581	twist homolog 2 (Drosophila)
284	SPINK6	1.71	0.711	404203	serine peptidase inhibitor, Kazal type 6
285	THBS2	1.71	0.384	7058	thrombospondin 2
286	KIAA1462	1.71	0.432	57608	KIAA1462
287	MGC13102	1.71	0.015	84283	hypothetical protein MGC13102
288	CSTB	1.71	0.94	1476	Cystatin B (stefin B)
289	GPM6B	1.71	0.043	2824	glycoprotein M6B
290	ZNF469	1.7	0.038	84627	zinc finger protein 469
291	MLPH	1.7	0.245	79083	melanophilin
292	C20orf161	1.7	1	90203	chromosome 20 open reading frame 161
293	CLEC11A	1.7	1	6320	C-type lectin domain family 11, member A /// C-type lectin domain family 11, member A
294	SERPINB4	1.7	0.009	6318	serpin peptidase inhibitor, clade B (ovalbumin), member 4
295	LOC440449	1.7	0.702	440449	hypothetical gene supported by AF086204

296	A2ML1	1.7	0.837	144568	alpha-2-macroglobulin-like 1
297	WNT5A	1.69	0.029	7474	wingless-type MMTV integration site family, member 5A
298	FKBP7	1.69	1	51661	FK506 binding protein 7
299	CDH11	1.69	0.103	1009	cadherin 11, type 2, OB-cadherin (osteoblast)
300	RAB11FIP1	1.69	0.092	80223	RAB11 family interacting protein 1 (class I)
301	POSTN	1.69	0.064	10631	periostin, osteoblast specific factor
302	TDO2	1.68	0.096	6999	tryptophan 2,3-dioxygenase
303	C10orf72	1.68	0.732	196740	Chromosome 10 open reading frame 72
304	PVRL3	1.68	1	25945	poliovirus receptor-related 3
305	KRTAP2-1	1.68	0.017	81872	keratin associated protein 2-1
306	RGMB	1.68	0.028	285704	RGM domain family, member B
307	DKFZp761D112	1.68	0.137	84257	hypothetical protein DKFZp761D112
308	232151_at	1.68	1	---	MRNA full length insert cDNA clone EUROIMAGE 2344436
309	EDNRA	1.67	0.701	1909	endothelin receptor type A
310	NRK	1.67	1	203447	Nik related kinase
311	COL5A2	1.67	0.087	1290	collagen, type V, alpha 2
312	ITGB3	1.66	0.018	3690	integrin, beta 3 (platelet glycoprotein IIIa, antigen CD61)
313	RAB11FIP1	1.66	1	80223	RAB11 family interacting protein 1 (class I)

314	RUNX2	1.66	1	860	runt-related transcription factor 2
315	FBLN5	1.66	0.426	10516	fibulin 5
316	228438_at	1.65	1	---	CDNA FLJ41321 fis, clone BRAMY2045299
317	SPRY1	1.65	0.063	10252	sprouty homolog 1, antagonist of FGF signaling (Drosophila)
318	HOXB2	1.65	0.044	3212	homeo box B2
319	CLEC11A	1.65	1	6320	C-type lectin domain family 11, member A
320	LOC389019	1.65	1	389019	Hypothetical LOC389019
321	1566766_a_at	1.65	0.138	---	MRNA full length insert cDNA clone EUROIMAGE 2344436
322	LNK	1.65	0.325	10019	lymphocyte adaptor protein
323	SERPINB9	1.64	1	5272	serpin peptidase inhibitor, clade B (ovalbumin), member 9
324	TFPI	1.64	1	7035	tissue factor pathway inhibitor (lipoprotein-associated coagulation inhibitor)
325	213817_at	1.64	0.087	---	MRNA; cDNA DKFZp586B0220 (from clone DKFZp586B0220)
326	BIRC4BP	1.64	1	54739	XIAP associated factor-1
327	ANPEP	1.64	1	290	alanyl (membrane) aminopeptidase (aminopeptidase N, aminopeptidase M, microsomal aminopeptidase, CD13, p150)
328	FGFBP1	1.64	1	9982	fibroblast growth factor binding protein 1

329	CTSK	1.64	0.298	1513	cathepsin K (pycnodysostosis)
330	CSS3	1.63	0.333	337876	chondroitin sulfatase 3
331	FBLN1	1.63	0.14	2192	fibulin 1
332	PKIB	1.63	1	5570	protein kinase (cAMP-dependent, catalytic) inhibitor beta
333	KLF9	1.63	0.308	687	Kruppel-like factor 9
334	227361_at	1.62	1	---	---
335	JAM3	1.62	1	83700	junctional adhesion molecule 3
336	IL1F5	1.62	0.19	26525	interleukin 1 family, member 5 (delta)
337	IGFBP5	1.62	0.79	3488	insulin-like growth factor binding protein 5
338	GFPT2	1.62	0.819	9945	glutamine-fructose-6-phosphate transaminase 2
339	GPR109B	1.62	0.185	8843	G protein-coupled receptor 109B /// G protein-coupled receptor 109B
340	EMILIN1	1.62	1	11117	elastin microfibril interfacier 1
341	EPB41L1	1.61	0.344	2036	Erythrocyte membrane protein band 4.1-like 1
342	CFL2	1.61	1	1073	cofilin 2 (muscle)
343	DENND2A	1.61	1	27147	DENN/MADD domain containing 2A
344	TGFB1I1	1.61	0.667	7041	transforming growth factor beta 1 induced transcript 1
345	235438_at	1.61	1	---	MRNA; cDNA DKFZp686E22185 (from clone DKFZp686E22185)
346	MYLK	1.6	1	4638	myosin, light polypeptide

					kinase
347	METRNL	1.6	0.083	284207	meteorin, glial cell differentiation regulator-like
348	LOC144501	1.6	0.156	144501	Hypothetical protein LOC144501
349	CXXC5	1.6	1	51523	CXXC finger 5 /// CXXC finger 5
350	SORT1	1.59	0.086	6272	sortilin 1
351	KITLG	1.59	0.649	4254	KIT ligand
352	TM4SF1	1.59	0.17	4071	transmembrane 4 L six family member 1
353	BGN	1.59	1	633	biglycan
354	RGC32	1.59	0.863	28984	response gene to complement 32
355	ARHGAP24	1.59	0.217	83478	Rho GTPase activating protein 24
356	AQP3	1.59	1	360	aquaporin 3
357	RNF144	1.59	1	9781	ring finger protein 144
358	GPR110	1.59	0.18	266977	G protein-coupled receptor 110
359	ICAM1	1.59	0.978	3383	intercellular adhesion molecule 1 (CD54), human rhinovirus receptor
360	FAM84A /// LOC400944	1.59	0.159	151354 /// 400944	family with sequence similarity 84, member A /// hypothetical LOC400944
361	TRIB2	1.59	0.118	28951	tribbles homolog 2 (Drosophila)
362	ICAM1	1.58	0.365	3383	intercellular adhesion molecule 1 (CD54), human rhinovirus receptor

363	KRTHA4	1.58	0.597	3885	keratin, hair, acidic, 4
364	HSPB8	1.58	0.377	26353	heat shock 22kDa protein 8
365	TBX2	1.58	0.212	6909	T-box 2
366	SPRR2G	1.58	0.113	6706	small proline-rich protein 2G
367	IL1RN	1.58	1	3557	interleukin 1 receptor antagonist
368	FYN	1.58	1	2534	FYN oncogene related to SRC, FGR, YES
369	FZD2	1.57	1	2535	frizzled homolog 2 (Drosophila)
370	SGNE1	1.57	1	6447	secretory granule, neuroendocrine protein 1 (7B2 protein)
371	11-Sep	1.57	1	55752	Septin 11
372	MSX1	1.57	0.047	4487	msh homeo box homolog 1 (Drosophila)
373	ICAM1	1.57	1	3383	intercellular adhesion molecule 1 (CD54), human rhinovirus receptor
374	BBOX1	1.57	1	8424	butyrobetaine (gamma), 2-oxoglutarate dioxygenase (gamma-butyrobetaine hydroxylase) 1
375	EPS8L1	1.57	0.76	54869	EPS8-like 1
376	STC2	1.56	0.106	8614	stanniocalcin 2
377	HES5	1.56	1	388585	hairy and enhancer of split 5 (Drosophila)
378	CDH11	1.56	0.056	1009	Cadherin 11, type 2, OB-cadherin (osteoblast)
379	UNC5B	1.56	1	219699	unc-5 homolog B (C. elegans)
380	CYP1B1	1.56	1	1545	cytochrome P450, family 1,

					subfamily B, polypeptide 1
381	GLIS3	1.55	1	169792	GLIS family zinc finger 3
382	AQP3	1.55	0.901	360	aquaporin 3
383	NES	1.55	1	10763	nestin
384	PXK	1.55	1	54899	PX domain containing serine/threonine kinase
385	EBF	1.55	1	1879	Early B-cell factor
386	ANK3	1.55	0.599	288	ankyrin 3, node of Ranvier (ankyrin G)
387	TGFB2	1.55	1	7042	transforming growth factor, beta 2
388	CYP1B1	1.54	1	1545	cytochrome P450, family 1, subfamily B, polypeptide 1
389	UACA	1.54	0.173	55075	uveal autoantigen with coiled-coil domains and ankyrin repeats
390	IL24	1.54	1	11009	interleukin 24
391	CNN3	1.53	0.174	1266	calponin 3, acidic
392	PRG1	1.53	1	5552	proteoglycan 1, secretory granule
393	ADAMTS2	1.53	1	9509	ADAM metalloproteinase with thrombospondin type 1 motif, 2
394	ROR1	1.53	0.053	4919	receptor tyrosine kinase-like orphan receptor 1
395	HYAL1	1.53	1	3373	hyaluronoglucosaminidase 1
396	VGL-3	1.53	1	389136	vestigial-like 3
397	CRIP2	1.53	0.428	1397	cysteine-rich protein 2
398	229427_at	1.52	0.936	---	CDNA FLJ12815 fis, clone NT2RP2002546

399	ECM1	1.52	0.27	1893	extracellular matrix protein 1
400	228823_at	1.52	1	---	Transcribed locus, weakly similar to XP_517454.1 PREDICTED: similar to hypothetical protein MGC45438 [Pan troglodytes]
401	ADAMTS2	1.52	1	9509	ADAM metalloproteinase with thrombospondin type 1 motif, 2
402	KLK7	1.52	0.867	5650	kallikrein 7 (chymotryptic, stratum corneum)
403	C9orf19	1.52	1	152007	chromosome 9 open reading frame 19
404	SORT1	1.52	0.688	6272	sortilin 1
405	LMO7	1.52	0.364	4008	LIM domain 7
406	LOC338773	1.52	1	338773	hypothetical protein LOC338773
407	TMEM45B	1.51	0.359	120224	transmembrane protein 45B
408	RUNX1T1	1.51	1	862	Runt-related transcription factor 1; translocated to, 1 (cyclin D-related)
409	211600_at	1.51	1	---	---
410	HECW2	1.51	1	57520	HECT, C2 and WW domain containing E3 ubiquitin protein ligase 2
411	PCOLCE	1.51	1	5118	procollagen C-endopeptidase enhancer
412	STC2	1.51	0.443	8614	stanniocalcin 2
413	COL1A1	1.51	0.513	1277	collagen, type I, alpha 1
414	SDC2	1.51	0.218	6383	syndecan 2 (heparan sulfate proteoglycan 1, cell surface-associated, fibroglycan)

415	CLCA4	1.51	0.943	22802	chloride channel, calcium activated, family member 4
416	CDKN2C	1.5	1	1031	cyclin-dependent kinase inhibitor 2C (p18, inhibits CDK4)
417	RGS4	1.5	0.237	5999	regulator of G-protein signalling 4
418	CSTF2T	1.5	1	23283	Cleavage stimulation factor, 3' pre-RNA, subunit 2, 64kDa, tau variant
419	GUCY1B3	1.5	1	2983	guanylate cyclase 1, soluble, beta 3
420	232759_at	1.5	1	---	---
421	SLC16A1	0.67	0.578	6566	solute carrier family 16 (monocarboxylic acid transporters), member 1
422	KIAA0746	0.67	0.251	23231	KIAA0746 protein
423	CLK4	0.67	0.575	57396	CDC-like kinase 4
424	MARVELD3	0.67	0.487	91862	MARVEL domain containing 3
425	KIAA1217	0.67	0.073	56243	KIAA1217
426	AADAACL1	0.67	1	57552	arylacetamide deacetylase-like 1
427	229296_at	0.66	0.687	---	---
428	MTA1	0.66	1	9112	metastasis associated 1 /// metastasis associated 1
429	DOCK5	0.66	0.255	80005	dedicator of cytokinesis 5
430	CKLF4	0.66	1	146223	chemokine-like factor superfamily 4
431	DOCK5	0.66	1	80005	Dedicator of cytokinesis 5
432	FST	0.66	1	10468	follistatin

433	AER61	0.66	1	285203	AER61 glycosyltransferase
434	HBXAP	0.66	1	51773	hepatitis B virus x associated protein
435	SFRP1	0.66	0.503	6422	secreted frizzled-related protein 1
436	MGC18216	0.66	1	145815	hypothetical protein MGC18216
437	ZNF395	0.66	0.16	55893	zinc finger protein 395
438	PRKAB2	0.66	1	5565	protein kinase, AMP-activated, beta 2 non-catalytic subunit
439	C6orf168	0.66	0.951	84553	chromosome 6 open reading frame 168
440	TNS4	0.66	0.364	84951	tensin 4
441	226478_at	0.66	1	---	---
442	IL6R	0.65	0.219	3570	interleukin 6 receptor
443	EGFR	0.65	1	1956	Epidermal growth factor receptor (erythroblastic leukemia viral (v-erb-b) oncogene homolog, avian)
444	MOBKL2B	0.65	1	79817	MOB1, Mps One Binder kinase activator-like 2B (yeast)
445	L1CAM	0.65	0.281	3897	L1 cell adhesion molecule
446	MOBKL2B	0.65	1	79817	MOB1, Mps One Binder kinase activator-like 2B (yeast)
447	BCL11A	0.65	1	53335	B-cell CLL/lymphoma 11A (zinc finger protein)
448	SLC7A5	0.65	1	8140	solute carrier family 7 (cationic amino acid transporter, y+ system), member 5

449	CARD10	0.65	0.212	29775	caspase recruitment domain family, member 10
450	NOTCH1	0.64	0.915	4851	Notch homolog 1, translocation-associated (Drosophila)
451	BCL11A	0.64	1	53335	B-cell CLL/lymphoma 11A (zinc finger protein)
452	ALDH4A1	0.64	0.365	8659	aldehyde dehydrogenase 4 family, member A1
453	C11orf32	0.64	0.32	442871	chromosome 11 open reading frame 32
454	NANOS1	0.64	0.096	340719	nanos homolog 1 (Drosophila)
455	HS6ST2	0.63	0.447	90161	heparan sulfate 6-O-sulfotransferase 2
456	C21orf91	0.63	0.266	54149	chromosome 21 open reading frame 91
457	C20orf23	0.63	0.45	55614	chromosome 20 open reading frame 23
458	212675_s_at	0.63	1	---	---
459	229699_at	0.63	0.46	---	---
460	NT5C2L1	0.63	1	221294	5'-nucleotidase, cytosolic II-like 1
461	TGFBR1	0.63	0.313	7046	transforming growth factor, beta receptor I (activin A receptor type II-like kinase, 53kDa)
462	AMIGO2	0.63	1	347902	adhesion molecule with Ig-like domain 2
463	YEATS4	0.63	0.483	8089	YEATS domain containing 4
464	TP73L	0.63	0.184	8626	tumor protein p73-like
465	MMP28	0.63	0.059	79148	matrix metalloproteinase 28

466	MMP28	0.62	0.036	79148	matrix metallopeptidase 28
467	SLC7A11	0.62	1	23657	solute carrier family 7, (cationic amino acid transporter, y+ system) member 11
468	TGFBR1	0.62	1	7046	transforming growth factor, beta receptor I (activin A receptor type II-like kinase, 53kDa)
469	MED18	0.62	1	54797	mediator of RNA polymerase II transcription, subunit 18 homolog (yeast)
470	ELAVL2	0.62	0.307	1993	ELAV (embryonic lethal, abnormal vision, Drosophila)-like 2 (Hu antigen B)
471	SLC30A1	0.62	0.045	7779	Solute carrier family 30 (zinc transporter), member 1
472	LOC441762	0.62	1	441762	Similar to CG7467-PA /// Similar to CG7467-PA
473	SOX7	0.61	1	83595	SRY (sex determining region Y)-box 7
474	MMP3	0.61	0.254	4314	matrix metallopeptidase 3 (stromelysin 1, progelatinase)
475	1555854_at	0.61	0.908	---	---
476	ALS2CR13	0.61	1	150864	amyotrophic lateral sclerosis 2 (juvenile) chromosome region, candidate 13
477	SOX7	0.61	1	83595	SRY (sex determining region Y)-box 7
478	SLC7A11	0.61	1	23657	solute carrier family 7, (cationic amino acid transporter, y+ system) member 11
479	TMEFF2	0.6	1	23671	transmembrane protein with EGF-like and two follistatin-

					like domains 2 /// transmembrane protein with EGF-like and two follistatin- like domains 2
480	AKAP1	0.6	0.131	8165	A kinase (PRKA) anchor protein 1
481	KIAA1509	0.6	1	440193	KIAA1509
482	USP31	0.6	0.045	57478	ubiquitin specific peptidase 31
483	TNFSF10	0.6	1	8743	tumor necrosis factor (ligand) superfamily, member 10 /// tumor necrosis factor (ligand) superfamily, member 10
484	EPPK1	0.59	0.144	83481	epiplakin 1
485	ATXN3	0.59	1	4287	Ataxin 3
486	HS6ST2	0.59	0.096	90161	heparan sulfate 6-O- sulfotransferase 2
487	KIAA0888	0.59	0.074	26049	KIAA0888 protein
488	DST	0.58	1	667	dystonin
489	LOC91614	0.58	1	91614	novel 58.3 KDA protein
490	IFNK	0.58	0.075	56832	interferon, kappa
491	SLC30A1	0.58	1	7779	solute carrier family 30 (zinc transporter), member 1
492	KLHL24	0.57	0.11	54800	kelch-like 24 (Drosophila)
493	NEFL	0.57	0.027	4747	neurofilament, light polypeptide 68kDa
494	DST	0.57	0.061	667	dystonin
495	DLL1	0.56	0.284	28514	delta-like 1 (Drosophila)
496	ABCG1	0.56	0.002	9619	ATP-binding cassette, sub- family G (WHITE), member 1
497	CMKOR1	0.56	0.04	57007	chemokine orphan receptor 1

498	FST	0.54	0.134	10468	follistatin
499	PAK3	0.54	0.455	5063	P21 (CDKN1A)-activated kinase 3
500	ZCCHC2	0.54	1	54877	zinc finger, CCHC domain containing 2
501	CBLB	0.54	0.008	868	Cas-Br-M (murine) ecotropic retroviral transforming sequence b
502	MTUS1	0.53	0.005	57509	mitochondrial tumor suppressor 1
503	UBE2B	0.49	1	7320	ubiquitin-conjugating enzyme E2B (RAD6 homolog)
504	SFRP1	0.46	1	6422	secreted frizzled-related protein 1
505	FST	0.44	0.03	10468	follistatin
506	CXCL14	0.43	0	9547	chemokine (C-X-C motif) ligand 14
507	CXCL14	0.39	0.003	9547	chemokine (C-X-C motif) ligand 14
508	MALAT1	0.17	1	378938	metastasis associated lung adenocarcinoma transcript 1 (non-coding RNA)

Supplemental Data 1: Up and down regulated genes for 24hr 0.3mM calcium treatment.

The list of genes above illustrates both up regulated and down regulated genes in response to 0.3mM calcium. The list is organized from the most significantly upregulated to the most significantly down regulated gene. (AccNum=Accession number)

References:

1. Alexa, A., J. Rahnenfuhrer, and T. Lengauer, *Improved scoring of functional groups from gene expression data by decorrelating GO graph structure*. *Bioinformatics*, 2006. **22**(13): p. 1600-7.
2. Tian, L., et al., *Discovering statistically significant pathways in expression profiling studies*. *Proc Natl Acad Sci U S A*, 2005. **102**(38): p. 13544-9.
3. Woltgens, J.H., et al., *Biom mineralization during early stages of the developing tooth in vitro with special reference to secretory stage of amelogenesis*. *Int J Dev Biol*, 1995. **39**(1): p. 203-12.
4. Chen, J., et al., *Calcium-mediated differentiation of ameloblast lineage cells in vitro*. *J Exp Zool B Mol Dev Evol*, 2009. **312B**(5): p. 458-64.
5. Fukumoto, S., et al., *Essential roles of ameloblastin in maintaining ameloblast differentiation and enamel formation*. *Cells Tissues Organs*, 2005. **181**(3-4): p. 189-95.
6. Fukumoto, S. and Y. Yamada, *Review: extracellular matrix regulates tooth morphogenesis*. *Connect Tissue Res*, 2005. **46**(4-5): p. 220-6.
7. Kubler, M., Lesot H, Ruch J V, *temporo-spatial distribution of matrix and microfilament components during odontoblast and ameloblast differentiation*. *Development Genes and Evolution*, 1988. **197**(4): p. 212-220.
8. Webb, P.P., et al., *Immunolocalisation of collagens in the developing rat molar tooth*. *Eur J Oral Sci*, 1998. **106 Suppl 1**: p. 147-55.

9. Fukumoto, S., et al., *Ameloblastin is a cell adhesion molecule required for maintaining the differentiation state of ameloblasts*. J Cell Biol, 2004. **167**(5): p. 973-83.
10. He, P., et al., *Ameloblast differentiation in the human developing tooth: effects of extracellular matrices*. Matrix Biol, 2010. **29**(5): p. 411-9.
11. Horiuchi, K., et al., *Identification and characterization of a novel protein, periostin, with restricted expression to periosteum and periodontal ligament and increased expression by transforming growth factor beta*. J Bone Miner Res, 1999. **14**(7): p. 1239-49.
12. Gillan, L., et al., *Periostin secreted by epithelial ovarian carcinoma is a ligand for alpha(V)beta(3) and alpha(V)beta(5) integrins and promotes cell motility*. Cancer Res, 2002. **62**(18): p. 5358-64.
13. Kruzynska-Frejtag, A., et al., *Periostin is expressed within the developing teeth at the sites of epithelial-mesenchymal interaction*. Dev Dyn, 2004. **229**(4): p. 857-68.
14. Rios, H., et al., *periostin null mice exhibit dwarfism, incisor enamel defects, and an early-onset periodontal disease-like phenotype*. Mol Cell Biol, 2005. **25**(24): p. 11131-44.
15. Thieberg, R.H., et al., *Sequential distribution of keratan sulphate and chondroitin sulphate epitopes during ameloblast differentiation*. Histochem J, 1999. **31**(9): p. 573-8.
16. Del Sal, G., et al., *The growth arrest-specific gene, gas1, is involved in growth suppression*. Cell, 1992. **70**(4): p. 595-607.

17. Kang, J.S., W. Zhang, and R.S. Krauss, *Hedgehog signaling: cooking with Gas1*. Sci STKE, 2007. **2007**(403): p. pe50.
18. Martinelli, D.C. and C.M. Fan, *Gas1 extends the range of Hedgehog action by facilitating its signaling*. Genes Dev, 2007. **21**(10): p. 1231-43.
19. Allen, B.L., T. Tenzen, and A.P. McMahon, *The Hedgehog-binding proteins Gas1 and Cdo cooperate to positively regulate Shh signaling during mouse development*. Genes Dev, 2007. **21**(10): p. 1244-57.
20. Dassule, H.R., et al., *Sonic hedgehog regulates growth and morphogenesis of the tooth*. Development, 2000. **127**(22): p. 4775-85.
21. Gritli-Linde, A., et al., *Shh signaling within the dental epithelium is necessary for cell proliferation, growth and polarization*. Development, 2002. **129**(23): p. 5323-37.
22. Takahashi, S., et al., *Differentiation of an ameloblast-lineage cell line (ALC) is induced by Sonic hedgehog signaling*. Biochem Biophys Res Commun, 2007. **353**(2): p. 405-11.
23. Brigstock, D.R., *The CCN family: a new stimulus package*. J Endocrinol, 2003. **178**(2): p. 169-75.
24. Rosen, C.J., *Insulin-like growth factor I and calcium balance: evolving concepts of an evolutionary process*. Endocrinology, 2003. **144**(11): p. 4679-81.
25. Takahashi, K., et al., *Induction of amelogenin and ameloblastin by insulin and insulin-like growth factors (IGF-I and IGF-II) during embryonic mouse tooth development in vitro*. Connect Tissue Res, 1998. **38**(1-4): p. 269-78; discussion 295-303.

26. Moussad, E.E. and D.R. Brigstock, *Connective tissue growth factor: what's in a name?* Mol Genet Metab, 2000. **71**(1-2): p. 276-92.
27. Friedrichsen, S., et al., *Gene expression of connective tissue growth factor in adult mouse.* Growth Factors, 2005. **23**(1): p. 43-53.
28. Shimo, T., et al., *Expression, gene regulation, and roles of Fisp12/CTGF in developing tooth germs.* Dev Dyn, 2002. **224**(3): p. 267-78.
29. Pauls, T.L., J.A. Cox, and M.W. Berchtold, *The Ca²⁺(-)-binding proteins parvalbumin and oncomodulin and their genes: new structural and functional findings.* Biochim Biophys Acta, 1996. **1306**(1): p. 39-54.
30. Berggard, T., et al., *Calbindin D28k exhibits properties characteristic of a Ca²⁺ sensor.* J Biol Chem, 2002. **277**(19): p. 16662-72.
31. Kutuzova, G.D., et al., *Calbindin D9k knockout mice are indistinguishable from wild-type mice in phenotype and serum calcium level.* Proceedings of the National Academy of Sciences, 2006. **103**(33): p. 12377-12381.

Appendix 3-Characterization of SV40-transfected human ameloblasts

Rationale:

In the previous appendix, we found the addition of extracellular calcium to our primary human ameloblast lineage cell culture led to upregulation of several extracellular matrix proteins [1]. Among the matrix proteins that were upregulated was collagen Type I; which was confirmed by qPCR analysis. *In situ* hybridization in human fetal tissue did not show expression of collagen Type I, though we did find positive expression in samples isolated by laser capture microdissection (results not shown). This discrepancy led us to critically assess composition of cells in our primary ameloblast lineage cell culture model. To determine the effects of calcium on a pure cell population, we derived an SV40 immortalized human ameloblast lineage cell line, and examined whether these cells could similarly respond to calcium and expresses collagen Type 1.

Materials and Methods

Cell culture and transformation

Primary ameloblast lineage cells were isolated from 18-23 week old human fetal tooth buds, obtained through the tissue-sharing program at UCSF. The incisor tissue mass was dispersed by 1 mg/ml of collagenase/dispase in PBS at 37°C for 2 hrs, and further digested with 0.05% trypsin with EDTA for 5 min at 37°C. Ameloblast lineage cells were selectively grown in a serum free keratinocyte selective media, KGM-2 from Cambrex (Walkersville, VA, USA) supplemented with 0.05 mM calcium [2-6]. Primary ameloblast lineage cells were cultured to passage two and transfected with pSV ori plasmid (containing the full SV40 genome) using Fugene 6 transfection, according to the manufacturer's instructions (Roche, Redwood City, CA, USA) [7]. We found that dental

mesenchymal cells were not readily transfected using this protocol, and non-transfected ameloblast lineage cells would not grow beyond passage three.

After transfection, viable cells were further grown in KGM-2 media for epithelial cell selection. Transfected cells were then passaged at a very low density to promote single cell colony formation. Individual colonies were then selectively transferred to individual plates by using cloning discs soaked with 0.05% trypsin. Images were captured using a phase contrast microscope (Nikon E800 system, Melville, NY, USA) at every passage to characterize the morphology of the transfected cells as compared to primary non-transfected ameloblast lineage cells.

Large T-antigen western blot analysis

SV40 transfected human ameloblast lineage cells (SV40-HA) cells were harvested from cell culture plates via 0.05% trypsin digestion for 5 min at 37⁰C. Cells were lysed by passage through a 20-gauge needle five times in the presence of RIPA buffer containing pepitadase inhibitors PMSF, Aprotinin, Leupeptin, and Pepstain A (Sigma-Aldrich, St. Louis, MO, USA). Cell lysates were immediately treated with SDS buffer and heated to 100⁰C for 5 min to denature all protein structure. Proteins were resolved on 10% SDS-PAGE gels and transferred onto nitrocellulose membranes (GE Healthcare, Piscataway, NJ, USA). After 1hr of blocking non-specific sites with 5% non-fat milk, the membranes were probed with primary antibodies, mouse anti-Large T-antigen and rabbit anti-actin as control (Santa Cruz Biotechnology, Santa Cruz, CA, USA) overnight at 4⁰C. The membrane was then washed and then probed with a horseradish peroxidase-conjugated anti-mouse secondary antibody for 1h at room temperature, followed by ECL detection (GE Healthcare, Piscataway, NJ, USA).

Immunocytochemistochemical localization of Large T-antigen and cytokeratin 14

SV40-HA cells at 80-100% confluence were fixed using 5% acetic acid and 95% CH₃OH for 30 min. Cells were washed three times with PBS 0.1% tween-20 for 5 min each. 5% BSA in PBS was used to block non-specific binding sites, and after 1 h at room temperature, the cells were incubated first with either mouse anti-cytokeratin 14 (Chemicon Intl. Inc, Temecula, CA, USA) or mouse anti-Large T-antigen (Santa Cruz Biotechnology, Santa Cruz, CA, USA) at 4⁰C overnight. After primary antibody incubation, cells were washed three times with PBS for 5 min each. Then the cells were incubated with fluorescein-conjugated anti-mouse secondary antibodies (Sigma-Aldrich Corp, St Louis, MO, USA). Parallel immunostaining experiments without primary antibody were used as a non-specific control. The immunopositive reaction was observed under a Nikon Eclipse E800 (Melville, NY, USA) fluorescent microscope and photographed using SimplePCI Version 5.3.1 software.

Gene expression of SV40-HA cells

SV40-HA cells were cultured to 80-100% confluence and were harvested via 0.05% trypsin digestion for 5 min at 37⁰C. Cells were then lysed and RNA extraction was accomplished by using RNAeasy Kit (Qiagen, Valencia, CA, USA). The amount of extracted RNA was measured via UV absorbance. Five milligrams of RNA from each sample was reverse transcribed into cDNA by Superscript II kit (Invitrogen, Carlsbad, CA, USA) and subsequently used for conventional PCR. PCR primers were designed to amplify human amelogenin, MMP-20 and human GAPDH transcripts (TABLE 1). PCR products were resolved on 1% agarose gel. A human fetal tooth cDNA library was used as a positive control for enamel matrix gene transcripts.

Table 1: Gene specific primers (amelogenin, MMP-20, and GAPDH as control)

Gene of interest	5' primer	3' primer
Amelogenin	GGCTGCACCACCAAATCATCC	CCCGCTTGGTCTTGTCTGTCG
MMP-20	CCAGGAGCAAATGCATGGGC	ATTGGTGAGATGGTTGCAAGA
GAPDH	ACCACAGTCCATGCCATCAC	TCCACCACCCTGTTGCTGTA

Aliquots of cDNA were also used to assess collagen Type I expression via real-time PCR system, using commercially synthesized primers (Applied Biosystems, Redwood City, CA).

Mineralization assay

Passage two primary ameloblast lineage cells and clone 9 (passage 13) SV40-HA cells were grown in KGM-2 media to 70-80% confluence. Calcium, at final concentrations of 0.1mM and 0.3mM, was added to the medium for 2 weeks to induce cell differentiation [1]. The media was then changed to induce mineralization, by adding media supplemented with 3.0mM calcium in addition to containing 10.0mM β -glycerolphosphate, and 50 mg/ml L-ascorbic acid as optimized for other mineral assays [8, 9]. Von Kossa staining was used to detect mineral formation after 4 weeks of treatment.

Results

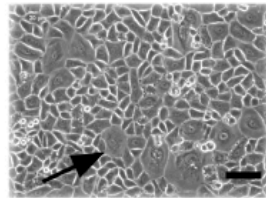
Cell morphology of SV40- human ameloblasts (SV40-HA)

Phase contrast microscopy of primary cells depicts colonies of tightly clustered small cobble stoned appearance cells with the occasional large rounded cells (Fig 1). We followed the cell morphology of our SV40-HA cells through to passage 13 and found

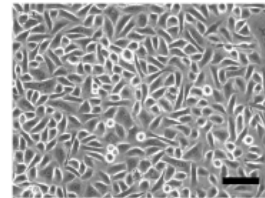
little to no difference in terms of cellular morphology between them and primary human ameloblast lineage cells (Fig 1).

FIG 1:

A)

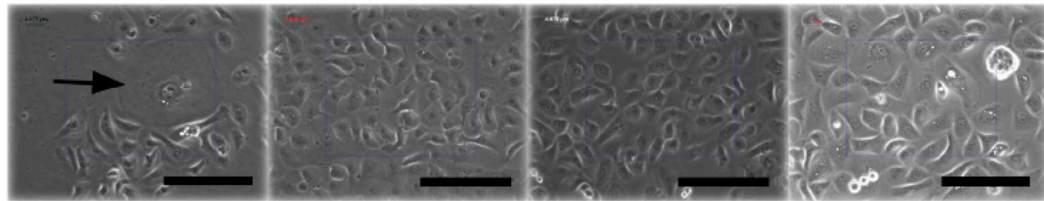


Primary P2



Primary P2

B)



P7

P8

P11

P13

Figure 1: Cellular morphology of SV40-HA cells

A) Passage two primary ameloblast lineage cells comprised of small cobblestone cells and large rounded cells (arrow).

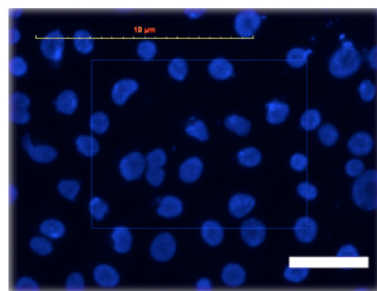
B) Passage 7-13, SV40-HA cells with similar small cobblestone cells and large rounded cells (arrow) Bar= 50 microns

Large-T antigen detection and localization

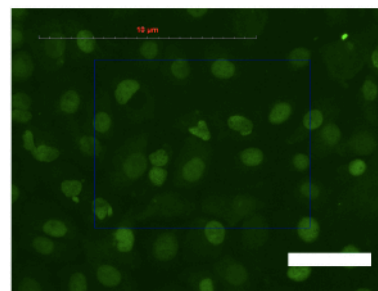
Cell lysates were obtained from several colonies. Large-T antigen was detected in the nucleus of transfected ameloblasts by immunofluorescent staining (Fig 2A). A band immunopositive for large-T antigen at approximately 92kDa was detected in all cell lysate samples (Fig 2B).

FIG 2:

A



DAPI + control



Anti-Large T Antigen

B

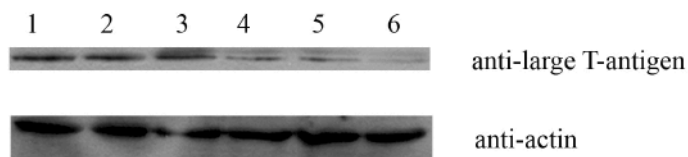


Figure 2: Large T-antigen localization

A) Immunofluorescent staining of Large T-antigen (green). Large T-antigen is localized to the nucleus (blue) Bar=50 micron

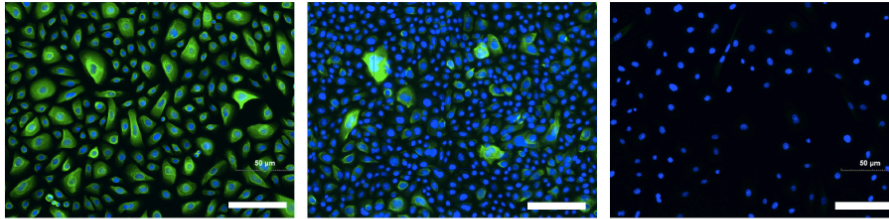
B) Western blot analysis of Large T-antigen expression. 1-6 represents different colonies. Top row represents positive bands for Large T-antigen and the bottom row represents loading control (actin).

Clonal selection by gene expression

Both amelogenin and MMP-20 expression were detected in only one clone (clone 9) of our SV40-HA colonies. Once identified, clone 9 was expanded and tested for cytokeratin 14 levels. Cytokeratin 14 expression was detected in clone 9, but with mixed levels of expression among cells (Fig 3A). Positive expression of amelogenin, MMP-20, and cytokeratin 14 suggests our SV40-HA cells appear to be at the same stage of differentiation as compared to our primary cells (Fig 3B).

FIG 3:

A)



Primary P2

Clone 9 P10

control

B)

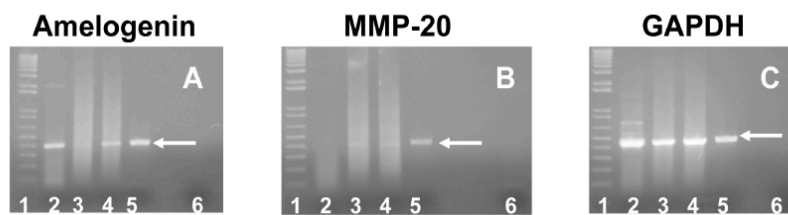


Figure 3: SV40-HA expression profile

A) Cytokeratin 14 expression (Green-CK14, blue-DAPI) is expressed by all primary cells, where as a more limited expression appears to be present in clone 9 passage 10 cells. The control panel shows primary human ameloblasts immunostained without primary antibody.

B) Semi-quantitative PCR with primers against amelogenin, MMP-20 and GAPDH.

Lane 1-DNA ladder, Lanes 2-4 where RNA isolated from different colonies of SV40-HA. Lane 5 positive control with human fetal tooth cDNA library, lane 6 negative control (water). Not all colonies express both amelogenin and MMP-20. Only Lane 4 (which is clone 9, passage 10) was positive for both amelogenin and MMP-20.

Collagen Type I expression in SV40-HA cells:

After we have established a pure clonal SV40-HA line we examined if our pure still retained their ability to express collagen Type I. qPCR results showed our SV40-HA cells express collagen Type I at the same relative level as that seen in our primary cell culture (Table 2).

TABLE 2:

	ΔCt	SD
Primary cells	11.47	0.36
SV40-HA cells	11.93	0.30

Table 2: No significant difference in the level of collagen Type I between primary human ameloblasts and SV40-HA cells. (P-value > 0.05)

Mineralization comparison between primary human ameloblasts vs. SV40-HA cells

At concentrations of 0.1mM and 0.3mM calcium, primary cells showed Von Kossa positive clusters after 4 weeks of treatment with the mineralization cocktail (Fig 4A). However, under the same conditions our clone 9 SV40-HA cells were not able to form von Kossa positive foci (Fig 4B).

FIG 4:

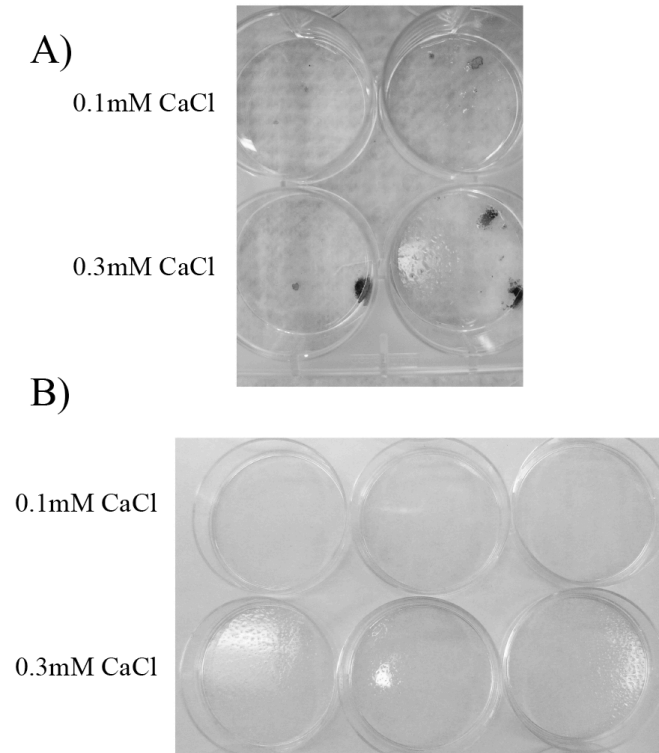


Figure 4: SV40-HA cells were unable to form Von Kossa positive clusters as compared to primary human ameloblast lineage cells.

A) Primary cell control-Von Kossa positive foci are seen as black clusters.

B) SV40-HA cells-no Von Kossa positive foci present at any concentration of calcium.

Discussion:

As discussed in appendix two, we found high levels of collagen Type I expression in our primary human ameloblast lineage cell culture. Those results led us to consider the level of heterogeneity in our primary cell population and if calcium was indirectly regulating ameloblast cellular functions. Expression of collagen Type I in our primary

cell culture was validated by real time PCR both from human ameloblast lineage cell lysates and mRNA isolated from ameloblasts by laser capture microscopy of human tooth fetal tooth buds (data not shown). In spite of this, *in situ* hybridization experiments were negative for collagen Type I expression by ameloblasts (data not shown). The combination of inconclusive evidence for collagen Type I expression in human ameloblasts and the presence of high levels collagen Type I in our cell primary cell culture caused some concern regarding our previous publication, where we found increased mineralization of our primary ameloblasts in response to elevated calcium [1]. We hypothesized that the positive mineralization could have been the result of a very heterogeneous primary cell culture containing a small proportion of mesenchymally derived cells, which were responsible for the collagen Type 1 expression and mineralized nodules. We explored this possibility by first developing a homogeneous immortalized ameloblast cell line using SV40 genome and then examining the levels of collagen Type I followed by assessing the mineralization capability of these cells.

Our SV40-HA cells were derived from one single colony and they expressed several major ameloblast markers, cytokeratin 14, amelogenin, and MMP-20. In addition to those ameloblast markers, our SV40-HA cells also expressed high levels of collagen Type I. We concluded our SV40-HA cells are of epithelial and not mesenchymal origin because they were derived from a single colony and after multiple passages they still retained high levels of cytokeratin 14 (epithelial cell marker).

Stellate reticulum cells are the only enamel organ epithelial cells that have been reported to express Type I collagen. Therefore, the fact that the SV40-HA cells express amelogenin [10], MMP-20 [11], cytokeratin 14 [12] and, more importantly, collagen Type I [13], suggests that the SV40-HA cells are derived from stellate reticulum. The exact role of the stellate reticulum still remains to be determined, and perhaps due to their unique position between the blood supply and the developing enamel, they function to provide a medium in which nutrients diffuse through to the ameloblasts.

SV40-HA cells were unable to produce the same mineral nodules as those seen in our primary cell culture, regardless of collagen Type I expression. This negative mineralization is consistent with the identity of these cells as stellate reticulum, which, even in the presence of Type 1 collagen, does not mineralize. We can then conclude that the mineralization nodules we saw in our primary cell culture were due to other cell types present in culture, and show the importance of other cell types for *in vitro* mineralization. The fact that the cells mineralized in the absence of serum containing media suggests that this mineralization is driven by epithelial rather than potentially contaminating mesenchymally derived cells.

Conclusion:

In summary, this study showed it was possible to maintain multiple passages of SV40 transfected human ameloblast lineage cells with retained primary cell like characteristics. SV40-HA cells were derived from one single colony and expressed

amelogenin, MMP-20, cytokeratin 14, and collagen Type I. This expression profile is indicative of stellate reticulum cells found in the enamel organ. These immortalized stellate reticulum cells were unable to form mineralization nodules as those seen in primary ameloblast lineage cell culture. This difference illustrates the importance of other cells or cellular factors needed to provide a mineral conducive environment. Further studies will be needed to determine what the other cell types are present in our primary cell culture and how those cells respond to calcium.

References

1. Chen, J., et al., *Calcium-mediated differentiation of ameloblast lineage cells in vitro*. J Exp Zool B Mol Dev Evol, 2009. **312B**(5): p. 458-64.
2. DenBesten, P.K., et al., *Characterization of human primary enamel organ epithelial cells in vitro*. Arch Oral Biol, 2005. **50**(8): p. 689-94.
3. Le, T.Q., et al., *The effect of LRAP on enamel organ epithelial cell differentiation*. J Dent Res, 2007. **86**(11): p. 1095-9.
4. Yan, Q., et al., *Differentiation of human ameloblast-lineage cells in vitro*. Eur J Oral Sci, 2006. **114 Suppl 1**: p. 154-8; discussion 164-5, 380-1.
5. Zhang, Y., et al., *JNK/c-Jun signaling pathway mediates the fluoride-induced down-regulation of MMP-20 in vitro*. Matrix Biol, 2007. **26**(8): p. 633-41.
6. Zhang, Y., et al., *Fluoride down-regulates the expression of matrix metalloproteinase-20 in human fetal tooth ameloblast-lineage cells in vitro*. Eur J Oral Sci, 2006. **114 Suppl 1**: p. 105-10; discussion 127-9, 380.

7. DenBesten, P., *Development and characterization of an SV40 immortalized porcine ameloblast like cell line*. Eur J Oral Sci, 1999(107): p. 276-281.
8. Maniatopoulos, C., J. Sodek, and A.H. Melcher, *Bone formation in vitro by stromal cells obtained from bone marrow of young adult rats*. Cell Tissue Res, 1988. **254**(2): p. 317-30.
9. Chen, J., et al., *Wnt/beta-catenin signaling plays an essential role in activation of odontogenic mesenchyme during early tooth development*. Dev Biol, 2009. **334**(1): p. 174-85.
10. Gutierrez-Cantu, F.J., et al., *Amelogenin and enamelysin localization in human dental germs*. In vitro cellular & developmental biology. Animal, 2011. **47**(5-6): p. 355-60.
11. Bourd-Boittin, K., et al., *Immunolocalization of enamelysin (matrix metalloproteinase-20) in the forming rat incisor*. The journal of histochemistry and cytochemistry : official journal of the Histochemistry Society, 2004. **52**(4): p. 437-45.
12. Tabata, M.J., et al., *Expression of cytokeratin 14 in ameloblast-lineage cells of the developing tooth of rat, both in vivo and in vitro*. Archives of Oral Biology, 1996. **41**(11): p. 1019-1027.
13. Webb, P.P., et al., *Immunolocalisation of collagens in the developing rat molar tooth*. Eur J Oral Sci, 1998. **106 Suppl 1**: p. 147-55.

Appendix 4: Detection and localization of CaSR in human ameloblasts

Rationale:

We found that calcium upregulated amelogenin expression (chapter two), and in this further study, we determined the possibility that this effect of calcium on amelogenin expression and upregulation of extracellular matrix proteins might be mediated by the calcium sensing receptor.

Materials/Methods:

Cell isolation and cell culture:

Primary ameloblast lineage cells were isolated from 18-23 week old fetal tooth buds, with permission obtained through the tissue-sharing program at UCSF, as previously described DenBesten *et al* in 2005 [1-5] as previously described in this chapter. Briefly, the tissue mass from these tooth buds was dispersed by the addition of 1 mg/ml collagenase/dispase mixture dissolved in PBS at 37°C for 2 hr. The tissue mass was further digested with 0.05% trypsin with EDTA for 5 min at 37°C. Ameloblast lineage cells were specifically selected for by keratinocyte selective media, KGM-2 w/o serum and supplemented with 0.05mM calcium.

RNA isolation and gene expression assays:

Total RNA was isolated from primary ameloblast cell cultures (control and 0.1mM calcium). Media was removed and plates were washed with PBS. Cells were scrapped from the plates following incubation in 0.05% trypsin for 5 min at 37°C, and total RNA was isolated using Qiagen's RNeasy Kit (Valencia, Ca). Purified RNA was quantified by UV spectroscopy on a Nanodrop (Thermo Fisher Scientific, Waltham, MA) and equal amounts of RNA from control and test samples were converted to cDNA by

Superscript III kit (Invitrogen, Carlsbad, Ca). Aliquots of the resulting cDNA were used for semi-quantitative PCR. CaSR primers: forward primer-AGGAAGTCT GTC CAC AAT GG and reverse primer- CAA TGA TCC CTT TCC TGG TC) were purchased from Elim Bio (Hayward, CA). CaSR expression levels were assessed by agarose gel electrophoresis.

Section preparation and immunofluorescent staining of paraffin sections:

Human fetal mandibles were isolated and dissected from fetal cadavers with permission from UCSF's Center for Human Research. Isolated human fetal mandibles and maxilla's were from 18-23 week old fetuses. The mandibles and maxillas were fixed with 4% PFA for 24hrs. After fixation, all samples were demineralized for 4 weeks in 10% EDTA. Demineralized samples were then paraffin embedded and sectioned at 5 μ m thicknesses. Some sections were stained with hemotoxylin and eosin, while other sections were used for immunofluorescent staining.

Paraffin samples were incubated with 5% BSA in PBS/0.1% Triton X-100 for 1 hr at room temperature to block non-specific binding. Samples were then incubated with primary antibodies against N-terminus of CaSR (Santa Cruz Biotech, Santa Cruz, Ca) and amelogenin overnight at 4° C. Control samples were incubated with purified rabbit IgG. Paraffin sections were then washed three times with PBS and incubated with secondary antibodies (Goat Anti-rabbit FITC conjugated 1:40, Sigma-Aldrich, St. Louis, MO) for 1 hr at RT. Sections were washed three more times with PBS and counterstained with Hoescht 1:10,000. Sections were then washed three times with PBS and mounted with permamount (Fisher, Pittsburg, PA). All samples were visualized by light microscopy

under epifluorescence on a Nikon E800 system (Nikon TMS, Melville, NY, USA) and SimplePCI imaging software version 5.3.1.

Results:

Paraffin sections of human fetal incisor tooth bud showed distinct localization of CaSR expression to pre-secretory and secretory ameloblasts. CaSR was expressed in early stage pre-secretory ameloblasts with slightly decreased expression up to the secretory stage (Fig 1C). We found that in CaSR expression in the secretory stage was highly variable with regions of high and low expression (Fig 1C). We distinguished early pre-secretory and secretory stage ameloblasts by assessing amelogenin expression (Fig 1B). In human ameloblast cell culture, we found abundant CaSR expression at the protein level, but only minimal levels of mRNA (Fig 2).

FIG 1:

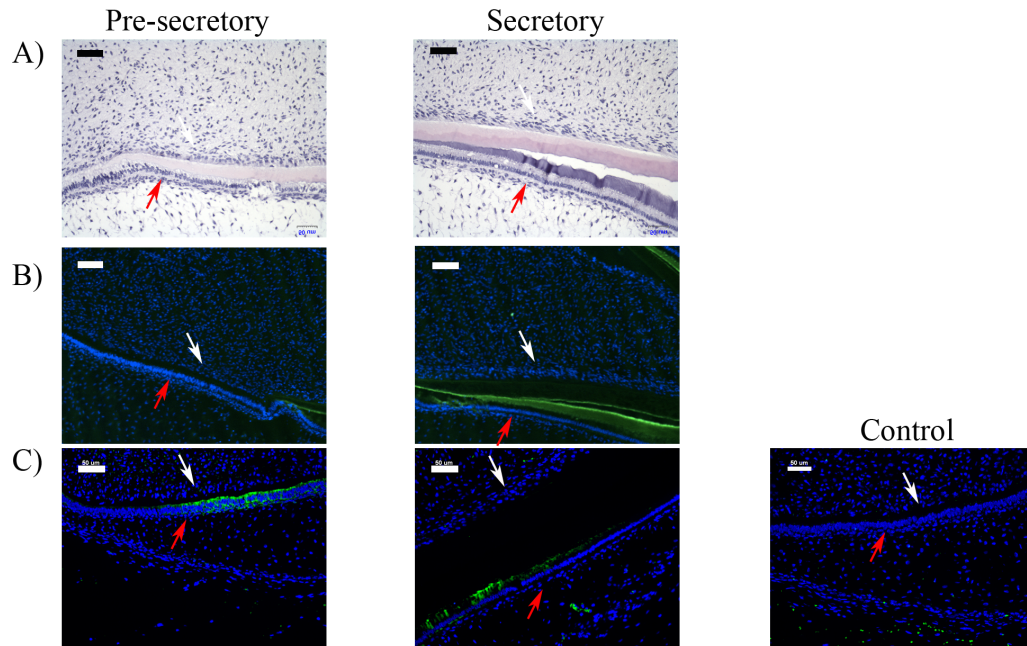


Figure 1-CaSR levels in human fetal tooth buds and human primary cell culture.

White arrows indicate odontoblasts, Red arrows indicate ameloblasts.

Images are taken from pre-secretory and secretory stage ameloblasts.

A) HE images showing pre-secretory and secretory ameloblasts along with some matrix formation.

B) The presence of amelogenin expression delineates secretory stage ameloblasts from pre-secretory stage ameloblasts (Green-amelogenin, Blue-Nuclei).

C) CaSR is expressed at high levels in pre-secretory ameloblasts, but in secretory ameloblasts CaSR expression was quite variable (Green-CaSR, Blue-Nuclei).

Last image is negative immunofluorescent control. Bar=50 μm

FIG 2:

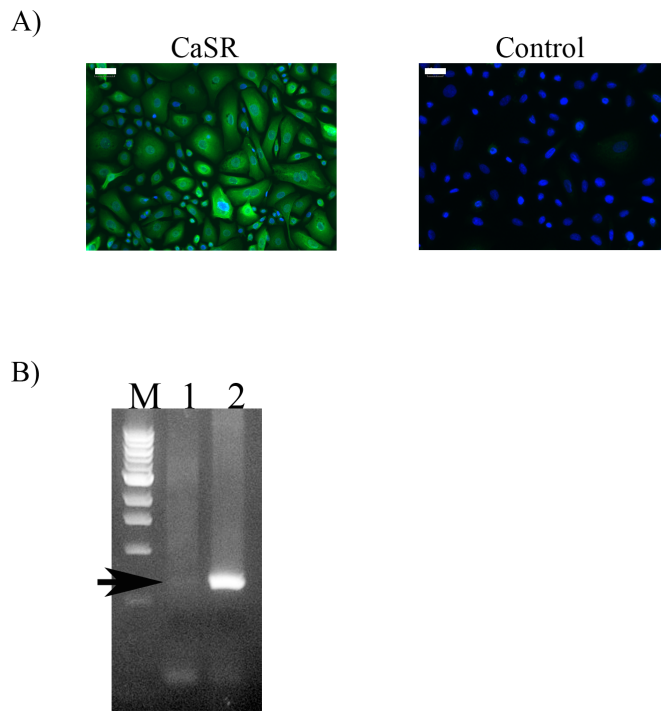


Figure 2-CaSR levels in human ameloblast primary cell culture.

A) Human primary ameloblast lineage cells showed very high levels of CaSR protein.

Green is positive CaSR expression on the left, and on the right is the negative control.

B) In contrast to the protein levels, only a small amount of CaSR mRNA was detected in

human ameloblast lineage cells (Arrow). M-marker, 1-primary human ameloblast

mRNA , 2-positive control mRNA from HEK-CaSR cells.

Conclusion:

In this study we confirmed CaSR expression in our human ameloblast lineage cells on both the protein and mRNA level. There was higher levels CaSR protein than CaSR mRNA, which suggests prolonged protein retention. Maturation of CaSR is highly dependent on proper folding during translation and requires numerous post-translational modifications, all of which require highly efficient protein synthesis machinery [6]. More recently, a conformational checkpoint for CaSR retention in the endoplasmic reticulum has been identified, which could explain the high levels of CaSR protein but low levels CaSR mRNA we see in our cultured cells [6]. CaSR is connected to multiple intracellular signaling pathways and the role of the CaSR in mediating amelogenin expression in ameloblasts requires further study.

References

1. DenBesten, P.K., et al., *Characterization of human primary enamel organ epithelial cells in vitro*. Arch Oral Biol, 2005. **50**(8): p. 689-94.
2. Le, T.Q., et al., *The effect of LRAP on enamel organ epithelial cell differentiation*. J Dent Res, 2007. **86**(11): p. 1095-9.
3. Yan, Q., et al., *Differentiation of human ameloblast-lineage cells in vitro*. Eur J Oral Sci, 2006. **114 Suppl 1**: p. 154-8; discussion 164-5, 380-1.
4. Zhang, Y., et al., *JNK/c-Jun signaling pathway mediates the fluoride-induced down-regulation of MMP-20 in vitro*. Matrix Biol, 2007. **26**(8): p. 633-41.

5. Zhang, Y., et al., *Fluoride down-regulates the expression of matrix metalloproteinase-20 in human fetal tooth ameloblast-lineage cells in vitro.* Eur J Oral Sci, 2006. **114 Suppl 1**: p. 105-10; discussion 127-9, 380.
6. Cavanaugh, A., et al., *Calcium-sensing receptor biosynthesis includes a cotranslational conformational checkpoint and endoplasmic reticulum retention.* J Biol Chem, 2010. **285**(26): p. 19854-64.

CHAPTER 2 CONCLUSION

The results from these studies of human ameloblast lineage cell provided insights into the role of extracellular calcium on amelogenesis. Extracellular calcium appears to regulate gene expression of both extracellular matrix proteins as well as enamel matrix proteins, specifically amelogenin. Calcium mediated upregulation of amelogenin expressions occurs specifically at the promoter and this is likely mediated through multiple cell signaling molecules. The effect of calcium on gene expression is dependent on both the level of calcium and the duration of exposure.

The presence of the CaSR in the developing ameloblast *in vivo* and *in vitro*, suggest that the CaSR may be a candidate for calcium related regulation of ameloblast differentiation. This question is addressed in the following chapter, where we characterized the effect of targeted CaSR ablation in epithelial cells.

CHAPTER 3-CASR TISSUE SPECIFIC KNOCKOUT MOUSE

Introduction

Enamel formation is controlled by specialized mineral forming epithelial cells called ameloblasts, which are derived from oral epithelial precursor cells found in the developing oral cavity [1]. Ameloblasts progressively mature from oral epithelial cells to terminally differentiated ameloblasts, and in doing so, they undergo changes in both cell morphology and gene expression [1].

Histodifferentiation of precursor ameloblasts begins in the bell stage of tooth formation, where ameloblast terminal differentiation is separated into different stages (i.e. presecretory, secretory, transition, maturation). These stages are distinguished from one another by cellular morphology and regulated gene expression of multiple enamel matrix proteins [2], including the amelogenins, which are critical for enamel formation [2].

Extracellular calcium at levels above 0.1 mM has been shown to regulate the formation of the enamel matrix by controlling amelogenin expression in hamster and human *in vitro* models [3, 4]. Both rat and human ameloblast cells grown in culture have been used to show that calcium affects ameloblast cell morphology, with increasing cellular organization [4, 5]. These studies showed calcium could have a specific role in ameloblast differentiation.

The role of intracellular calcium levels on ameloblast cellular function is not well defined. Many published studies have focused on calcium transport through ameloblasts, and the potential role of calcium transporters calbindin 28K and

calbindin 9K, on calcium export to the extracellular matrix [6]. Calbindin 28K is strongly expressed by maturation stage ameloblasts, while calbindin 9K is only weakly expressed [7, 8], leading to a proposed function of calbindin 28K in ameloblast calcium transport. Several recent studies on calbindin 28K null mouse models showed very minimal effects on enamel formation [9, 10]. Other calcium interacting proteins such as Ca-ATPases are also expressed in ameloblasts, but little evidence is available regarding their direct role in amelogenesis [6].

The role of extracellular calcium on ameloblast function has focused on the calcium sensing receptor (CaSR) [11, 12]. CaSR was discovered in bovine parathyroid cells, where it monitors fluctuations in the level of serum calcium and responds accordingly via parathyroid hormone expression and secretion [12, 13]. CaSR is expressed in multiple cell types (most notably fibroblasts, osteoblasts, and keratinocytes) [11], some of which directly regulate calcium while others do not [14]. More importantly with regards to tooth development, CaSR was localized at the apical border of secretory ameloblasts in multiple species [15, 16], and has been proposed to have a role in modulating ameloblast function as enamel mineralization progresses [4, 17, 18].

In vivo studies using germ-line CaSR^{-/-} mice, which we will refer to as CaSR^{-/-} from now on, further support a possible link between CaSR and enamel formation. Ho *et al* [19] characterized mineral formation in a mouse model lacking CaSR activity, and found incomplete mineral formation in all mineralized tissues (bone, dentin, enamel). Subsequently, Sun *et al* [20] used this same mouse model to focus more specifically on tooth formation, and concluded that CaSR was required for

tooth formation. This particular mouse model has very high PTH and calcium levels with poor survival beyond weaning. The authors later showed that when the same CaSR^{-/-} mice, with severely hypomineralized enamel, were crossed with PTHrP^{-/-} mice, the phenotype was partially rescued [20]. These studies suggest that the effect of CaSR on tooth formation is related to its role in modulation of serum calcium concentrations.

Two major limitations exist in both these studies that make it difficult to determine the extent of CaSR function in enamel formation. The first limitation relates to CaSR expression in multiple cell types, and therefore, a germ-line knockout mouse model would potentially make it difficult to determine if the reduced mineralization phenotype was a direct result of lost CaSR function in ameloblasts or an indirect result of deregulated calcium homeostasis. The second limitation is related to how the germ-line knockout mouse was generated. Both studies used a knockout mouse in which the neomycin cassette was inserted into exon 5 of the full length CaSR gene. The drawback to this method of disrupting CaSR activity is the fact that an alternatively spliced variant of CaSR exists, which lacks exon 5 [21]. The result of this splice variation is CaSR transcripts without the inserted neomycin cassette. This truncated CaSR, lacking 77 amino acids in the extracellular domain, compensates to some degree the loss of full-length CaSR [22].

In this study we used a mouse line that specifically addresses both limitations to determine whether the CaSR can directly affect ameloblast function. We analyzed a tissue specific CaSR knockout mouse (K14-Cre-CaSR^{-/-}) line generated in the Bikle lab [23] that was made by mating a mouse with Cre

recombinase transcribed under the control of the cytokeratin 14 (K14) promoter, and a second mouse in which exon 7 of CaSR is flanked by two lox sites. The result of mating these two mice is deletion of exon 7, which codes for the transmembrane region of the CaSR, specifically in epithelially derived cells. Cytokeratin 14 is known to be synthesized by the enamel organ epithelium, with no expression in the dental mesenchyme, thus making this an ideal model to address the question of whether the CaSR can modulate ameloblast directed enamel formation and mineralization [24]. To enhance the potential effects of the CaSR ablation, we treated the K14-Cre-CaSR^{-/-} mice with either low calcium diet (normal calcium levels in the diet are 1.3% and our low calcium diet was 0.02%) or drinking water supplemented with 50 ppm fluoride.

METHODS:

K14-Cre-CaSR^{-/-} model

FloxCaSR mice were generated as described by Tu *et al* [23] and they were crossed with mice that express Cre recombinase under the control of the K14 promoter. The mouse CaSR gene and the RF8 ES cells were derived from 129Sv mice, while the K14-Cre mice were C57Bl6. The offspring of a cross between K14-Cre mice and FloxCaSR mice yielded a mixed background mouse that has the CaSR gene knocked-out specifically in cell types expressing K14. These mice express a truncated version of CaSR lacking exon 7, which contains the transmembrane domain and intracellular domain, which result in a loss of signaling capacity [23].

The efficiency of the conditional knockout mice in the tooth enamel organ was determined by quantifying the expression of full length CaSR mRNA in enamel tooth organs of 3-week old wild type and K14-Cre-CaSR^{-/-} mice. Mandibles were isolated and the cervical loop region was micro-dissected away from the bone, and digested in collagenase (2%) (Worthington, Lakewood, NJ) for 4 hrs on ice. After 4 hrs of collagenase treatment the epithelial layer was mechanically separated from the mesenchymal layer and mRNA was isolated by Qiagen's RNeasy kit (Valencia, CA). The amount of total RNA isolated from each sample was measured using a NANODROP (Thermo Scientific, Wilmington, DE), and equal amounts of RNA were reverse transcribed into cDNA by Invitrogen's Superscript III kit (Carlsbad, CA). Real-time PCR and semi-quantitative PCR using primers specific for exon 7 of the full-length CaSR transcript were used to assess the knockout efficiency in enamel epithelial cells (lox 7up: 5'---TGTGACGGAAAACATACTGC---3', Lox7 low: 5'---CGAGTACAGGCTTTGATGC---3').

Sybergreen green reactions using Lox7up and low primers were conducted at 58°C annealing/extension temperature (Sybergreen master mix was from Roche, Redwood City, CA, Real-Time PCR system from Applied Biosystems, Redwood City, CA). For semi-quantitative PCR, the annealing temperature was 50°C with an extension time of 30 sec and the level of CaSR was assessed by agarose gel separation.

Histological and immunohistochemical characterization of tooth organs

Both wild type and K14-Cre-CaSR^{-/-} were sacrificed at 3-days and 2-month-old. Three-day-old mice mandibles were immerse-fixed in 4% paraformaldehyde for 30 min at 4°C. Mandibles from 2-month-old mice were immerse-fixed in 4% paraformaldehyde for 24 hrs at 4°C, followed by demineralization using 10% EDTA pH 8.0 for four weeks.

The mandibles were processed for paraffin embedding and sectioned at 5 µm thick sections. Paraffin embedded sections were de-waxed and used for HE staining as well as immunofluorescent staining. Sections were incubated overnight at 4° C with primary antibodies specific for C-terminal domain of CaSR (gift from Bikle lab) (ain press) and amelogenin (generated by our lab) [25]. After three washes with PBS, the sections were incubated with secondary antibodies conjugated with FITC (Sigma-Aldrich, St. Louis, MO) for one hour at room temp. The sections were then washed again and counterstained for nuclei by Hoescht (Invitrogen, Carlsbad, CA). Images were taken with a Nikon Eclipse E3800 microscope (Melville, NY) using a digital camera and SimplePCI imaging software version 5.3.1.

Relative enamel matrix gene expression from isolated mandibles analyzed by qPCR

Mandibles from three separate wild type and K14-Cre-CaSR^{-/-} mice given a normal diet were dissected, frozen at -20°C overnight, and then crushed with a microtube pestle. mRNA was isolated using a MicroRNAeasy kit from Qiagen (Valencia, CA), quantified (NanoDrop, Thermo Fisher Scientific, Waltham, MA), and

converted to cDNA using Invitrogen's (Carlsbad, CA) Superscript III kit with the use of random primers. Aliquots of the resulting cDNA were used for gene expression assays. Relative expression of amelogenin, MMP-20, ameloblastin, and GAPDH from mandibles of wild type and K14-Cre-CaSR^{-/-} mice was analyzed by real-time PCR system, using commercially synthesized primers (Applied Biosystems, Redwood City, CA).

Micro X-ray Computed Tomography (Micro XCT):

Wild type and K14-Cre-CaSR^{-/-} mice were maintained on a normal diet, low calcium diet, and with water containing 50 ppm fluoride for four weeks after weaning. For all groups, after four weeks treatment the animals were sacrificed, the mandibles dissected free of other tissues, cleaned and stored in 70% ethanol at 4°C until micro-CT analysis. Computer tomography scans were obtained using a MicroXCT-200 (Xradia Inc., Concord, CA, USA). A 2X objective was used to obtain resolutions of approximately 11.3 µm, respectively. X-rays were set to 75 kV (molars and surrounding bone only) and amperage selected accordingly such that the power was kept at 6 W. Each tomograph was reconstructed from 2100 radiographic projections obtained from scan angles ranging from -104° to 104° and exposure times were adjusted to yield 8,000 to 13,000 counts per pixel of each recorded radiograph approximating 25% of the original X-ray intensity passing through the specimen and arriving at the detector. All specimens were submerged in 70% ethanol to avoid imaging artifacts due to drying while scanning. 3D images

were reconstructed from the recorded X-ray projections using reconstruction software (XMReconstructor, Version 7.0.2817, Xradia Inc., Concord, CA, USA).

Micro XCT Data analysis:

After XMR reconstruction, data from each sample were converted into dicom data format for image processing and quantification. A specific density threshold was set for each sample using Dolphin Imaging software (Chatsworth, CA). Relative intensity for enamel and dentin was measured in Hounsfield units through Dolphin imaging. The region of the highest intensity of Hounsfield units both in the enamel and dentin were used for comparisons between samples. Measurements were made at the same section of each sample (mesial root of the 1st molar, distal root of the 1st molar, mesial root of the 2nd molar, and the distal root of the 2nd molar). The relative ratio of enamel image intensity to dentin image intensity was used to calculate the initiation of enamel mineralization between samples. Statistical analyses (described below) were conducted to test for significance in mineral density. The enamel thickness of incisors, 1st and 2nd molars were directly measured using Dolphin Imaging software (Chatsworth, CA).

Statistics:

The relative gene expression of K14-Cre-CaSR^{-/-} and wild type mice was compared using paired Student *t*-test. Differences in mineral intensity and enamel thickness were assessed by ANOVA followed by direct comparisons between K14-Cre-CaSR^{-/-} and wild type mice using unpaired Student *t*-testing.

RESULTS:

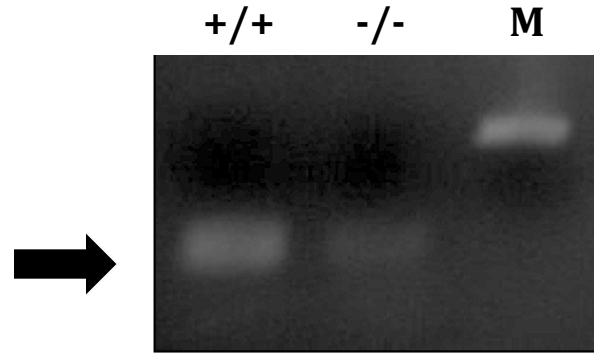
K14-Cre-CaSR^{-/-} mice showed high tissue specificity with a variable knockout efficiency

CaSR exon 7, which was the conditionally deleted transmembrane/ intracellular segment in the in the K14-Cre-CaSR^{-/-} mouse could be amplified in enamel organs of both the wild type and K14-Cre-CaSR^{-/-} mice (Fig 1A). Semi-quantitative PCR (Fig 1A) showed a reduction in expression of transcripts containing exon 7 in the K14-Cre-CaSR^{-/-} mice as compared to the wild type mice, and further analysis by qPCR (using the same primer sequences) quantified the reduction as a 5-fold decrease in the amplification of exon 7 of K14-Cre-CaSR^{-/-} mice (data not shown).

Similarly, when we compared the protein levels between the K14-Cre-CaSR^{-/-} and wild-type mice, using an antibody specific for the C-terminus, we found reduced immunostaining for the CaSR (Fig 1B). The reduction in CaSR was seen in intracellular vesicles of secretory stage ameloblasts and perinuclear staining in maturation stage ameloblasts. However, consistent with our mRNA analysis, residual cytoplasmic CaSR remained present in K14-Cre-CaSR^{-/-} mouse sections. We did not see a difference in the level of CaSR in mesenchymally derived cells, such as odontoblasts or osteoblasts (Fig 1B).

FIG 1:

A)



B)

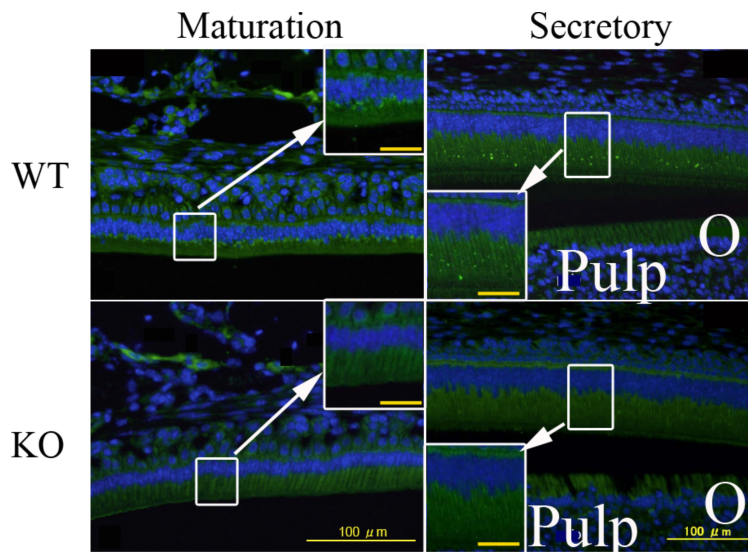


Figure 1: CaSR expression and cellular localization in maturation and secretory stage ameloblasts showing incomplete K14-Cre-CaSR^{-/-} knockout efficiency.

A) Primers specific for exon 7 of CaSR, which is the deleted region in

K14-Cre-CaSR^{-/-} mice, were used to assess the knockout efficiency. Wild-type (+/+) mice showed amplification of transcripts containing exon 7, while K14-Cre-CaSR^{-/-} mice (-/-) showed reduced amplification of the same transcripts.

B) An antibody specific for the C-terminus (exon 7 translated region including the transmembrane domain and intracellular domain) was used to assess CaSR protein levels. These are sagittal sections through a mouse mandible, where green fluorescence represents CaSR and blue fluorescence represents nuclear staining. In secretory stage ameloblasts (right images), CaSR localized intensely to discrete vesicles in the wild-type mouse, and this localization was not evident in the K14-Cre-CaSR^{-/-} mouse. In the maturation stage ameloblast (left images), CaSR was highly localized to the perinuclear region, and this was not seen in K14-Cre-CaSR^{-/-} mice. Insets represent higher magnification images of the designated white boxes. (yellow bar = 100 micron, O = odontoblasts)

K14-Cre-CaSR^{-/-} mice presented with no obvious changes on overall tooth morphology or ameloblast cellular morphology.

There were no obvious differences in the appearance, length, and shape of the erupted portion of the incisors between K14-Cre-CaSR^{-/-} and wild type mice (Fig 2). Histologically we did not find any obvious differences in cell morphology and organization at all stages of ameloblast differentiation when comparing wild type

and K14-Cre-CaSR^{-/-} mice (Fig 3). Additionally, the distribution of the epithelially derived supporting structures (stratum intermedium and stellate reticulum) was similar in K14-Cre-CaSR^{-/-} and wild type mice (Fig 3).

FIG 2:

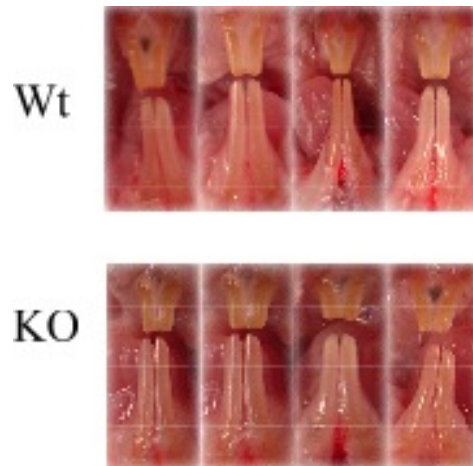


Figure 2: Normal appearance of the erupted incisors isolated from K14-Cre-CaSR^{-/-} mice.

Digital images were taken of erupted incisors from wild type (Wt) and K14-Cre-CaSR^{-/-} (KO) mice. No differences in length, color, and shape were visible between the wild type and K14-Cre-CaSR^{-/-} mice were present.

FIG 3:

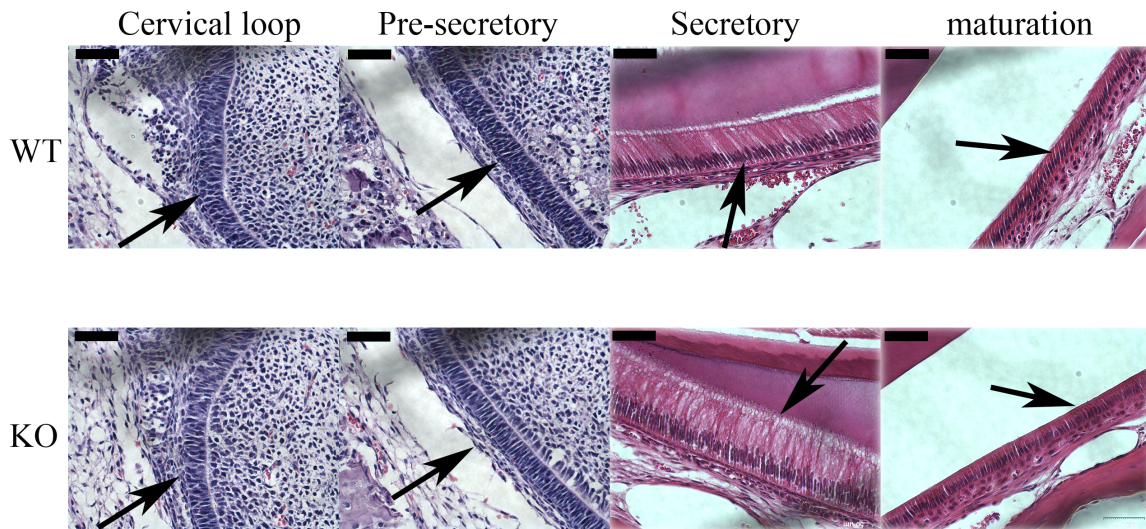


Figure 3: Normal ameloblast cellular morphology and organization in K14-Cre-CaSR^{-/-} mice.

HE staining of sagittal sections of mandibles isolated from both wild-type (Wt) and K14-Cre-CaSR^{-/-} (KO) mice. Normal cellular (compared to wild type sample) architecture and organization was evident in K14-Cre-CaSR^{-/-} samples (bottom row) at all four stages of differentiation. Black arrows indicate ameloblasts, scale bar 50 micron)

Enamel matrix expression profile analysis of wild-type and K14-Cre-CaSR^{-/-} mouse tooth organs showed no significant differences between the two groups..

No significant differences in the relative amounts of amelogenin, MMP-20 or ameloblastin mRNA in K14-Cre-CaSR^{-/-} mice compared to wild type mice (Table 1). Consistent with this mRNA data, levels of amelogenin protein between the K14-Cre-

CaSR^{-/-} and wild type mouse were unchanged in immunofluorescent staining of 3-day old mice mandibles (Fig 4).

TABLE 1:

AMELOGENIN

	Δ Ct	SD
Wild-type	5.20	0.34
K14-Cre-CaSR^{-/-}	6.23	0.83

AMELOBLASTIN

	Δ Ct	SD
Wild-type	9.94	0.45
K14-Cre-CaSR^{-/-}	10.05	0.76

MMP-20

	Δ Ct	SD
Wild-type	15.03	0.37
K14-Cre-CaSR^{-/-}	16.03	0.89

Table 1: Normal enamel matrix gene expression in K14-Cre-CaSR^{-/-} mice.

qPCR analysis of the major enamel matrix genes (amelogenin, ameloblastin, and MMP-20) showed no statistical difference between wild-type and K14-Cre-CaSR^{-/-} mice (P>0.05 paired t-test).

FIG 4:

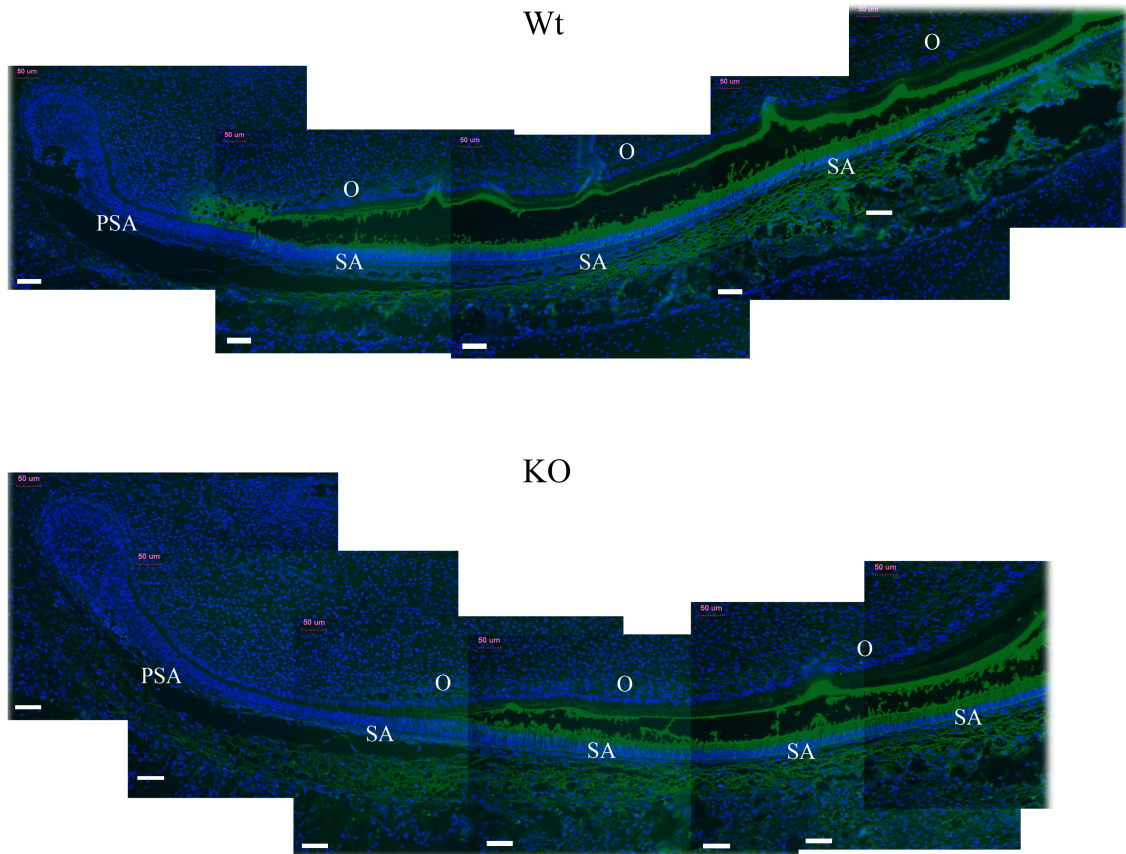


Figure 4: Normal amelogenin protein expression and localization in K14-Cre-CaSR^{-/-} mice.

Sagittal section of 3-day-old mouse incisor wild type (top) and K14-Cre-CaSR^{-/-} (bottom). No difference in terms of localization of amelogenin was detectable between the K14-Cre-CaSR^{-/-} and wild type mice when focusing on pre-secretory (PSA) to secretory (SA) ameloblasts (odontoblasts-O, bar=50 micron). Green-amelogenin, Blue-nuclei.

Enamel mineralization is initiated earlier in K14-Cre-CaSR^{-/-} mice as compared to wild type mice:

There was no difference in the thickness of enamel in the lower incisor, and lower 1st and 2nd molars between wild type and K14-Cre-CaSR^{-/-} mice (Table 2). However, on closer examination of the lower incisors, K14-Cre-CaSR^{-/-} mice showed earlier enamel formation as compared to the wild type mice (Fig 5). Mineralization began just distal to distal root of the second molar in K14-Cre-CaSR^{-/-} mice compared to at the distal root of the first molar in wild type mice (Fig 5). The relative mineral intensity was assessed as a ratio of the measured by image intensity of the developing incisor enamel relative to the image intensity of the developing incisor dentin. This ratio was determined at four specific stages: underlying either the mesial root of the first molar, the distal root of the first molar, the mesial root of the second molar and the distal root of the second molar. Using triplicate samples we found consistent early mineral formation in the incisors of K14-Cre-CaSR^{-/-} mice (Fig 6). The presence of fluoride in the drinking water or reduced calcium in the diet both significantly enhanced this early enamel formation phenotype (Fig 5,6)

TABLE 2:

NORMAL DIET

	Incisor (mm)	SD	1 st molar (mm)	SD	2 nd molar (mm)	SD
Wild-type	1.4	0.06	1.2	0.06	1.2	0.06
K14-Cre-CaSR^{-/-}	1.4	0.06	1.2	0.0	1.3	0.0

LOW CALCIUM DIET

	Incisor (mm)	SD	1 st molar (mm)	SD	2 nd molar (mm)	SD
Wild-type	1.4	0.1	1.2	0.2	1.2	0.1
K14-Cre-CaSR^{-/-}	1.4	0.1	1.0	0.2	1.2	0.06

50 PPM FLUORIDE WATER

	Incisor (mm)	SD	1 st molar (mm)	SD	2 nd molar (mm)	SD
Wild-type	1.3	0.06	1.1	0.06	1.3	0.0
K14-Cre-CaSR^{-/-}	1.3	0.06	1.0	0.1	1.3	0.1

Table 2: K14-Cre-CaSR^{-/-} showed no difference in the thickness of enamel.

Coronal sections generated by Dolphin Imaging were used to measure the enamel thickness at the incisor, 1st molar, 2nd molar for both wild type and K14-Cre-CaSR^{-/-} mice. There was no difference in the thickness enamel at all three regions (ANOVA P>0.05).

FIG 5:

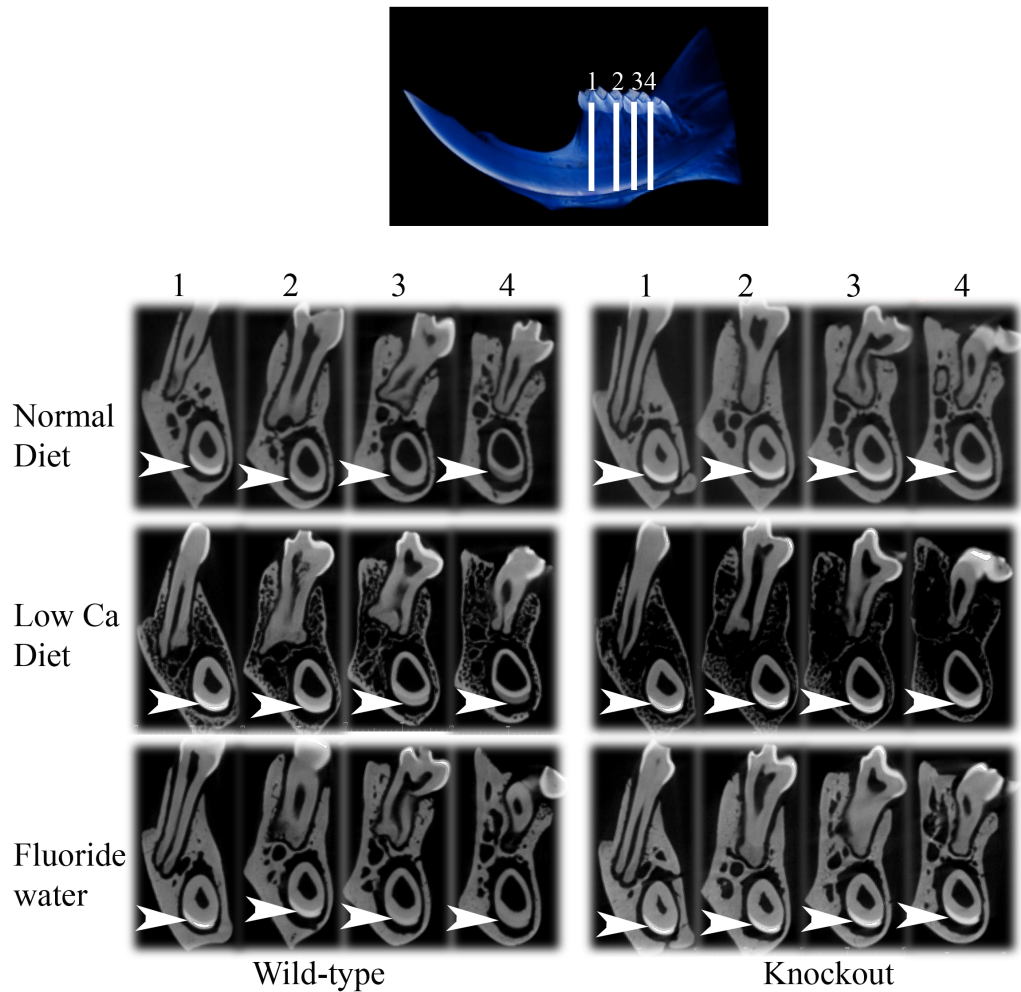
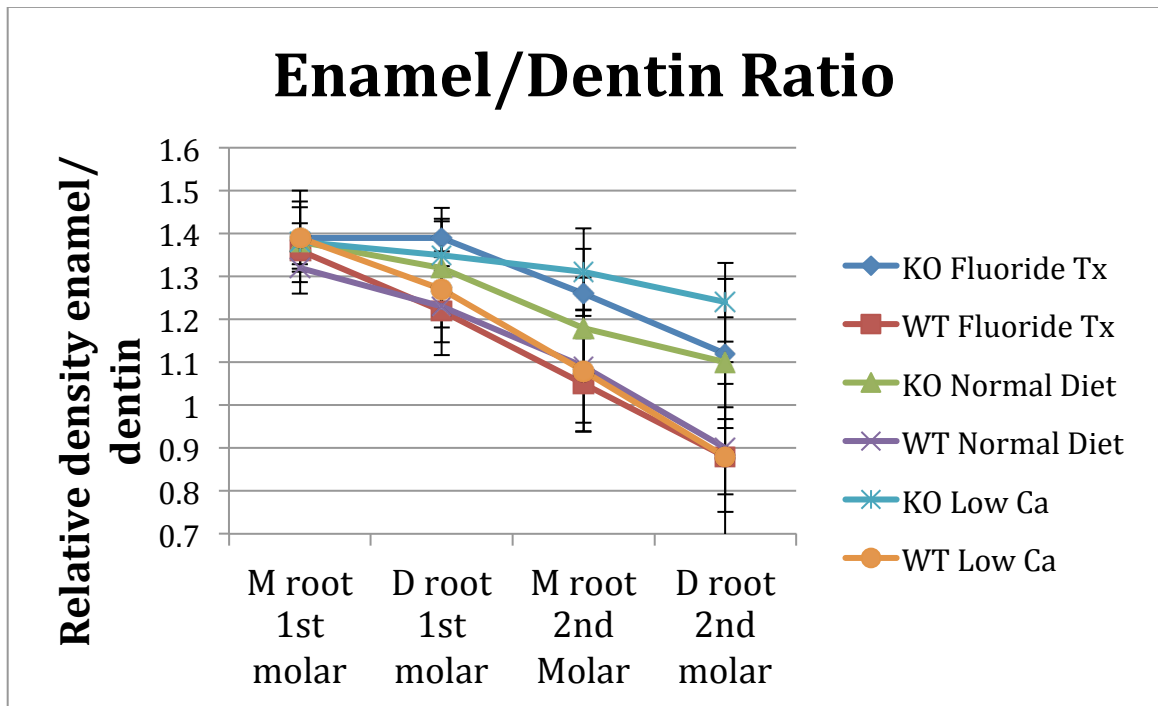


Figure 5: Coronal sections from Micro-CT scans showed early enamel formation in $K14-Cre-CaSR^{-/-}$ mice.

One representative mouse sample from each treatment group and genetic background was used for this image composite. For each mandible four coronal sections were generated using Dolphin Imaging Software. Each section was generated at the mesial root of the first molar **(1)**, distal root of the first molar **(2)**, mesial root of the second molar **(3)**, and distal root of the second molar **(4)**, location

of the sections are shown in the 3D volumetric view (top image). White arrows indicate the developing enamel of the lower incisor. Incisor enamel formation started by the distal root of the second molar in K14-Cre-CaSR^{-/-} mice of from all three-treatment groups; whereas, for the wild-type mice, enamel formation began by the distal root of the 1st molar for all three-treatment groups.

FIG 6:



	M Root 1 st Molar	D Root 1 st Molar	M root 2 nd Molar	D root 2 nd Molar
Normal Diet WT vs. KO (P-value)	0.191	0.161	0.118	0.066 (#)
Fluoride Water WT vs. KO (P-value)	0.484	0.076 (#)	0.040 (*)	0.050 (*)
Low Ca Diet WT vs. KO (P-value)	0.458	0.166	0.046 (*)	0.029 (*)

Figure 6: *Early enamel formation in K14-Cre-CaSR^{-/-} mice quantified by comparing relative mineral intensity of the developing incisor enamel and dentin.*

Relative intensities were assessed by comparing the highest Hounsfield units of both enamel and dentin of the developing incisor at the designated regions determined in figure 5 **(1,2,3,4)**. The readings were measured using coronal sections generated by Dolphin Imaging at the mesial root of the 1st molar, distal root 1st molar, mesial root of the 2nd molar, and the distal root of the 2nd molar. Readings for each group was measured using triplicate samples. Knockout mice had higher enamel to dentin relative mineral intensity ratio at the distal root of the second molar compared to wild-type mice (ANOVA $p < 0.05$). Direct comparisons between knockout and wild-type mice showed that both a reduction of calcium from the diet and the addition of fluoride in the drinking water were able to enhance the early enamel formation phenotype (t-test, $P < 0.05$ starting at the mesial root of the 2nd molar to the distal root of the 2nd molar).

Discussion:

The calcium sensing receptor is a key membrane bound receptor, whose activity regulates multiple cellular processes. CaSR^{-/-} knockout mouse studies have shown CaSR is instrumental in regulating mineralization of bone, enamel, and dentin [19, 20]. However, determining what specific role CaSR has in each of these tissues has been difficult due expression of CaSR in a multitude of tissues, including tissues critical for calcium homeostasis. Additionally, recent evidence has shown that the germ-line knockout of CaSR, functionally, may be incomplete due to the

presence of an alternatively spliced variant of CaSR, which retains some residual activity [23].

Chang *et al* [23] showed that a tissue specific CaSR knockout mouse model (Type I collagen-Cre-CaSR^{-/-}) helped in accurately deciphering what the direct role of CaSR is on osteoblast differentiation. These authors also found a significant difference in the viability of their mouse model versus that of the germ-line knockout model. Based on this premise we sought to determine what the direct role of CaSR activity is on enamel formation and in our study we characterized the effect of reducing CaSR activity specifically in cytokeratin 14 expressing cells, which included mouse ameloblast lineage cells.

The difference between using a germ line knockout mouse model as opposed to a tissue specific knockout mouse model was clearly seen in the difference in overall size of the mandible and teeth of our K14-Cre-CaSR^{-/-} mice model. The size, length, and shape of the erupted incisors and molars from our K14-Cre-CaSR^{-/-} mice were the same as the wild-type mice, which was in contrast to the CaSR^{-/-} mouse characterized by Sun *et al* [20], whom showed significantly smaller mandibles and teeth. This difference between the two mouse models provides evidence to support the view that CaSR may not be as critical for tooth formation as described by Sun *et al*. Also in their study, Sun *et al* found when they crossed CaSR^{-/-} mice with PTHrP^{-/-} mice almost a complete rescue of the initial phenotype occurred [20]. The combination of their results with PTHrP^{-/-} mice crossed CaSR^{-/-} mice and our findings lend strong support for a more specialized role for CaSR as compared to a master regulator of tooth size and shape as previously thought.

Further evidence for a more specialized role has come from several *in vitro* and *in vivo* studies that have shown a direct relationship between calcium and ameloblast cellular function [4, 5, 26-28]. Because of its significant relationship with calcium signaling we sought to evaluate the effects of decreased CaSR activity on ameloblast cellular function. Histologic examination of the developing incisor showed no difference in the morphology or organization between wild type and K14-Cre-CaSR^{-/-} mice. Furthermore, we found no significant difference in enamel matrix gene expression, specifically amelogenin, ameloblastin, and MMP-20, between the wild type and K14-Cre-CaSR^{-/-} mice. These results showed that CaSR is likely not the only receptor responsible for transmitting changes in extracellular calcium intracellularly; this would therefore suggest that other redundant mechanisms may regulate this calcium effect.

A possible mechanism is the ability of other members of the G-protein coupled receptor (GPCR) family to bind calcium and activate intracellular signals. More specifically, CaSR belongs to a superfamily of GPCR's and among these family members there exists some degree of redundant calcium signaling [14]. GPCR family C members share at least 20% amino acid identity in their transmembrane domain and they constitute a wide range of different receptors with very specific functions [29]. Among these members of family C, several receptors can respond to elevated levels of calcium in a manner similar to CaSR. mGluRs 1,3, and 5 can sense calcium over a range of 0.1mM to 10mM (well within the range of calcium levels in the enamel matrix), and mGluR2 receptor responding to altered calcium levels at a much higher threshold [30]. Furthermore, mGluRs 1,3, and 5 contain specific serine

residues in their extracellular domain that is required for calcium binding [30]. However, the level of cooperative binding of these putative calcium binding sites differs significantly from CaSR, where CaSR has a Hill coefficient of 3, mGluRs have a Hill coefficient of 1 [30-34]. Currently there have been no studies evaluating the expression pattern of these mGluR proteins in ameloblast lineage cells, though recently we have identified positive expression of mGluR1 in a microarray analysis of human ameloblast lineage cells (data not shown).

In addition to mGluRs, the function of GABA_B receptor is also modulated by changes in the level of extracellular calcium [35]. However, calcium by itself does not directly activate GABA_B receptors but in fact calcium potentiates the stimulatory action of GABA on G-protein activation [35]. Taken together, the abilities of other GPCR's to bind calcium and activate multiple downstream pathways shows that there is a level of degeneracy between GPCR's, which could contribute extracellular calcium signaling and explain the lack of any significant cellular changes of ameloblasts from K14-Cre-CaSR^{-/-} mice.

To determine whether the CaSR has a role in the initiation of enamel formation, we evaluated the timing of enamel formation in our K14-Cre-CaSR^{-/-} mouse model. Using microCT scans of K14-Cre-CaSR^{-/-} and wild-type mice, we found a subtle but detectable difference in the timing of enamel formation between the two mice. K14-Cre-CaSR^{-/-} mice showed earlier enamel formation as compared to wild type mice; however, images from several different mice showed high variability. Subsequently, we quantified this effect of the CaSR in generating earlier enamel formation; we found no statistically significant differences, with a p-value of 0.066.

We further hypothesized that the high variability in the expression of the early enamel formation phenotype was exacerbated by the variable efficiency of the CaSR knockout. We were only able to detect a 5-fold reduction of intact CaSR in enamel organ epithelial cells from K14-Cre-CaSR^{-/-} mice. Likewise, immunofluorescent imaging of both secretory and maturation stage ameloblasts from K14-Cre-CaSR^{-/-} mice confirmed reduced expression of full length CaSR and not its complete ablation.

The combination of variable expressivity and incomplete knockout efficiency led us to explore other methods to further reduce the local calcium concentrations in the developing enamel matrix. We therefore analyzed the effects of a low calcium diet (change from 1.3% to 0.02%) and increased fluoride in the drinking water (50 ppm fluoride) on modulation of enamel matrix formation by the CaSR. Both fluoride and calcium are known to regulate ameloblast cellular function [33-38], and some studies have shown that calcium protects against the adverse effects of fluoride on ameloblast function [26, 36]. We determined the addition of fluoride and reduction in calcium would offer a significant enough of a change in the chemical environment of the developing enamel to possibly enhance the early enamel formation phenotype we saw in our K14-Cre-CaSR^{-/-} mice [26, 37].

When we compared wild-type mice to the K14-Cre-CaSR^{-/-} mice treated with either a reduction in dietary calcium treated or with fluoride we found significantly earlier enamel formation in K14-Cre-CaSR^{-/-} mice. K14-Cre-CaSR^{-/-} mice from both treatment groups consistently began enamel formation around the distal root of the second molar as compared to wild-type mice, where enamel was first detected between the 1st and 2nd molar (P<0.05). In a separate set of experiments we

confirmed both treatments, individually, did not have a direct effect on enamel initiation in wild-type mice. Similar comparisons using K14-Cre-CaSR^{-/-} mice, mice showed no significant differences in timing of initiation of mineral formation between fluoride treated and low calcium diet versus normal a normal diet. Based all the aforementioned mineral intensity comparisons, we can conclude that CaSR regulates the timing of enamel formation and the reduction of calcium in the diet or the addition of fluoride to the drinking water enhanced this phenotype, but independently each treatment did not affect enamel initiation.

This phenotype of an earlier enamel formation were similar to those of Zhang *et al*, whom examined the role of the vitamin-D receptor (VDR) on enamel formation [38]. Zhang *et al* found the enamel of the lower incisor mineralized early, starting at the second molar in VDR^{-/-} mice compared to the 1st molar in control mice. This phenotype was independent of the level of calcium because VDR^{-/-} mice on a high calcium diet still maintained this phenotype [38]. This result indicated a more direct and specific role of VDR in enamel formation. VDR is expressed in ameloblasts and is localized to the nucleus, however its exact role on amelogenesis is not well characterized [39]. Zhang *et al* attributed their enamel mineralization phenotype to a possible disruption in the paracellular and transcellular calcium transport pathways [38].

Calcium transport from the blood to the enamel matrix is a fairly complicated and stage specific phenomenon. Calcium either can pass in between ameloblasts or through them depending on which stage of differentiation (i.e. ruffled ended or smooth ended ameloblasts) [40]. Paracellular transport of calcium can be easily

explained by the tremendous calcium gradient present between the papillary layer (10^{-3}mM) and the enamel matrix (10^{-5}mM). This significant difference in calcium concentrations provides the environment for a high rate of diffusion [41]. However, the transcellular transport of calcium can be comparably slower than the paracellular route, in large part due to regulation by various channels and pumps. At the enamel matrix side, intracellular calcium is actively pumped outside of the ameloblasts by Ca-ATPase [42-44]. Once the calcium ions are in the enamel matrix they can rapidly redistribute throughout the entirety of the matrix and so making the apparent rate limiting step of enamel crystal formation the transport of calcium from the papillary layer to inside the ameloblasts [40].

Both VDR and CaSR could potentially regulate calcium transport to the enamel matrix by shuttling calcium between transcellular and paracellular pathways. First, VDR activity directly controls the expression of two specific calcium channels, TRPV5 and 6 [45]. The expression of these calcium channels at the basolateral border results in a transport of calcium down its concentration gradient intracellularly [45]. A decrease in TRPV5 and 6 levels at the basolateral surface would result in a build-up of extracellular calcium on the papillary side until it then flows down its concentration gradient into the developing enamel matrix via the paracellular route. Second, the expression of VDR is dependent on the level of extracellular calcium and the activity of CaSR. Upon calcium binding, CaSR triggers the activation of Sp1 transcription factor, which then leads to the upregulation of VDR. This VDR regulation, by CaSR, is mediated through the Erk1/2 MAPK pathway [46]. CaSR regulation of VDR would presumably also control TRV5 and 6 levels. Our

results and that of Zhang *et al*, suggest CaSR is involved in the initiation process of enamel formation, and it does so by functioning upstream of VDR. Further studies will be needed to evaluate the expression levels of calcium channels (TRPV 5 and 6) as well as VDR in our K14-Cre-CaSR^{-/-} mice model.

In addition to the early enamel formation phenotype in VDR^{-/-} mice, Zhang *et al* [38] also found that the enamel of the VDR^{-/-} mice was more susceptible to acid erosion than the wild-type counterparts, and this data infers a weakened enamel microstructure. The authors proposed that this phenotype could offer some explanation as to why certain patients are more susceptible to dental decay than others. The literature does not mention any specific enamel defect associated with patients whom lack CaSR function, at the same time, none of those studies assessed the patients dental decay susceptibility. It would definitely be of interest to determine if our K14-Cre-CaSR^{-/-} has a similar response to acid erosion, and if patients with Familial Hypocalciuric Hypercalcaemia (inactivating mutations of CaSR) are more susceptible to dental decay. Obviously, further studies are needed to explore and define what the mechanisms are behind this early enamel formation phenotype

In summary, our studies suggest that CaSR activity alone is not directly responsible for the phenotypes seen in both the Ho *et al* and Sun *et al* studies. Our epithelial specific K14-Cre-CaSR^{-/-} mice showed normal length, shape, and color of the enamel seen in the erupted mandibular incisor, as compared to the dramatically reduced and hypoplastic enamel seen in the Sun *et al* study. Moreover, CaSR alone

does not control ameloblast cellular function and gene expression as seen in our histologic sections and gene expression assays. Under a normal diet, K14-Cre-CaSR^{-/-} mice did show slightly earlier mineralization compared to the wild type mice. This early enamel formation phenotype was more pronounced in both the low calcium diet and the high fluoride water treatment groups. This phenotype could be the result of CaSR indirectly regulating the expression of two specific calcium channels (TRPV5 and 6) through VDR activity. Further experiments are needed to understand how these proteins work to direct enamel formation.

References:

1. Thesleff, I., X.P. Wang, and M. Suomalainen, *Regulation of epithelial stem cells in tooth regeneration*. C R Biol, 2007. **330**(6-7): p. 561-4.
2. Fincham, A.G., J. Moradian-Oldak, and J.P. Simmer, *The structural biology of the developing dental enamel matrix*. J Struct Biol, 1999. **126**(3): p. 270-99.
3. Lyaruu, D.M., et al., *Localization of calcium in differentiating odontoblasts and ameloblasts before and during early dentinogenesis and amelogenesis in hamster tooth germs*. J Histochem Cytochem, 1985. **33**(6): p. 595-603.
4. Chen, J., et al., *Calcium-mediated differentiation of ameloblast lineage cells in vitro*. J Exp Zool B Mol Dev Evol, 2009. **312B**(5): p. 458-64.
5. Kukita, A., et al., *Primary and secondary culture of rat ameloblasts in serum-free medium*. Calcif Tissue Int, 1992. **51**(5): p. 393-8.

6. Hubbard, M.J., *Calcium transport across the dental enamel epithelium*. Crit Rev Oral Biol Med, 2000. **11**(4): p. 437-66.
7. BAILLEUL-FORESTIER, I., et al., *Immunolocalization of Vitamin D Receptor and Calbindin-D28k in Human Tooth Germ*. Pediatric Research, 1996. **39**(4): p. 636-642.
8. Elms, T.N. and A.N. Taylor, *Calbindin-D 28K Localization in Rat Molars During Odontogenesis*. J Dent Res, 1987. **66**(9): p. 1431-1434.
9. Turnbull, C.I., et al., *Calbindin independence of calcium transport in developing teeth contradicts the calcium ferry dogma*. J Biol Chem, 2004. **279**(53): p. 55850-4.
10. Kutuzova, G.D., et al., *Calbindin D9k knockout mice are indistinguishable from wild-type mice in phenotype and serum calcium level*. Proceedings of the National Academy of Sciences, 2006. **103**(33): p. 12377-12381.
11. Bikle, D.D., et al., *Calcium- and vitamin D-regulated keratinocyte differentiation*. Mol Cell Endocrinol, 2001. **177**(1-2): p. 161-71.
12. Garrett, J.E., et al., *Molecular cloning and functional expression of human parathyroid calcium receptor cDNAs*. J Biol Chem, 1995. **270**(21): p. 12919-25.
13. Brown, E.M., *Cloning and characterization of extracellular Ca sensing receptor from bovine parathyroid glands*. Nature, 1993(366): p. 575-580.
14. Brown, E.M. and R.J. MacLeod, *Extracellular calcium sensing and extracellular calcium signaling*. Physiol Rev, 2001. **81**(1): p. 239-297.
15. Bawden, W.J., *Immunohistochemical localization of Gq α , PLC β , Gi α , PKA,*

- Endothelin B, and extracellular calcium sensing receptor during early amelogenesis.* Journal of Dental Research, 2000(79): p. 1896-1909.
16. Mathias, R., *Identification of calcium sensing receptor in developing tooth organ.* J Bone Miner Res, 2001(12): p. 2238-2244.
 17. Mathias, R.S., et al., *Identification of the calcium-sensing receptor in the developing tooth organ.* J Bone Miner Res, 2001. **16**(12): p. 2238-44.
 18. Moran, R.A., E.M. Brown, and J.W. Bawden, *Immunohistochemical localization of Galphaq, PLCbeta, Galphai1-2, PKA, and the endothelin B and extracellular Ca²⁺-sensing receptors during early amelogenesis.* J Dent Res, 2000. **79**(11): p. 1896-901.
 19. Ho, C., et al., *A mouse model of human familial hypocalciuric hypercalcemia and neonatal severe hyperparathyroidism.* Nat Genet, 1995. **11**(4): p. 389-94.
 20. Sun, W., et al., *Alterations in phosphorus, calcium and PTHrP contribute to defects in dental and dental alveolar bone formation in calcium-sensing receptor-deficient mice.* Development. **137**(6): p. 985-92.
 21. Oda, Y., et al., *The calcium sensing receptor and its alternatively spliced form in keratinocyte differentiation.* J Biol Chem, 1998. **273**(36): p. 23344-52.
 22. Rodriguez, L., et al., *Expression and functional assessment of an alternatively spliced extracellular Ca²⁺-sensing receptor in growth plate chondrocytes.* Endocrinology, 2005. **146**(12): p. 5294-303.
 23. Chang, W., et al., *The extracellular calcium-sensing receptor (CaSR) is a critical modulator of skeletal development.* Sci Signal, 2008. **1**(35): p. ra1.

24. Tabata, M.J., et al., *Expression of cytokeratin 14 in ameloblast-lineage cells of the developing tooth of rat, both in vivo and in vitro*. Archives of Oral Biology, 1996. **41**(11): p. 1019-1027.
25. DenBesten, P.K., et al., *Characterization of human primary enamel organ epithelial cells in vitro*. Arch Oral Biol, 2005. **50**(8): p. 689-94.
26. Bronckers, A.L., et al., *Effect of calcium, given before or after a fluoride insult, on hamster secretory amelogenesis in vitro*. Eur J Oral Sci, 2006. **114 Suppl 1**: p. 116-22; discussion 127-9, 380.
27. Lyaruu, D.M., et al., *The effect of fluoride on enamel and dentin formation in the uremic rat incisor*. Pediatr Nephrol, 2008. **23**(11): p. 1973-9.
28. Yamaguti, P.M., V.E. Arana-Chavez, and A.C. Acevedo, *Changes in amelogenesis in the rat incisor following short-term hypocalcaemia*. Arch Oral Biol, 2005. **50**(2): p. 185-8.
29. Kolakowski, L.F., Jr., *GCRDb: a G-protein-coupled receptor database*. Receptors & channels, 1994. **2**(1): p. 1-7.
30. Kubo, Y., T. Miyashita, and Y. Murata, *Structural basis for a Ca²⁺-sensing function of the metabotropic glutamate receptors*. Science, 1998. **279**(5357): p. 1722-5.
31. Bai, M., et al., *Expression and characterization of inactivating and activating mutations in the human Ca²⁺-sensing receptor*. The Journal of biological chemistry, 1996. **271**(32): p. 19537-45.

32. Brown, E.M., *Extracellular Ca²⁺ sensing, regulation of parathyroid cell function, and role of Ca²⁺ and other ions as extracellular (first) messengers.* *Physiological reviews*, 1991. **71**(2): p. 371-411.
33. Brown, E.M., et al., *Cloning and characterization of an extracellular Ca(2+)-sensing receptor from bovine parathyroid.* *Nature*, 1993. **366**(6455): p. 575-80.
34. Gama, L. and G.E. Breitwieser, *A carboxyl-terminal domain controls the cooperativity for extracellular Ca²⁺ activation of the human calcium sensing receptor. A study with receptor-green fluorescent protein fusions.* *The Journal of biological chemistry*, 1998. **273**(45): p. 29712-8.
35. Wise, A., et al., *Calcium sensing properties of the GABA(B) receptor.* *Neuropharmacology*, 1999. **38**(11): p. 1647-56.
36. Bronckers, A.L., L.L. Jansen, and J.H. Woltgens, *A histological study of the short-term effects of fluoride on enamel and dentine formation in hamster tooth-germs in organ culture in vitro.* *Arch Oral Biol*, 1984. **29**(10): p. 803-10.
37. Bronckers, A.L., et al., *Antagonism of fluoride toxicity by high levels of calcium but not of inorganic phosphate during secretory amelogenesis in the hamster tooth germ in vitro.* *Arch Oral Biol*, 1989. **34**(8): p. 625-36.
38. Zhang, X., et al., *Normalisation of calcium status reverses the phenotype in dentin, but not in enamel of VDR-deficient mice.* *Archives of Oral Biology*, 2009. **54**(12): p. 1105-1110.
39. Bailleul-Forestier, I., et al., *Immunolocalization of vitamin D receptor and calbindin-D28k in human tooth germ.* *Pediatr Res*, 1996. **39**(4 Pt 1): p. 636-42.

40. Kawamoto, T. and M. Shimizu, *Pathway and Speed of Calcium Movement from Blood to Mineralizing Enamel*. Journal of Histochemistry & Cytochemistry, 1997. **45**(2): p. 213-230.
41. Aoba, T. and E.C. Moreno, *The enamel fluid in the early secretory stage of porcine amelogenesis: chemical composition and saturation with respect to enamel mineral*. Calcif Tissue Int, 1987. **41**(2): p. 86-94.
42. Sasaki, T. and P.R. Garant, *Mitochondrial migration and Ca-ATPase modulation in secretory ameloblasts of fasted and calcium-loaded rats*. Am J Anat, 1987. **179**(2): p. 116-30.
43. Sasaki, T. and P.R. Garant, *Ultracytochemical demonstration of ATP-dependent calcium pump in ameloblasts of rat incisor enamel organ*. Calcif Tissue Int, 1986. **39**(2): p. 86-96.
44. Sasaki, T. and P.R. Garant, *A study of post-secretory maturation ameloblasts in the cat by transmission and freeze-fracture electron-microscopy*. Arch Oral Biol, 1986. **31**(9): p. 587-96.
45. van de Graaf, S.F.J., et al., *Regulation of the epithelial Ca²⁺ channels TRPV5 and TRPV6 by 1[alpha],25-dihydroxy Vitamin D3 and dietary Ca²⁺*. The Journal of Steroid Biochemistry and Molecular Biology, 2004. **89-90**: p. 303-308.
46. Ca^v±adillas, S., et al., *Upregulation of parathyroid VDR expression by extracellular calcium is mediated by ERK1/2-MAPK signaling pathway*. American Journal of Physiology - Renal Physiology, 2010. **298**(5): p. F1197-F1204.

CONCLUSION

Tooth formation is highly dependent on signaling molecules and how they interact with their downstream targets. The role of calcium in enamel development has been overlooked, with most of the attention focused on organic signaling molecules or enamel matrix proteins [1, 2]. A combination of *in vitro* studies and case studies on human diseases, in which serum calcium regulation was significantly changed, suggested that calcium might have a role in regulating ameloblast differentiation and enamel formation [3-6]. The goals of this thesis project was two fold, first to determine both the effects of extracellular calcium on ameloblast cellular function and second to determine what role the calcium sensing receptor plays in the process of enamel formation.

The *in vitro* results reported in this thesis determined the importance of calcium in enamel matrix formation. We found that the effect of calcium on ameloblast gene expression was dose dependent and time dependent, where ameloblasts responded to high and low levels of calcium very differently. In short exposure times, low levels calcium induced upregulation of basement membrane and extracellular matrix proteins, whereas relatively high calcium concentrations led to increased enamel matrix protein expression. These results offer an intriguing scenario where different concentrations of calcium in the developing matrix regulate the expression of different assortment of matrix genes. As the level of extracellular calcium increases during the secretory stage, amelogenin expression increases and as the level drops during mineralization, so does the level of amelogenin.

One surprising finding from our *in vitro* studies were the high levels of collagen Type I, expression because up to now there have been no studies showing positive collagen Type I expression in ameloblast lineage cell culture. This expression of

collagen Type I in our primary cell culture prompted us to critically assess the cellular composition of our primary cell culture, and we suggest that the source of the collagen Type I expression in our primary cell culture and our SV40-HA cells to be from stellate reticulum cells. A homogeneous population of immortalized stellate reticulum cells proved unable to form mineralization nodules in contrast to our heterogeneous primary ameloblast lineage cells. These results illustrate the importance other cell types, found in the enamel organ, for mineralization. Further studies will be needed to determine which cell or cells are required for mineralization *in vitro*. Data gained this thesis and by these future studies will move the field of enamel formation one step closer to the main goal of synthesizing human enamel *de novo*.

The data from our *in vitro* studies clearly showed a cellular response to extracellular calcium. The fact that our human primary ameloblast lineage cells responded so effectively to elevated levels of calcium led us to evaluate what molecules involved in calcium signaling could be responsible for these results. The primary candidate for mediating extracellular calcium signaling is CaSR, which we determined to be expressed in our human ameloblast lineage cell culture. To determine the role of CaSR in enamel formation and ameloblast cellular function, we evaluated and characterized an epithelial specific tissue CaSR knockout (K14-Cre-CaSR^{-/-} mouse).

Studies prior to this one discovered that germ-line CaSR^{-/-} mice displayed dramatically hypoplastic enamel [7, 8], but these studies could not determine whether the hypoplastic enamel was due to a direct loss of CaSR function in ameloblasts or an indirect loss of calcium regulation. In our study we found an effect of the CaSR in the timing of enamel initiation. Micro-CT comparison of wild-type and K14-Cre-CaSR^{-/-}

mice showed significantly earlier enamel formation in mice that had a reduced level of CaSR activity. Additionally, this enamel initiation phenotype was enhanced through the addition of fluoride in the drinking water and through the reduction of calcium in the diet.

The early enamel initiation phenotype found in our K14-Cre-CaSR^{-/-} mice was similar to that reported in studies on VDR null mice [9]. The fact that both our mice and the VDR null mouse share the same phenotype would suggest that they are both integrated in the same pathway, with evidence showing CaSR mediated regulation VDR expression [10]. The ramifications of this early initiation phenotype are not clear and still need to be further evaluated. One intriguing possibility was described by Zhang *et al*, where they showed VDR^{-/-} mice were more susceptible to acid erosion compared to wild-type mice [9]. Further studies are needed to evaluate the levels VDR and to assess the enamel micro-strength in our K14-Cre-CaSR^{-/-} mice.

In summary, the results from this thesis have provided further evidence supporting the role of extracellular calcium in human amelogenesis. Extracellular calcium functions to induce gene expression of a variety of different matrix proteins. The exact mechanism of how extracellular calcium regulates ameloblast gene expression is not clear, but our in vitro experiments show it appears to occur independent of CaSR levels (Fig 1,2). CaSR activity does appear to contribute to the timing of enamel formation, though clearly other factors are involved as well, most importantly VDR and calcium channels such as TRPV5/6 (Fig 1,2). There have been no reports of severe enamel defects in patients with mutations in CaSR, but if CaSR alters the timing of initiation of enamel mineralization, it is possible that a loss of CaSR function could affect a patient's resistance to caries. The next phase of experiments using our K14-Cre-CaSR^{-/-}

^{-/-} mice should be focused on evaluating the physical properties of enamel under normal conditions and under cariogenic conditions, as well as evaluating the levels of VDR, TRPV5 and 6 in ameloblasts. Should a difference exist between the K14-Cre-CaSR^{-/-} and wild-type mouse then a human clinical study evaluating the caries risk of patients diagnosed with Familial Hypocalciuric Hypercalcaemia should be considered.

Fig 1:

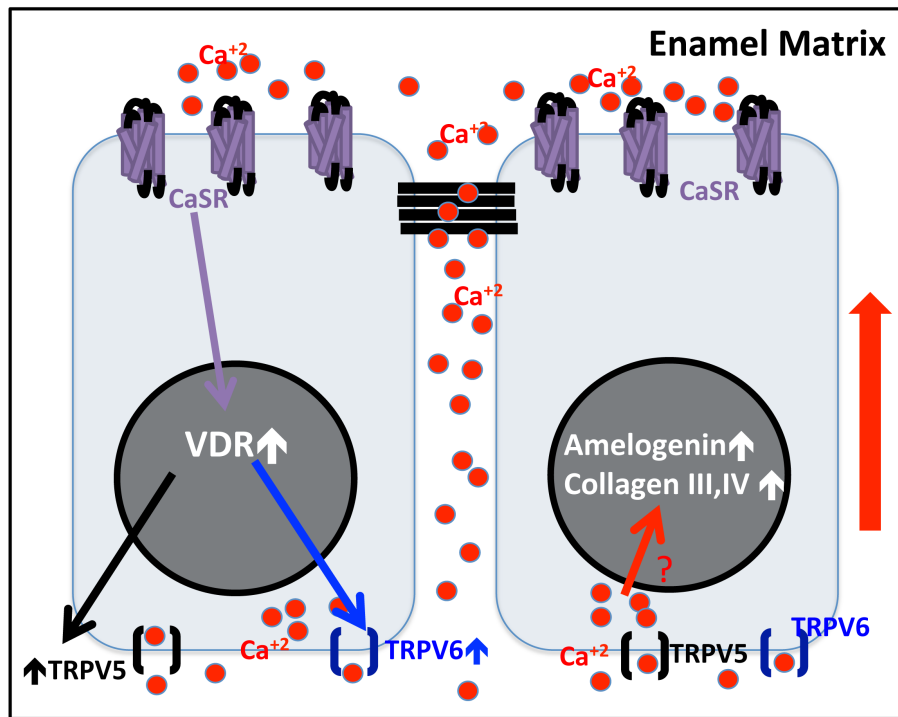


Figure 1: Proposed model for CaSR and calcium function during amelogenesis.

The cartoon is a depiction of secretory stage ameloblasts responding to calcium during amelogenesis under normal CaSR activity. The left cell shows activated CaSR triggers VDR upregulation, presumably through ERK/MAPK pathway, which then

increases the expression of two calcium channels, TRPV5 and 6. The expression of TRPV5 and 6 maintains a balance between intracellular and paracellular calcium transport (as indicated by the length of the red arrow on the right). The right cell illustrates that the increased levels of TRPV5 and 6 allows calcium to pass intracellularly, where it then triggers upregulation of amelogenin and other matrix proteins though via a mechanism that is yet to be determined.

FIG 2:

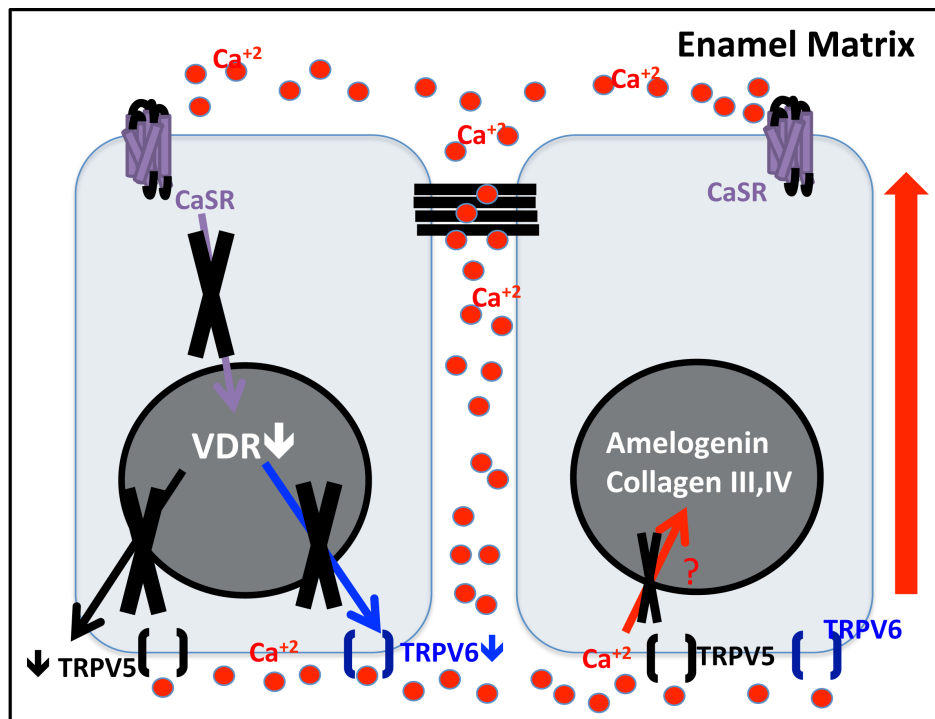


Figure 2: Proposed model for reduced CaSR activity.

The cartoon is a depiction of secretory stage ameloblasts responding to calcium during amelogenesis in the absence of adequate CaSR signaling. The left cell illustrates how reduced CaSR activity fails to trigger VDR upregulation, which then

results in reduced the level TRPV5 and 6. The loss of TRPV5 and 6 leads to a shift in calcium transport paracellularly, which ultimately allows for more rapid calcium diffusion into the enamel matrix (as indicated by the length of the red arrow on the right). The right cell illustrates how reduced intracellular levels of calcium potentially translate to decreased levels amelogenin and other matrix proteins.

References-


1. Simmer, J.P. and A.G. Fincham, *Molecular mechanisms of dental enamel formation*. Crit Rev Oral Biol Med, 1995. **6**(2): p. 84-108.
2. Tompkins, K., *Molecular mechanisms of cytodifferentiation in mammalian tooth development*. Connect Tissue Res, 2006. **47**(3): p. 111-8.
3. Woltgens, J.H., et al., *Biom mineralization during early stages of the developing tooth in vitro with special reference to secretory stage of amelogenesis*. Int J Dev Biol, 1995. **39**(1): p. 203-12.
4. Kukita, A., et al., *Primary and secondary culture of rat ameloblasts in serum-free medium*. Calcif Tissue Int, 1992. **51**(5): p. 393-8.
5. Koch, M.J., et al., *Enamel hypoplasia of primary teeth in chronic renal failure*. Pediatr Nephrol, 1999. **13**(1): p. 68-72.
6. Nunn, J.H., et al., *Oral health in children with renal disease*. Pediatr Nephrol, 2000. **14**(10-11): p. 997-1001.
7. Ho, C., et al., *A mouse model of human familial hypocalciuric hypercalcemia and neonatal severe hyperparathyroidism*. Nat Genet, 1995. **11**(4): p. 389-94.

8. Sun, W., et al., *Alterations in phosphorus, calcium and PTHrP contribute to defects in dental and dental alveolar bone formation in calcium-sensing receptor-deficient mice*. *Development*. **137**(6): p. 985-92.
9. Zhang, X., et al., *Normalisation of calcium status reverses the phenotype in dentin, but not in enamel of VDR-deficient mice*. *Archives of Oral Biology*, 2009. **54**(12): p. 1105-1110.
10. Cavalladas, S., et al., *Upregulation of parathyroid VDR expression by extracellular calcium is mediated by ERK1/2-MAPK signaling pathway*. *American Journal of Physiology - Renal Physiology*, 2010. **298**(5): p. F1197-F1204.

Publishing Agreement

It is the policy of the University to encourage the distribution of all theses, dissertations, and manuscripts. Copies of all UCSF theses, dissertations, and manuscripts will be routed to the library via the Graduate Division. The library will make all theses, dissertations, and manuscripts accessible to the public and will preserve these to the best of their abilities, in perpetuity.

I hereby grant permission to the Graduate Division of the University of California, San Francisco to release copies of my thesis, dissertation, or manuscript to the Campus Library to provide access and preservation, in whole or in part, in perpetuity.

 8/29/11
Author Signature Date